NEUROMUSCULAR NETWORKING CONNECTIVITY IN SENSORIMOTOR IMPAIRMENTS AFTER STROKE

ZHOU SA

PhD

The Hong Kong Polytechnic University

2023

The Hong Kong Polytechnic University

Department of Biomedical Engineering

Neuromuscular Networking Connectivity in Sensorimotor Impairments after Stroke

Zhou Sa

A thesis submitted in partial fulfilment of the requirements for the degree of Doctor of Philosophy

August 2022

CERTIFICATE OF ORIGINALITY

I hereby declare that this thesis is my own work and that, to the best of my knowledge and belief, it reproduces no material previously published or written, nor material that has been accepted for the award of any other degree or diploma, except where due acknowledgement has been made in the text.

_____(Signed)

ZHOU SA (Name of student)

ABSTRACT

More than half of stroke survivors experience both sensory and motor impairments in the upper extremity (UE), limiting their independence in daily living tasks. Neuroplastic processes of neuromuscular networking connectivity, including connectivity among cortical areas (i.e., cortico-cortical connectivity) and that between the sensorimotor cortex and muscle effectors (i.e., cortico-muscular connectivity), in central-and-peripheral nerves systems, is the basis of sensorimotor rehabilitation after stroke. However, little has been done on an effective neurological evaluation of sensorimotor impairments after stroke. This was primarily caused by the absence of systemic assessments on the altered neuromuscular networking connectivity in sensorimotor impairments and its evolution in the recovery process after stroke. Current sensorimotor evaluation post-stroke relied on traditional clinical assessments through manual operation and visual observation, with disadvantages of subjectiveness, low accuracy, and low repeatability. Therefore, the purpose of this project was to investigate the neuromuscular networking connectivity in post-stroke sensorimotor impairments and recovery in rehabilitation, including 1) the functional connectivity (FC) among cortical areas in fine tactile sensation after stroke, 2) the pathway-specific cortico-muscular coherence (CMC) in the motion compensation from the proximal upper limb to the fine motor control of distal fingers, 3) integrated sensorimotor evaluation of post-stroke cortical rearrangement in sensory-/motor-level neuromuscular electrical stimulation (NMES), and 4) the closed-loop neurorehabilitation effects of a CMC-Electromyogram (EMG)-driven NMES-robot after stroke, as in the following four studies:

In the first study, the whole-brain 64-channel electroencephalogram (EEG) was recorded in both stroke (n=8) and unimpaired participants (n=8) during the fabric

stimulation. The FC among cortical areas and the networking structure in the brain were then estimated using EEG coherence and graph theory analyses. Results suggested that the tactile impairments post-stroke had increased inter-hemispheric connectivity and cortical activities mainly in the unaffected hemisphere and attentional areas for compensation to the ipsilesional somatosensory areas.

In the second study, synchronous EEG and electromyography (EMG) recordings were conducted from the sensorimotor cortical areas and both distal and proximal UE muscles in stroke (n=14) and unimpaired (n=11) participants during fine motor control of distal fingers. The directed CMC (dCMC) in descending, i.e., from EEG to EMG, and ascending pathways i.e., from EMG to EEG, and the corticomuscular conduction delay were analyzed. Results suggested that the post-stroke compensatory motions from the proximal elbow-shoulder to the precise control of distal fingers had the shifted descending predominance from the fingers towards the proximal elbow-shoulder joints, excessive sensory feedbacks in distal finger, and extended conduction delay for descending control in target muscles.

In the third study, sensory- and motor-level NMES to the hand-wrist extensors with synchronized whole-brain 64-channel EEG recordings were conducted in stroke (n=15) and unimpaired (n=20) participants. The NMES cortical neuromodulation was analyzed by event-related desynchronization/synchronization (ERD/ERS) and FC analyses based on EEG signals. Results suggested that sensory-/motor-level NMES and EEG effectively captured the cortical rearrangement in post-stroke sensorimotor impairments, presenting altered hemispheric dominance in cortical activation, over inhibition in cortical recovery, reduced cortical interaction with the ipsilesional hemisphere, and cortical compensation from neighboring regions.

In the fourth study, a randomized control trial was performed to compare the rehabilitation effectiveness of the CMC-EMG-triggered NMES-robot (n=16) and CMC-EMG-triggered Robot (n=11) for hand-wrist recovery after stroke. We assessed the rehabilitation effectiveness of these systems with both behavioral, i.e., clinical scores, and neurological measures, i.e., CMC, dCMC, and the levels of EMG activation. Results suggested that the CMC-EMG-triggered NMES-robot exhibited better motor outcomes than the CMC-EMG-triggered robot for the precise hand-wrist motor restoration after stroke. The additional NMES assistance in the system could enhance improvements on voluntary motor functions in target muscles and the re-distribution of central-and-peripheral voluntary motor efforts (CAP-VME) among UE muscles for motor relearning, contributing to the cortical sensorimotor integration for the closed-loop neurorehabilitation on target muscles.

In conclusion, the neuromuscular networking connectivity could be effective to evaluate the systemic neurological changes in sensorimotor impairments and recovery post-stroke.

PUBLICATIONS ARISING FROM THE THESIS

Journal papers

1. Zhou, S., Huang, Y., Jiao, J., Hu, J., Hsing, C., Lai, Z., ... & Hu, X. (2021). Impairments of cortico-cortical connectivity in fine tactile sensation after stroke. Journal of NeuroEngineering and Rehabilitation, 18(1), 1-18.
2. Zhou, S., Guo, Z., Wong, K., Zhu, H., Huang, Y., Hu, X., & Zheng, Y. P. (2021). Pathway-specific cortico-muscular coherence in proximal-to-distal compensation during fine motor control of finger extension after stroke. Journal of Neural Engineering, 18(5), 056034.
3. Guo, Z.*, Zhou, S.*, Ji, K., Zhuang, Y., Song, J., Nam, C., ... & Zheng, Y. (2022). Corticomuscular integrated representation of voluntary motor effort in robotic control for the recovery of hand-wrist functions. Journal of Neural Engineering, 19(2), 026004. **(* indicates the co-first authorship)**
4. Zhou, S., Ye, F., Chan N, Song J., Han Y., Hu, X., & Zheng, Y. (2022). Integrated sensorimotor evaluation of cortical rearrangement after stroke with sensory-/motor-level neuromuscular electrical stimulation (NMES) and electroencephalography (EEG). Computer Methods and Programs in Biomedicine. Under Revision.
5. Zhou, S., Zhang, J., Hu, X. (2022). Automatic theranostics for long-term neurorehabilitation after stroke. Frontiers in Aging Neuroscience. Submitted.
6. Zhou, S., Guo, Z., Song J., Ye, F., Hu, X., & Zheng, Y. (2022). Closed-loop neurorehabilitation assisted by CMC-EMG-triggered NMES-Robot after stroke : a randomized controlled trial. Neural Network. In preparation.

Conference proceedings:

1. Zhou, S., Huang, Y., Jiao, J., Hu, J., Hsing, C., Lai, Z., Hu, X. Impairments of Cortico-cortical Connectivity in Fine Tactile Sensation after Stroke, IEEE-EMB Hong Kong-Macau Joint Chapter Student Project Competition 2020
2. Zhou, S., Guo, Z., Huang, Y., Jiao, J., Hu, J., Hsing, C., Lai, Z., Hu, X. Neuromuscular Networking Connectivity on Sensorimotor Impairments after Stroke, IEEE-EMB Hong Kong-Macau Joint Chapter Student Project Competition 2021
3. Zhou, S., Guo, Z., Huang, Y., Jiao, J., Hu, J., Hsing, C., Lai, Z., Hu, X., & Zheng, Y, Neuromuscular Networking Connectivity on Sensorimotor Impairments after Stroke, 1st Asia-Pacific Neuroscience Student Congress and HKSAN 2nd Annual Conference (APNSC-HKSAN) 2021

Patents:

1. Hu, X.L., W. Rong, Li, W.M., Guo, Z.Q., Zhou, S. A cortico-muscular coupling-based voluntary motor controlled rehabilitation training system. China. Applicant: The Hong Kong Polytechnic University. Application number: 2021114954087. Filed on 9 Dec, 2021.

ACKNOWLEDGEMENTS

My deepest gratitude goes to my chief supervisor, Dr. Xiaoling Hu, for her supervision, patient guidance, and tremendous support in my research. I have received valuable experiences and knowledge under her inspiration and guidance of my PhD study.

I would like to sincerely thank my co-supervisor, Prof. Yong-ping Zheng, for his trust and support in this research and warm encouragement throughout the study.

I would like to extend my thanks to my colleagues and other members of the team, Dr. Yanhuan Huang, Dr. Qiuyang, Qian, Dr. Chingyi Nam, Dr. Ziqi Guo, and Mr. Fuqiang Ye, Mr. Legeng Lin, Mr. Jianing Zhang, and Miss Wanyi Qing for their assists in human subject experiments and friendly support in daily life. Many thanks go to them for their time and efforts in this study.

I would like to express my gratefulness to all participants in this research, for their time and effort.

I am fortunate and honored to have my family, who supported me with unconditional love, faith, and encouragement.

TABLE OF CONTENTS

LIST OF FIGURES

LIST OF TABLES

LIST OF ABBREVIATIONS

ALDs	Activities of daily livings
M1	Primary motor cortex
SI	Primary somatosensory cortices
SII	Secondary somatosensory cortices
FMA	Fugl-Meyer Assessment Scale
FIM	Functional Independence Measurement
MAS	Modified Ashworth Score
ARAT	Action Research Arm Test
NSA	Nottingham Sensory Assessment
RASP	Rivermead assessment of somatosensory
QST	Quantitative sensory testing
FC	Functional connectivity
PET	Positron emission tomography
EEG	Electroencephalography
fMRI	Functional magnetic resonance imaging
TMS	Transcranial magnetic stimulation
MEPs	Motor evoked potentials
CMC	Cortico-muscular coherence
dCMC	Directional cortico-muscular coherence
NMES	neuromuscular electrical stimulation
VME	Voluntary motor efforts
CAP-VME	Central-and-peripheral voluntary motor efforts
CPM	Continuous passive mode
CIMT	Constraint-induced movement therapy
NDT	Neurodevelopmental treatment
BCI	Brain computer interface
MI	Motor imagery
SMA	Supplementary motor area

ME	Motor execution
EMG	Electromyography
RCT	Randomized control trials
SFC	Stimulation induced functional connectivity
MMSE	Mini-Mental State Examination
Ahemi	Affected hemisphere
Uhemi	Unaffected hemisphere
ImCoh	Imaginary coherence
Sig-FC	Significant FC
FDR	False discovery rate
Lhemi	Left hemisphere
Rhemi	Right hemisphere
Alimb	Affected limb
Ulimb	Unaffected limb
Llimb	Left limb
Rlimb	Right limb
HL	Hemispheric lateralization
PMC	Premotor cortex
APB	Abductor pollicis brevis
ECR	Extensor carpi radialis
S1	Primary somatosensory area
SMA	Supplementary somatosensory area
FD	Flexor digitorum
BIC	Biceps brachii
ED	Extensor digitorum
TRI	Triceps brachii
iMVC	Isometric maximum voluntary contraction
MPF	Mean power frequency
ANOVA	Analysis of Variance
EFs	Effect sizes

SEM	Standard error of mean
CMCT	Central motor conduction delay
ERD/ERS	Event-related desynchronization/synchronization
ICA	Independent component analysis

CHAPTER 1
INTRODUCTION

1.1 Stroke

1.1.1 Overview

Stroke has been the leading cause of persistent adults motor disability [1]. According to the World Stroke Organization: Global Stroke Fact Sheet 2022, stroke has been ranked not only the 2nd primary reason for death, but also the 3rd primary reason for disability all over the word. Globally, there was approximately over US$721 billion (0.66% of the global GDP) in the stroke-associated costings [1]. Over the past two decades (1990-2019), the stroke-associated economic burden presented a substantial increase, where the raised incident strokes is 70.0%, the deaths rate of stroke is 43.0%, and the prevalence was 102.0%) [1]. In Hong Kong, stroke ranked the fourth cause of death in 2020, where there was 3,164 registered deaths and the crude death was 42.3 per 100 000 persons [2].

Stroke is a medical syndrome in which cell death was induced by interrupted or reduced blood flow to the brain [2]. The main reasons includes the alteration in vascular structures and a blood vessel rupture or blockage of the blood supply [3]. According to the onset pathogenesis, stroke can be classified into ischemic stroke, where the blood supply is blocked by a blood clot, accounting for 85% of all cases; hemorrhagic stroke, where a cerebral blood artery was already weak bursts [3]. As the most common type of stroke, ischemic stroke is also regarded as a cerebral infarction brought on by a constricted brain artery and a markedly reduced blood flow [4]. A hemorrhagic stroke is characterized by a blood vessel rupture or leak [5]. The two types of stroke both result

in the brain receiving insufficient oxygen and nutrients, which results in permanent cell death [5].

The International Classification of Function, Disability and Health framework published by the World Health Organization, divides stroke effects on individual into four principal categories, namely pathology (disease or diagnosis), impairment (symptoms and signs), limitations on activity (disability), and restrictions on participation (handicap) [6]. Among the main symptoms, e.g., communication problems, emotional disturbances, and post-stroke fatigue, motor deficits are commonly observed manifesting the muscular weakness, which generally leads to the paralysis in more severe cases, leaving survivors unable to move certain parts of their bodies [6]. Hemiparesis is the most common motor deficits after stroke, which leads to both sensory and motor deficits on both contralateral upper and lower limbs to the lesion site [7]. Severe motor deficits typically involve the somatosensory impairments on the touch sensation, thermal sensation, pain, and proprioception [7] [8]. It could further limit the motor functions in both upper and lower limbs for grasp, grip, walk, balance, and stand [8]. Stroke survivors could also have movement deficits such as drop foot, muscle spasticity, and poor stamina [7]. The symptoms of a stroke can last from a few minutes to several years, depending on the individual [6]. In some circumstances, these effects are modest and temporary, while in others they can be significant and long-lasting [6]. Notably, neurological difficulties will be evident on the left upper and lower limbs when a stroke lesion was on the right hemisphere, and vice versa, because the left and right hemisphere regulate the opposing sides of the body [6]. These effects are related to lesions that affect the arterial blood flow to the middle cerebral area [6].

1.1.2 Sensorimotor impairments after stroke

More than half stroke survivors suffer from both sensory and motor deficits in their affected UE [8] [9]. It was reported that only 11.6% of stroke survivors were able to recover the UE functions to normal levels at the chronic stage [1]. In contrast, up to 80% of stroke survivors were able to regain the basic walking function following the sub-acute stage after a stroke with the help of lower limb motor rehabilitation [1]. The post-stroke upper limb motor impairments typically manifest as muscle weakness or contracture, spasticity, discoordination among muscles, and impaired motor control [10]. These motor impairments decrease the ability to move and coordinate muscles and joints in their affected UE, particularly for the distal UE, e.g., finger and wrist in hand joints, leading to difficulties to complete routine tasks, e.g., reaching, grabbing, eating, dressing, and holding objects [10]. Lower levels of self-dependence and living quality are manifested in motor impairments after a stroke, which could severely affect the activities of daily livings (ALDs) [10].

In addition to motor impairments, more than 50% of stroke patients had significantly sensory deficits or sensory loss, including impairments on the touch, temperature, pain, and proprioception [11]. It has also been found that poorer motor functions were correlated with the sensory impairments after stroke [12]. There are two types of somatosensation, i.e., exteroception and proprioception [11]. The exteroception mainly refers to the superficial and cutaneous sensation perceived by the mechanoreceptors, thermoreceptors and nociceptors on the skin [11]. The proprioception, also known as kinesthesia, refers to the sensation on movement, action, and location, which is mediated by proprioceptors with mechanosensory neurons in muscles, tendons, and joints [11] [13]. Both types of somatosensory impairments could exacerbate the motor impairments related to “learned-disuse” after stroke [8]. It was because that the tactile and proprioceptive impairments can make it difficult for a stroke person to safely

explore and interact with their environment, which would reduce their autonomy, independence, sociability, and quality of life [13]. Stroke survivors frequently reported pain and discomfort due to somatosensory impairment in the clinical assessments [13] [14]. According to previous studies on sensorimotor impairments, partial sensory recovery can form progressively and subconsciously during the spontaneous recovery after stroke even in the absence of dedicated sensory rehabilitation [13]. Recent studies on sensory rehabilitation after stroke suggested that specific sensory therapies could lead to higher improvements in both sensory and motor recovery [15]. Despite both motor and sensory impairments can limit the functional outcomes of treatment programs after stroke, sensory functions are often neglected in stroke rehabilitation that have a bias towards motor functions [11] [16]. Sensorimotor integration was known to be important in functional restoration after a stroke because voluntary motion, e.g., postural stabilization and motor dexterity, requires the precise coordination of multisensory and motor information. Many neuroimaging studies suggested that primary motor cortex (M1) participated in processing somatosensation [12] [8]. It was found that the M1 had both functional and anatomical connectivities to both primary and secondary somatosensory cortices (SI and SII), which coordinated to finish the sensorimotor tasks in daily life [17]. Researchers further found that stroke survivors with reduced cortical activation in sensory areas could experience poorer outcomes after rehabilitation [8] [18]. Therefore, it is crucial to develop an integrated evaluation and restoration on sensorimotor impairments after stroke.

1.1.3 Clinical assessments for sensorimotor impairments after stroke

Traditional clinical assessments with straightforward measures of behavioral changes after stroke have been widely accepted by therapists to evaluate the extent of sensorimotor impairments. Traditional assessments of motor function in upper limb

post-stroke rely on the clinical scores, such as the Fugl-Meyer Assessment Scale (FMA) [19], Functional Independence Measurement (FIM) [20], Modified Ashworth Score (MAS) [21], Action Research Arm Test (ARAT) [22]. Although it has been used for clinical and research purposes due to its straightforward to perform and interpret, these approaches are qualitative descriptions of motor performance regarding muscle strength, synergies, and tone, etc. [23]. Also, the scores could vary greatly across examiners. In other words, the traditional assessments are not objective enough in the descriptions of motor performance [24]. More importantly, these physical assessments are lack of neurophysiological detections to reflect the functional neuroplastic processes related to task performance, and thus have a ceiling effect in describing the motor impairments [25]. Due to the lack of sensitive behavioral measures in clinical examinations, subtle movement alteration caused by decreased motor precision, such as compensatory motion, postural instability, and hand dexterity, have proven particularly difficult to identify. The ARAT, for instance, places too much emphasis on task completion without adequate consideration to how the work is carried out, such as the excessive activities at elbow and wrist parts during hand clutching. Therefore, the objective and sensitive evaluation directly based on neural responses is needed for the evaluation of motor functions in stroke patients.

Sensory impairments are generally evaluated by the two-point discrimination and monofilament tests or measured as sub-scores in clinical assessments including Fugl-Meyer Sensory Scale [19], Nottingham Sensory Assessment (NSA) [26], Rivermead assessment of somatosensory (RASP) [27], performance Erasmus MC altered version of the NSA (Em-NSA) [28] and Quantitative sensory testing (QST) [13]. However, these assessment methods suffer from highly subjective and poor reliability without the neurological detections [13]. The reason is that the subjective nature of tactile sensation

makes these assessments difficult to be performed accurately. For example, in the two-point discrimination test described by Weber [29], the points of calipers are held by the examiner against the skin of patients at different distances from each other. The test determines the patient's ability to identify two close points in contact with skin, and how fine the ability is according to the distinguishable minimal distance. The pressure that the examiners apply to the finger to stimulate tactile sensation has a significant impact on the test outcomes, as does the patients' response and comprehension of small variations [11]. Therefore, the test results would be affected by patients' alertness, audition, ability to cooperate and comprehend. This means that many cognitive and neurological processes are involved in current tactile assessments, which further makes the results highly subjective. Hence, objective evaluation directly based on the neural responses are necessary and essential for both motor and tactile functions post-stroke.

1.2 Neuromuscular Networking Connectivity in Sensorimotor Impairments after Stroke

The restoration of sensory and motor functions after stroke highly depends on the neural reorganization in central-and-peripheral nerve systems on sensorimotor functions [30]. The neural reorganization in sensorimotor impairments could be indicated by altered neural connectivity among cortical areas (i.e., cortico-cortical connectivity), and that between the motor cortex and the muscle effectors (i.e., cortico-muscular connectivity) due to the relocation of the cortical center after the brain lesion [31]. Previous studies have reported that stroke survivors with better recovery after the treatment recruited other sensorimotor related cortical networks to compensate for the impaired motor cortex in the brain [31]. The neural reorganization in the motor-related areas was promoted along with improved motor performance after intensive physical practice with a task-oriented training of the affected lower limb [32]. Similar findings have also

been reported in the recovery of tactile sensation post-stroke [33]. Neural reorganization in the sensory-related areas was facilitated in the recovery of tactile functions post-stroke, where cortical connectivity was enhanced between somatosensory regions and distributed brain networks [34]. Hence, it is essential to understand the dynamics of neural reorganization regarding the impairments and recovery of sensory and motor functions after stroke, with the purpose of promoting the rehabilitation strategy planning for effective treatments.

1.2.1 Cortical connectivity in sensorimotor impairments after stroke

Functional connectivity (FC) can capture the dynamic cortical rearrangement in motor activities after a stroke, which shows how information interacts among cortical regions [35]. The neurophysiological foundation for the post-stroke FC analysis is that functional neuroplastic processes frequently occurs in many brain regions, which could reorganize remote and local areas in relation to the lesion site and would further lead to the cortical rearrangement and connectivity disturbance [36]. For example, Seitz et al. moved beyond the investigations of the localized cortical activation and conducted the first FC study on stroke patients to characterize the lesioned brain as an integrated and reorganized functional network, where the Positron emission tomography (PET)-based FC was analyzed at rest and during finger movement [3]. The results revealed the recovery-related networks spatially overlay the contralesional thalamus and occipital cortex, suggesting that remote network changes induced by focal lesion site could facilitate motor recovery. In recent years, the breakthrough using electroencephalography (EEG) or using functional magnetic resonance imaging (fMRI) in FC analysis provides the technical basis for a conceptualization of the brain reorganization after stroke motor impairments [31]. To clarify the network contribution of contralesional hemisphere to motor rehabilitation after stroke, Gerloff et al. utilized

EEG and transcranial magnetic stimulation (TMS) to compare EEG-based FC and TMS-induced motor evoked potentials (MEPs) in the stroke and unimpaired participants [37]. The results found enhanced cortical rearrangement in the premotor cortex than the primary sensorimotor and parietal cortex in contralesional hemisphere in stroke patients, suggesting that the increased contralesional activity in higher-order cortical regions probably facilitated the motor recovery process. In general, the FC analysis of the reduced motor function after stroke frequently shows a redistribution trend from the ipsilesional to the contralesional hemisphere. However, the cortical reconfiguration related to sensory abnormalities post-stroke is little understood in contrast to the intensively researched motor impairments. The cortical rearrangement in the perception of light touch still require research.

1.2.2 Cortico-muscular connectivity in sensorimotor impairments after stroke

In addition to the connectivity disturbance among cortical regions in the brain, neural reorganization post-stroke also leads to alterations in the connectivity between the sensorimotor cortex and effector muscles during the movement activity [38]. This kind of connectivity can be described by the cortico-muscular connectivity (CMC), which has been adopted to measure the neuroplastic processes in the cortical-muscular control process in acute, subacute, and chronic stroke patients [39]. The CMC in post-stroke sensorimotor impairments could be shaped by the dysfunction of the neural circuits between the brainstem and spinal cord, e.g,, over-active brainstem-to-muscle pathways after post-stroke disinhibition may contribute to uncoordinated muscle activities particularly for proximal limb and trunk muscles. For example, it was reported that the severity of motor impairment after stroke was correlated with the poorer integrity in ipsilesional corticospinal tracts and enhanced integrity in contralesional reticulospinal tracts. For the post-stroke muscular discoordination, the flexion synergy expression has

been found to be correlated with the deactivation in ipsilesional motor cortex and corticospinal pathways, the progressive recruitment of the contralesional cortex, and excessive activation of contralesional reticulospinal pathways.

The functional recovery of upper limb could be evaluated by the CMC analysis during the muscle movements [40]. For instance, Mima et al. investigated the CMC to evaluate the cortical control to the upper limb muscles in subcortical stroke patients during the tonic contraction by each individual muscle. The hand and forearm muscles, but not the biceps, were found to have considerably smaller CMCs on the paretic side, suggesting the difference between the cortical controls to different segments in the upper limb due to lesioned motor cortex [41]. Fang et al. revealed significantly smaller CMC for proximal upper limb in stroke than healthy controls during a reaching task with shoulder flexion and elbow extension [42]. Meng et al. used CMC analysis to investigate the conduction delay from the sensorimotor cortex to the distal upper limb, which found significantly extended conduction delay of the cortical control in the stroke-affected side compared to the stroke-unaffected side. Notably, the shifted motor-related area post-stroke was also localized by the most significant CMC in cortical areas, which provides additional information for the brain reorganization after stroke [43]. In summary, these studies demonstrated that the cessation of information transfer in the sensorimotor system post-stroke could be represented by the changes of CMC, suggesting the potential utility of CMC in uncovering the focalized motor-related area after brain reorganization post-stroke.

There are not only the descending motor pathways (the efferent pathways), but also the ascending somatosensory pathways (the afferent pathway) involved in the cortico-muscular connectivity [40]. Directional cortico-muscular coherence (dCMC) can reveal the motor commands from brain to muscle in descending pathways, and the sensory

feedbacks from muscle to brain in the ascending pathways within the close-loop sensorimotor control system [44]. For functional recovery following a stroke, the simultaneous neurodegeneration of the sensory and motor systems is essential [45]. Previous studies on directed cortico-muscular connectivity have found a higher strength of connectivity in both ascending and descending pathways in stroke patients than the unimpaired controls [46]. Recently, Bao et al. used the directional cortico-muscular interactions to investigate pathway-specific CMC in the neuromuscular electrical stimulation (NMES) assisted pedaling control after stroke. Results found that NMES could only modulate the sensory feedback in the ascending pathways, which indicated the potential utility of directional cortico-muscular connectivity in illuminating the motor recovery post-stroke [40]. Therefore, functional changes of dCMC were essential to be investigated to explain the pathway-specific changes in closed-loop sensorimotor control after stroke.

1.3 Sensorimotor Rehabilitation After Stroke

1.3.1 Efficient training standards for sensorimotor restoration

According to previous systematic reviews on randomized control trials and neuroimaging studies, basic principles for an effective rehabilitation [47], including 1) Early recuperation together with voluntary effort, 2) Rigorous practice with accurate repeats, and 3) Integrated sensorimotor rehabilitation, have been defined with the purpose of improving the functional independence in daily tasks after stroke, as follows:

1) Early recuperation together with voluntary effort

Substantial evidence has pointed out that effective stroke rehabilitation should be initiated as soon as possible after a stroke [47]. Effective motor restoration has been relied on the self-participation and voluntary efforts in motion practice after stroke [48].

The voluntary motor efforts (VME) in the neuromuscular network have been confirmed to be essential for improving the motor restoration in target muscles compared to training with continuous passive mode (CPM) [49]. Early physical training combined with VME can enhance the neuroplastic processes in central-and-peripheral nerve systems, improving the motor outcomes after the treatment [49].

2) Rigorous practice with accurate repeats

Although no particular intensity level was suggested for the rehabilitation training after stroke in formulated guidelines, repetitive motion practice with a high intensity would greatly benefit the efficient motor restoration in the paretic UE [50]. Meanwhile, substantial evidence through neuroimaging techniques, such as PET and fMRI, and TMS confirmed that a high intensity training with high repetition facilitated neuroplastic processes in cortical areas and corticospinal pathways [51].

3) Integrated sensorimotor rehabilitation

Somatosensory system was known to participate various motion tasks in activities of daily living [9]. Restoration of somatosensory functions were essential for effective motor recovery after stroke [11]. Better sensory function can lead to better motor outcomes for stroke survivors, while sensory deficits have been found to be significantly associated to decreased functional mobility and inhibited ADLs [12]. Effective sensory training has been found to improve the motor restoration in rehabilitation programs after stroke [13].

1.3.2 Conventional therapeutic interventions

Standard therapeutic intervention should be given once the symptoms were stabilized after stroke [47]. This typically occurs one to two days after the stroke, despite expecting to stay in the hospital for an extended period of time is unrealistic for stroke

patients at the sub-acute stage [47]. Due to resource constraints, such labor shortage and economic burdens, intensive therapeutic treatments are frequently not available to every stroke patients, even in developed countries [1]. Several conventional rehabilitation strategies have been applied to assist stroke patients regain basic sensorimotor functions for activities of daily living [47]. The Bobath method [52] and constraint-induced movement therapy (CIMT) [53] are the most frequently used strategies in clinics.

1) Constraint-induced motor therapy

Constraint-induced motor therapy is a physical therapeutic approach that has demonstrated significant success in the recovery of severely impaired UE [53]. It has also been demonstrated to be effective in restoring the "learned-disuse" after stroke [53]. The three main principles of CIMT are: (1) intensive, repetitive, structured training of the arm with the greatest impact; (2) immobilization of the arm with the least impact; and (3) application of a set of behavioral techniques to translate the benefits from the clinic into everyday life (thereby producing functional results) [53]. Clinical results on the effectiveness of this technique showed that CIMT intensity was strongly correlated with outcomes and that this was resource-intensive [54]. Additionally, the CIMT was found to be more suitable for stroke persons with moderate to severe impairments [54].

2) Bobath approach

The Bobath method, also referred to as neurodevelopmental treatment (NDT), is a manual therapy with widely application in stroke rehabilitation training [52]. This method seeks to improve motor relearning for an effective motor control in different tasks, contributing to task engagement and performance [52]. This therapy combines speech and language therapy, occupational therapy, and physical therapy [55]. It

focuses on improving the interaction with the world and surrounds in stroke survivors, engaging them in daily activities, and communicating about their needs in terms of all aspects of their lives, beyond the recovery training itself [52].

1.3.3 Rehabilitation Robots-Assisted Therapeutic Interventions

Rehabilitation robots has been developed to assist the rehabilitation training after stroke, with advantages of high intensity, high repeatability, and cost-effective [56]. According to the control strategies and the user's participation, there are three main types of rehabilitation robots currently with passive, active, and interactive training mode [57]. In passive-mode rehabilitation robots, continuous passive motion was provided to patients without requiring their active participation [57]. The improvement in patients trained by passive robots, however, is still minimal and cannot be sustained in a long-term since there is not enough sensory stimulation and no voluntary inputs from the patients [57]. In contrast, interactive-mode rehabilitation robots offer adaptive help based on the motor performance of the stroke patients [58]. Active-mode rehabilitation robots provide motion assistance based on the voluntary motor intention of the stroke survivors, although frustration and poor motivation could be caused if there is insufficient assistance [48]. A variety of robots have been developed for the UE rehabilitation, with specialized training needs and to assist particular joints [58]. Previous clinical trials have investigated the rehabilitation effectiveness of these robots [58]. In contrast to those with continuous passive motions (CPM), rehabilitation robots triggered by the active intention or efforts in the participant have demonstrated higher efficacy [48].

Closed-loop neurorehabilitation promoting the excitation in both efferent and afferent cortico-muscular pathways is the dominant force to drive functional neuroplastic processes in both central and peripheral nerve systems in post-stroke recovery [49]. It

was because that the voluntary motion requires both descending motor control and ascending sensory feedbacks for precise coordination between the motor and muti-sensory systems, particularly in the fine hand motions, e.g., hand dexterity and postural stabilization [59] [10]. Among the rehabilitation robots, voluntary movement-driven control and NMES (i.e., the motor-level NMES throughout this Chapter) sensorimotor feedback have been employed as key strategies for promoting closed-loop neurorehabilitation after stroke [60].

1.3.3.1 CMC-EMG-triggered control

Current rehabilitation robots mostly adopted the central-intention-triggered and peripheral-effort-triggered strategies for the voluntary movement-driven [49]. However, little has been done on an effective control design engaging the voluntary motor efforts from both central and peripheral nerve systems for the closed-loop neurorehabilitation in motion practice after stroke. The central-intention-triggered control mainly refers to the brain computer interface (BCI), where the user's movement intention was identified during motor imagery (MI) without the need for motor execution (ME) [60]. According to fMRI studies, MI and ME have similar brain activation patterns, e.g., activation of both contralateral sensorimotor and supplementary motor area (SMA) [61]. BCI-MI intervention has been found to be effective for those severely impaired persons, such as the spinal cord injury, since it can bypass any compromised peripheral neuromuscular circuits [62]. However, the efficacy of BCI-MI intervention has been questioned in stroke rehabilitation. For instance, in a previous randomized control trial on subacute stroke, a similar motor outcome was achieved in participants with BCI-MI intervention compared to those with passive motion once traditional forms of physical therapy were eliminated [60].

In peripheral-effort-triggered robots, electromyography (EMG) was frequently applied to represent the voluntary motor efforts in target muscles with residual motor abilities after stroke [48]. The EMG envelope could be proportional to the output force in a target muscle with robustness against the cancellation effects among disco-ordinated muscles and high signal-to-noise ratio in comparison with the kinetic/kinematic signals [48]. Nonetheless, robotic misdrive could be triggered by the involuntary EMG in muscular spasticity, which occurred in the passive contraction from compensatory motion in synergistic muscles or the releasing challenges following earlier contractions[63]. Despite neural sources of spasticity was largely unknown, the spasticity was not controlled by the brain, but rather associated with the over-activated upper motor neurons on the spinal cord which had origins from the brainstem after losing the cortical control in the efferent pathways [64]. Unexpected motor improvements in the proximal UE, e.g., shoulder and elbow, were commonly obtained after the rehabilitation program, despite only EMG recordings and motion assistance in the distal UE, e.g., hand and wrist joints, due to the motor compensation from proximal joints to distal joints in the UE [50]. Nonetheless, the post-stroke compensatory motion in traditional physical therapy or device assisted motion practice has been corrected by visual observation and manual operation, which was labor-demanding and inaccurate in the precise motions [65]. Therefore, the central-intention-triggered and peripheral-effort-triggered robots had limited effectiveness on the motor restoration in the target muscles, presenting a lack of the inhibition cortical and muscular compensation. Effective robotic control engaging the central-to-peripheral VME in motor practice was needed for the closed-loop neurorehabilitation after stroke.

The central and peripheral VME have been engaged separately in robotic control. Although a few hybrid BCI systems driven by both EEG and EMG signals were

proposed [66], there was a lack of significant improvements of efficacy in hybrid BCI systems after stroke compared to the EEG- and EMG-driven systems. The robotic misdriving could still occurred with the involuntary EMGs in MI and MA, due to the lack of central-to-peripheral VME in motion practice. The corticomuscular coherence has been adopted to extract the central-to-peripheral VME with the estimation of the spectral correlation between EEG and EMG. It could quantify the neural synchronization between the sensorimotor cortex and target muscles in voluntary movements [67]. For example, the attenuation and moved location regarding the peak CMC have been connected to the impairment levels of motor deficiency after stroke [68]. In our previous work, a CMC-EMG-triggered NMES-robot system employing CMC as an indicator of central-to-peripheral VME was developed to provide guidance and assistance for the extension and flexion in hand and wrist joints in stroke patients [49]. Our device could engage the central-to-peripheral VME in the user by the CMC-EMG-triggered control and provide sensorimotor feedbacks to the user by the NMES-robot. A pilot trial confirmed that our developed system could contribute to precise restoration on hand and wrist joints, showing inhibition on cortical and muscular compensation, and improvements of the central-to-peripheral VME among UE muscles [49]. However, little was know on its rehabilitation effectiveness for the closed-loop neurorehabilitaion in both descending and ascending pathways after stroke. This was mostly caused by a dearth of understanding on the contribution of NMES sensorimotor feedback to the precise hand-wrist rehabilitaiton in the CMC-EMG-triggered NMES-robot system.

1.3.3.2 Neuromuscular Electrical Stimulation

Neuromuscular electrical stimulation is an integrated sensorimotor technique with controllable stimulation intensities enabling the selective sensory (sensory-level NMES)

and motion (motor-level NMES) inputs to a target muscle by depolarizing the respective sensory and motor axons via electrical currents on the skin [69] [70]. Sensory-/motor-level NMES has been applied in stroke survivors with various impairment levels in both clinical and home-based settings for sensorimotor restoration, due to its advantages of noninvasiveness and low cost [69] [70]. Motor-level NMES, also known as the functional electrical stimulation (FES), has been integrated into rehabilitation robots, to provide sensorimotor feedbacks once detected voluntary motor efforts in stroke survivors. Previous neuroimaging studies reported that both efferent, i.e., descending, and afferent, ascending, pathways were activated by motor-level NMES. Motor units on target muscles was recruited in motor-level NMES not only by the direct activation of descending motor neurons, but also by the indirect activation of corticospinal tracts via the activation of ascending sensory neurons due to the cortical sensorimotor integration [69]. However, little was known on the rehabilitation effectiveness of motor-level NMES for the closed-loop neurorehabilitation after stroke. The primary cause of this was an absence of neurological assessments of the pathway-specific corticomuscular communication in motor-level NMES-assisted rehabilitation programs. Previous randomized control trials (RCT) mainly investigated the rehabilitation effectiveness of motor-level NMES from the peripheral level with traditional manual assessments [48] [60]. It was found that motor-level NMES could contribute to release spasticity, improve muscle weakness, and reduce compensatory motion related with “learned-disuse” after stroke [48]. For example, a recent meta-analysis on BCI-driven rehabilitation systems found that BCI-driven NMES systems achieved better motor outcomes in the UE after stroke than BCI-driven robots after the training [60]. Results found that the motor improvements indicated by the pooled effect

size was significantly higher in the BCI-driven NMES systems than the NMES alone and other intervention, without significant improvements in BCI-driven robots.

1.4 Objectives of the Study

1.4.1 Research Gaps

Neuromuscular networking connectivity including both cortico-cortical and cortico-muscular connectivity has been investigated in both sensory and motor impairments after stroke. However, sensorimotor evaluation has been conducted manually and verbally through the traditional clinical scores in stroke survivors, without direct neurological detection. Several research gaps exist, as below:

1) Lack of effective neurological evaluation on post-stroke fine tactile sensation

Fine tactile sensation participates in the motor initiation and planning in voluntary movements. However, without direct cortical detection, the conventional measurements of fine tactile deficits in clinical practice had limited reliability. In contrast to the substantially studied cortical rearrangement related with motor deficits, less was known on the cortical rearrangement in sensory deficits following stroke. Therefore, it is necessary to investigate the changes of FC and the networking structure among cortical areas in fine tactile sensation after stroke.

2) Lack of effective neurological assessments on fine motor control after stroke

Motor compensation from proximal UE to distal hand movements with impaired control precision is commonly observed after stroke. The closed-loop neuromuscular systems, involving both afferent (ascending) and efferent (descending) corticomuscular pathways, was recruited in the fine motor control. Maladaptive neuroplastic processes brought on by compensatory movements after a stroke has been mistaken for motor recovery in clinical settings because its contributions to task performance gains. In the

absence of sensitive behavioral measures, subtle compensation with impaired motor precision in target muscles have gone undetected. Therefore, it was essential to investigate the post-stroke pathway-specific corticomuscular communication in motor compensation from proximal UE to fine motor control of the distal fingers.

3) Lack of effective integrated sensorimotor evaluation after stroke

Sensory functions are often neglected in post-stroke clinical assessments that have a bias towards motor functions. Uncontrollable sensorimotor stimulation in the manual operation of traditional clinical assessments led to subjectiveness in the clinical assessments. On the other hand, recent neuroimaging studies via EEG conducted either sensory or motor evaluations separately. There is also a limited applicability to severely impaired persons in dCMC-based measurements on precise movement control. NMES is an integrated sensorimotor technique with controllable stimulation intensities enabling the selective sensory (sensory-level NMES) and motion (motor-level NMES) inputs to a target muscle. Therefore, it is necessary to investigate an integrated sensorimotor evaluation of cortical rearrangement after stroke by analyzing the cortical neuromodulatory effects of sensory-/motor-level NMES based on EEG signals.

4) Lack of effective assessment for the closed-loop neurorehabilitation of CMC-EMG-triggered NMES-robot after stroke

Closed-loop neurorehabilitation promoting the excitation in both efferent and afferent cortico-muscular pathways is the dominant force to drive functional neuroplastic processes in post-stroke central-and-peripheral nerve systems. In our previous work, a CMC-EMG-triggered NMES-robot system employing CMC as an indicator of central-to-peripheral VME was developed to provide guidance and assistance for hand-wrist practice after stroke. However, little was known on its rehabilitation effectiveness for

the closed-loop neurorehabilitation in both descending and ascending pathways after stroke. There was a lack of understanding on the contribution of NMES sensorimotor feedback to the precise motor restoration of hand and wrist joints in the developed system.

1.4.2 Research Objectives

The purpose of this project was to investigate the neuromuscular networking connectivity in fine tactile sensation, fine motor control, integrated sensorimotor evaluation, and the sensorimotor recovery after stroke.

The objectives of this study include:

1) To investigate the functional connectivity among cortical areas in fine tactile sensation after stroke.

2) To investigate the pathway-specific corticomuscular connectivity in post-stroke compensation from the proximal upper limb to the fine control of distal fingers movements.

3) To investigate the integrated sensorimotor evaluation of cortical rearrangement in sensory-/motor-level NMES after stroke.

4) To investigate the closed-loop neurorehabilitation effects of CMC-EMG-triggered NMES-robot in hand and wrist joints after stroke.

CHAPTER 2

IMPAIRMENTS OF FUNCTIONAL CONNECTIVITY AMONG CORTICAL AREAS IN FINE TACTILE SENSATION AFTER STROKE

2.1 Introduction

Fine tactile sensation participates in voluntary motor activities after stroke. The sensation information was adopted in motor planning and correction to the desired targets for precise motor control [11] [12] [13]. However, its neuronal dynamics in the impairments and recovery were poorly understood, because of the overlooked sensory function in stroke rehabilitation. Due to the lack of a direct neurological evaluation, typical clinical assessments for the fine tactile sensation are unreliable and inconsistent [11]. In the two-point discrimination test, the test reliability was easily affected by the examiner's force applied to the fingertips, i.e., varied stimulation pressure, when the tactile stimulation was generated. Meanwhile, the post-stroke cognitive impairments could influence the discriminative levels with respective to subtle differences among stimulation [11]. Additionally, the neuroplastic process is a common occurrence in many different areas of the brain, including remote and local regions from the lesion site following a stroke. This cortical rearrangement could further disrupt cortical connectivity, as suggested in studies on motor impairments after stroke [36] [31]. When stroke patients performed motor or cognitive tasks, a redistribution pattern was frequently found from the lesional to the non-lesional side of the brain [71] [72]. The neuroplastic processes related to post-stroke sensory abnormalities were little understood, in contrast to the intensively researched motor impairments. This was due

to the lack of knowledge on the cortical rearrangement mechanisms in the context of fine tactile sensation.

Functional connectivity (FC) in the post-stroke sensory impairments has been investigated through neuroimaging techniques of the resting-state functional magnetic resonance imaging (rsfMRI) for the purpose of identifying the altered cortical rearrangement patterns [34] [33]. For example, the FC in rsfMRI was adopted to investigate its correlation with the restoration of tactile sensibility after a stroke. The findings showed that throughout the first six months following a stroke, the resting-state FC among somatosensory regions and the visual and attentional areas could attribute to the enhanced tactile sensation functions [34]. Additionally, Goodin et al. employed rsfMRI to examine how different hemispheric lesion sites affected the functional connectivity of touch sensibility in stroke patients. [33]. In comparison to stroke participants with lesions in left hemisphere and unimpaired participants, stronger FC was observed over the ipsilesional primary somatosensory cortex (S1) and inferior parietal regions in post-stroke individuals with left hemiplegia. These investigations, however, only identified changes in resting-state brain networks in stroke survivors, due to the relative low time resolution of fMRI. Because the sensitivity of sensory receptors gradually was altered in response to a steady stimulus for sensory adaptation, fMRI is insufficient for the identification of cortical processes in transient tactile stimulation. [73]. The results on resting-state FC related to tactile deficits following a stroke could be insufficient to explain the mechanisms underlying the FC alteration in tactile sensation, which involved a dynamic neural process [74].

EEG provides a higher time resolution than fMRI and has been applied to capture the transient neural firing patterns in task states [75] [76]. The EEG-based FC can, therefore, capture the neural communication among cortical areas. It has been used to measure

the brain connectivity changes during cognitive and motor tasks after stroke [77] [78] [37]. For example, the EEG-based FC in chronic stroke participants was contrasted with unimpaired participants during a 25% maximum handgrip task [78]. The findings showed that the post-stroke sensorimotor area had stronger FC connecting with the ipsilesional supplementary motor area (SMA) compared to the unimpaired individuals, suggesting that there was dynamical compensation for the stroke-related brain lesion. The post-stroke cortical rearrangement during a fast finger extension task has also been examined using the EEG-based FC. It revealed higher intensity of FC over motor area connecting the SMA within the contralesional hemisphere after stroke than that of unimpaired controls [37]. Even though the EEG-based FC was successfully investigated for motor-related neuroplastic processes after stroke, the tactile sensation related neuroplastic processes after stroke has not been investigated yet.

The graph theory-based technique can illustrate the change in cortical connections in its functional networking structure [79] [80]. In this regard, EEG channels on various cortical sites was identified as nodes and their FCs were identified as linkages in the topological representation [81]. The graph theory analysis was used to highlight the alterations of brain networking structures caused by stroke, ranging from local (such as a single brain area) to global (such as the entire brain) [35]. It has been applied to examine the dynamic information integration and brain interactions in post-stroke motor or cognitive activities [82], e.g., the functional brain organization in stroke patients while they were tapping their fingers. The researchers found ineffective brain networks in stroke patients who were less able to transfer and reorganize information either from distant brain areas or within a local area compared to the unimpaired [35]. Furthermore, motor outcomes assessed by the clinical assessments of FMA was correlated to the decrease of graph theoretical features, including the global and local

efficiency and the interhemispheric connection density after a 3-month rehabilitation program in the chronic stroke [83]. To comprehend the functional brain structure in relation to the sensory-related Cortical rearrangement, however, little has been done on post-stroke fine tactile impairments using the EEG-based graph theoretical approach.

This study used functional connectivity analysis derived from EEG to examine how brain connectivity changed after stroke during the fine tactile sensation induced by the textile fabrics. We hypothesized that the post-stroke FC changes in fine tactile impairments could present cortical compensation from the ipsilesional hemisphere and distributed visual and attention networks. The whole-brain 64-channels EEG was recorded in both stroke (n=8) and unimpaired participants (n=8), prior to and following the contact of the forearm with a piece of cotton cloth. The EEG coherence approach was then used to analyze functional connectivity [84]. The fabric stimulation induced functional connectivity (SFC) was further measured through a non-parametric statistical test regarding the FCs [85]. The graph theory-based approach was used to evaluate the networking brain structure in post-stroke fine tactile sensation.

2.2 Methods

2.2.1 Subject recruitment

This study was approved from the Human Subjects Ethics Subcommittee of Hong Kong Polytechnic University. The stroke participants to be recruited should satisfy the inclusion criteria, as follows: (1) >6 months of stroke onset with subcortical unilateral brain lesion; (2) No deficits in vision, cognition, or attention (Mini-Mental State Examination (MMSE) score >21) [86]; (3) Mild-to-moderate spasticity at the finger, wrist and elbow joints, MAS<3 [21]; (4) No any other types of neurological deficits except stroke; (5) Moderate sensory deficits with the light touch=1 in the Fugl-Meyer

Assessment (FMA) sensation sub-score. The control participants should meet the criteria of right-handed and no somatosensory impairments or any other neurological or psychiatric disorders. Finally, we recruited a total of 16 participants with equal numbers of stroke and unimpaired participants (age-matched, $p = 0.56$, independent t-test). The participants' demographic data and the stroke participants' clinical scores are summarized in Tables 2-1 and 2-2, respectively. All participants in both groups were aware of the experiment purpose. All of them provided signed the written consents. In this study, all stroke participants had a stroke onset of more than 10 years at the very chronic stage. Because of the "learned nonuse" in affected UE and the daily compensation in unaffected UE, in the stroke-affected side was defined as non-dominant side, and the unaffected side was defined as the dominant side [87].

2.2.2 EEG recordings in fine tactile sensation

A relative humidity of 60%±5% and a temperature between 18 ˚C and 20 ˚C comprised the conditions within the quiet room in which the experiment took place. The participants were asked to place their upper limbs on a soft cushion after they seated. The experimental setup is showed in Figure 2-1a. Subsequently, in line with the standard international 10–20 system, the 64-channel EEG cap (BP-01830, Brain Products Inc.) was worn onto the subject for whole-brain signal recording. Every electrode was prepped below 5 kΩ in terms of impedance. Ear plugs and eye masks were provided to the participants to minimize any audio and visual interference. The participants were required to avert active mental tasks, falling asleep, and motion throughout EEG recordings, to ensure the tactile sensation as the only exogenous attentional input to the participant.

The fabric that comes into direct contact with the skin possesses the properties of 40x20cm in size, a weight of 127.7±0.8 g/m2, 100% cotton, 0.39±0.01mm thickness,

and plain woven which, in turn provokes fine tactile stimulation [88]. It was found that cortical sensory responses could be induced in reaction to the surface texture and moderately light material of the textile fabric, thus making it an appropriate material for the experiment [89]. The widespread conception of pure cotton as comfortable and among the most widely available and utilized textile fabrics in day-to-day life led to its selection [90]. The cotton fabric was statically loaded onto the inner forearm for 13 s to induce the fine tactile stimulation [88]. The inner forearm was selected because of the richness of C-tactile (CT) afferents for light touch sensation, which was also commonly used for used for the fabric stimulation [91].

The timeline and stimulation protocol are demonstrated in Figure 2-1b. Three trials of fabric stimulation on the left and right forearms were conducted in a random order with simultaneous EEG recordings in every participant. A fabric stimulus consisting of 13 seconds each and a baseline test consisting of 30 seconds each made up the format of each individual trial. A period of 30 seconds void of stimulation where the participant sits quietly comprises the baseline test. Fine tactile sensation was attained by slightly loading the fabric sample onto the inner forearm and sustaining for 13 seconds, per the fabric stimulus. The two groups experienced equivalent experimental protocol.

EEG signals were recorded concurrently throughout the experiment (sampling frequency: 1000 Hz). These signals were depurated again to eliminate artifacts linked to potential ocular movements via independent component analysis (ICA) [92], re-referenced in line with the mean of all electrodes, and pre-processed offline through a band-pass filter ranging between 1 Hz to 45 Hz following the recordings. Each segment influenced by artifacts was excluded by conducting a visual inspection. Consistent data length and the constancy of the signals were facilitated by maintaining the period in which the transient sensory adaptation principally took place, namely, the initial 12

seconds of data without artifacts from the onset in each of the experimental conditions—baseline or fabric stimulation. Subsequently, the additional division into trials of 4 seconds occurred within the EEG signals without reference and the ground and possessing 62-channels each. Each of the subject groups had 288 trials ($N = N_{\text{experimental condition}} \times N_{trial} \times N_{forearm} \times N_{subject}$, where $N_{\text{experimental condition}} = 2$, i.e., the conditions of fabric stimulation and baseline period, $N_{trial} = 9$, $N_{forearm} = 2$, $N_{subject} = 8$) produced for them. For individuals with right hemiplegia, their EEG electrode positions were reversed across the mid-sagittal plane. This enabled the elevation of the statistical power as demonstrated in practice with stroke patients as well as the execution of group analysis on the eight stroke subjects.

2.2.3 Functional connectivity estimation

The cortical information communication was illustrated by functional connectivity (FC). In line with the calculations of prior motor functional research, the imaginary coherence (ImCoh) was used to calculated FC in the whole brain [84]. The ImCoh can reach a value of zero as there is a time lag of 0 between signals when common mode noise occurred, thereby enabling the suppression of the false connectivity provoked by volume conduction. This approach generated weighted values (0-1) on each frequency, where the higher the ImCoh values, the stronger the FC at a frequency. The ImCoh is the imaginary part of coherency, C_{ij}, which is the normalization form of the cross-spectrum of EEG i and j :

$$C_{ij} = \frac{S_{ij}(f)}{(S_{ii}(f)S_{jj}(f))^{1/2}} \tag{2-1}$$

The complex Fourier transforms of the terms $\hat{x_j}(f)$ and $\hat{x}_i(f)$ are represented as $x_j(f)$ and $x_i(f)$, respectively. The expectation value, the complex conjugate, and the cross-

spectrum between signals are denoted by $< >$, *, and $S_{ij}(f) =< x_i(f)x_j^*(f) >$, respectively. A 0.5-Hz frequency resolution was adopted by partitioning the EEG into 2-s overlapping segments in every calculation. Then, the fabric stimulation-induced FC was extracted from the FCs in fabric stimulation trials against those in baseline trials.

The EEG frequency band linked to tactile sensation was determined to be the beta band, i.e., 15–30 Hz, that was implemented for FC estimation [88, 93]. The ImCoh spectra is demonstrated in Figure 2-1c. The peak ImCoh in fabric stimulation exhibited a statistical distinction with the baseline in both groups (P<0.05, pared t-test). Further analyses would be implemented in three sub-bands in the beta—beta 1 ranging between 15–19 Hz, beta 2 ranging between 20–25 Hz, and beta 3 ranging between 26–30 Hz—in line with the waveform of the ImCoh spectra.

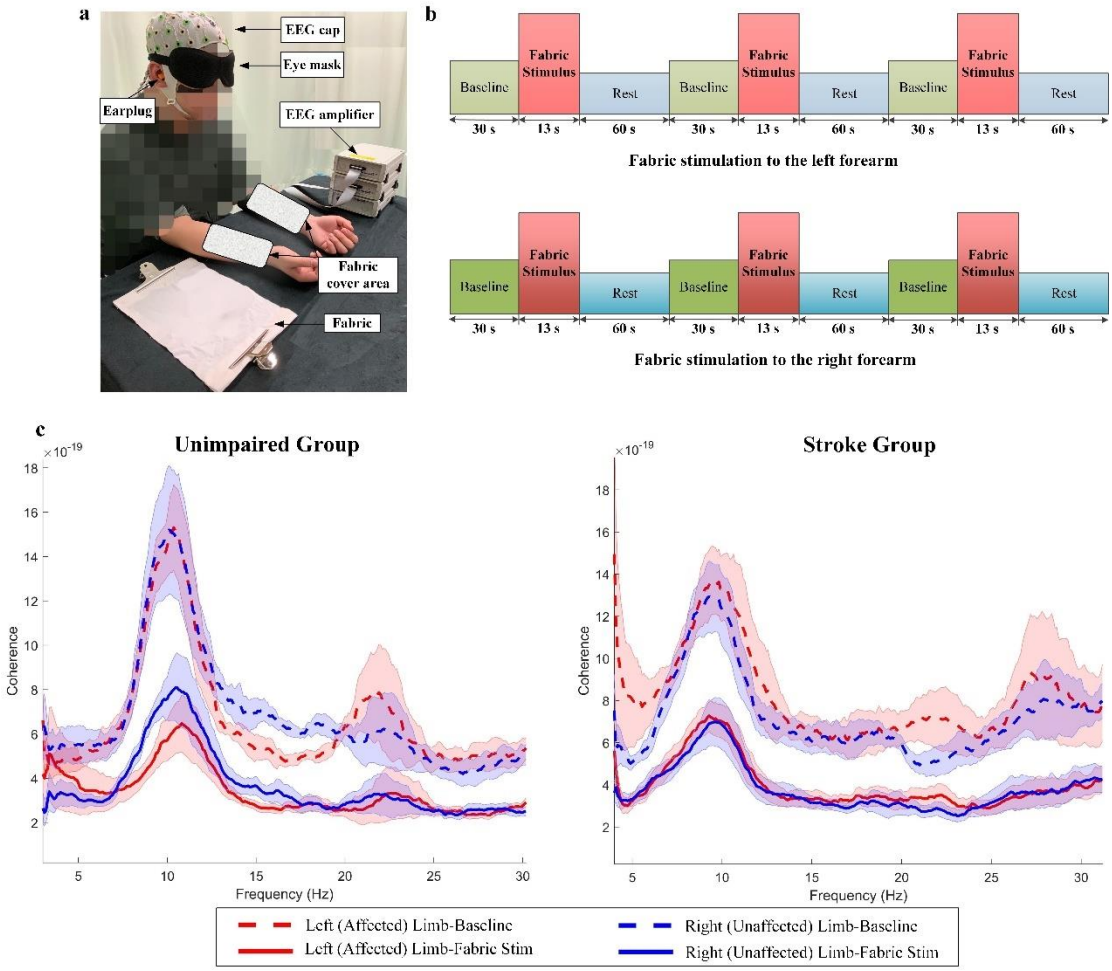

Figure 2-1. Experimental setup (A) and Experimental protocol (B); (C) Averaged ImCoh spectra in both groups.

2.2.4 Fabric stimulation induced functional connectivity

The SFC was attained via the cluster-based permutation test based on the pair-wise comparison on the FCs [85]. A significance level of 0.05 was adopted to identify the significant FC (Sig-FC) in fabric stimulation against the baseline [85]. As demonstrated in Figure 2-2, the permutation test and the computation of cluster-level statistics comprised the two main parts of the cluster-derived permutation test.

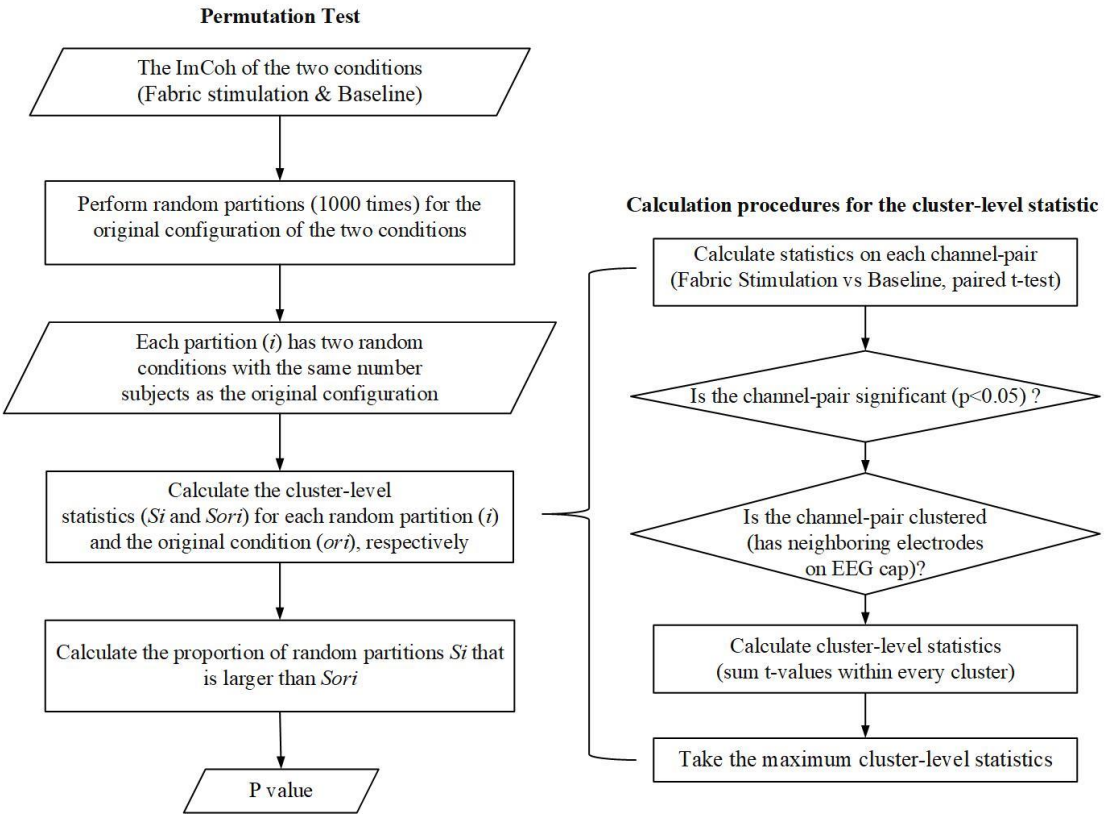

Figure 2-2. Flow chart presenting the computing processes of the cluster-derived permutation test.

2.2.5 Networking brain structure

Based on the graph theory, the networking brain structures at different scales in the fine tactile sensation were analyzed using all Sig-FCs [94], as practiced in studies on post-

stroke motor functions [95]. The estimation processes of the networking brain structure with 10 EEG channels are illustrated in Figure 2-3. To preserve the significant FCs against the baseline, a statistical comparison regarding the fabric stimulation FCs against baseline FCs was first carried out (paired t-test with multiple comparison correction of false discovery rate (FDR), P<0.05). The Sig-FCs and FCs without significance were encoded using an adjacency matrix with binary values of 1 and 0, respectively. In this study, the whole-brain 62-EEG channels were used to build the networking brain structure, after discarding the ground and reference channels. Based on the networking brain structure, the topological features were determined at large, intermediate, and small scales [35].

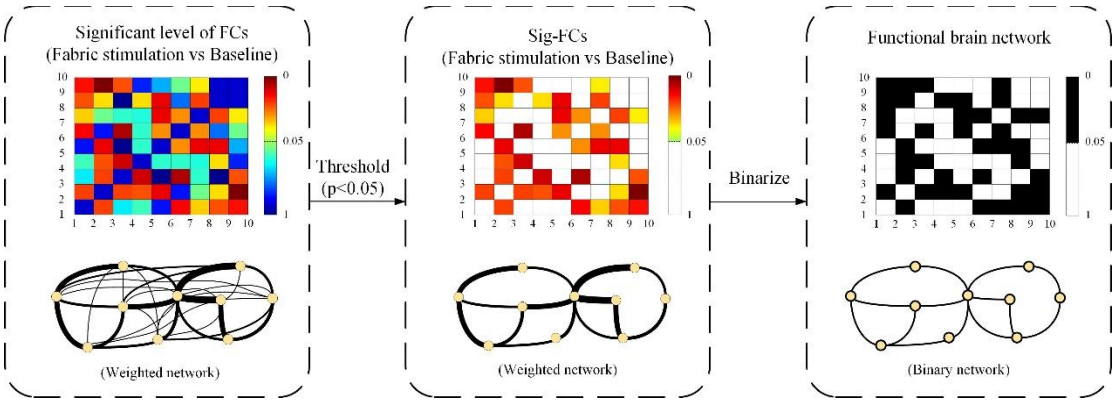

Figure 2-3. Estimation of the networking brain structure. For presentation purposes, the brain network possessing 10 EEG channels was utilized.

To measure the global features of the networking brain structure, smallworldness (SW), local efficiency (E_{loc}), and global efficiency (E_{glo}) were utilised as the three large-scale features that also served to depict efficacious whole-brain communication in reaction to fine tactile sensation. The hemispheric-level information transfer was assessed via the intermediate-scale features. By measuring the density of FC within and between the right (Rhemi) and left (Lhemi) hemispheres, or the unaffected (Uhemi) and affected

(Ahemi) after stroke, the networking brain structure at the intermediate-scale was investigated utilizing the features of intradensity K_{intra} and interdensity K_{inter} [94]. In reaction to fabric stimulation, the involvement of local brain regions is ascertained via the implementation of small-scale features. The centrality of nodes in relation to the links within and between the two hemispheres is represented by the intradegree D_{intra} and interdegree D_{inter} respectively, which was extracted on each EEG channel and embodied the local characteristics of the networking brain structure.

Upon the fabric stimulation being implemented to the distinct forearms, a statistical comparison was undertaken between the corresponding D_{intra} and D_{inter} values where the small-scale features computed in equations 7 and 8 served as the basis. Through the use of the unaffected limb as a baseline, SFC asymmetry within brain regions in the stroke-affected limb could be portrayed via such a comparison. An equivalent method was used utilising the right limb as a baseline in the unimpaired subject group [71] [35]. The statistical comparison between each group regarding the fabric stimulation of the two forearms was carried out via the implementation of the paired t-test ($P<0.05$) following the Shapiro-Wilk test ($P>0.05$) to confirm standard distribution [96]. Several comparison corrections were enabled via the application on all nodes of the FDR correction ($P<0.05$). Then, the topography of each group facilitated the visualization on each node of the substantial variances between the stimulation enacted on the two forearms.

2.2.6 Statistical comparison on brain networks

The global efficiency (E_{glo}), local efficiency (E_{loc}), smallworldness (SW), interdensity K_{inter} and intradensity K_{intra}, were confirmed to have the normal distribution ($P>0.05$) through the Shapiro-Wilk test of normality. The variances between the fabric

stimulation to the unaffected limb (Ulimb) and the affected limb (Alimb) in the stroke group regarding each brain network index are compared via the paired t-test ($P<0.05$). Additionally, stimulation to the right limb (Rlimb) and the left limb (Llimb) was compared in the unimpaired group alongside the networking features in this area through the implementation of the paired t-test. The statistical significance in this study was the $P<0.05$. The SPSS version 20 (SPSS, Chicago, IL) was adopted for the execution of all statistical analyses in this study.

2.3 Results

2.3.1 SFC topographic changes after stroke

SFC topographies in both groups are shown in Figure 2-4. The greatest alteration was observed in the S1 area and the contralateral sensorimotor region was usually covered by the SFC in the unimpaired participants. The ipsilateral hemisphere displayed narrower distribution over the contralateral hemisphere which, in turn, characterized the distribution of SFC upon the implementation of stimulation to the left forearm, as demonstrated in Figure 2-4a. The ipsilateral increase was observed on the ipsilateral side while contralateral decrease occurred on the contralateral side, signifying an elevation and drop in the intensity of SFC, respectively. Two FC clusters situated within C1 and C2 were displayed by the SFC with respect to the distribution. Partial coverage was observed in the parietal (P6), frontal (F8), and temporal (TP8, T8, FT8, FT10) lobes while S1 (CP2, CP4, CP6, FC6, C4, C6) comprised the focus of coverage. Only one of the 14 channels on the SFC topography was not a contralateral channel, thereby producing a 92% hemispheric lateralization degree. The average SFCs intensity in the ipsilateral brain was +8.88 while the average SFCs intensity in the contralateral brain was -29.

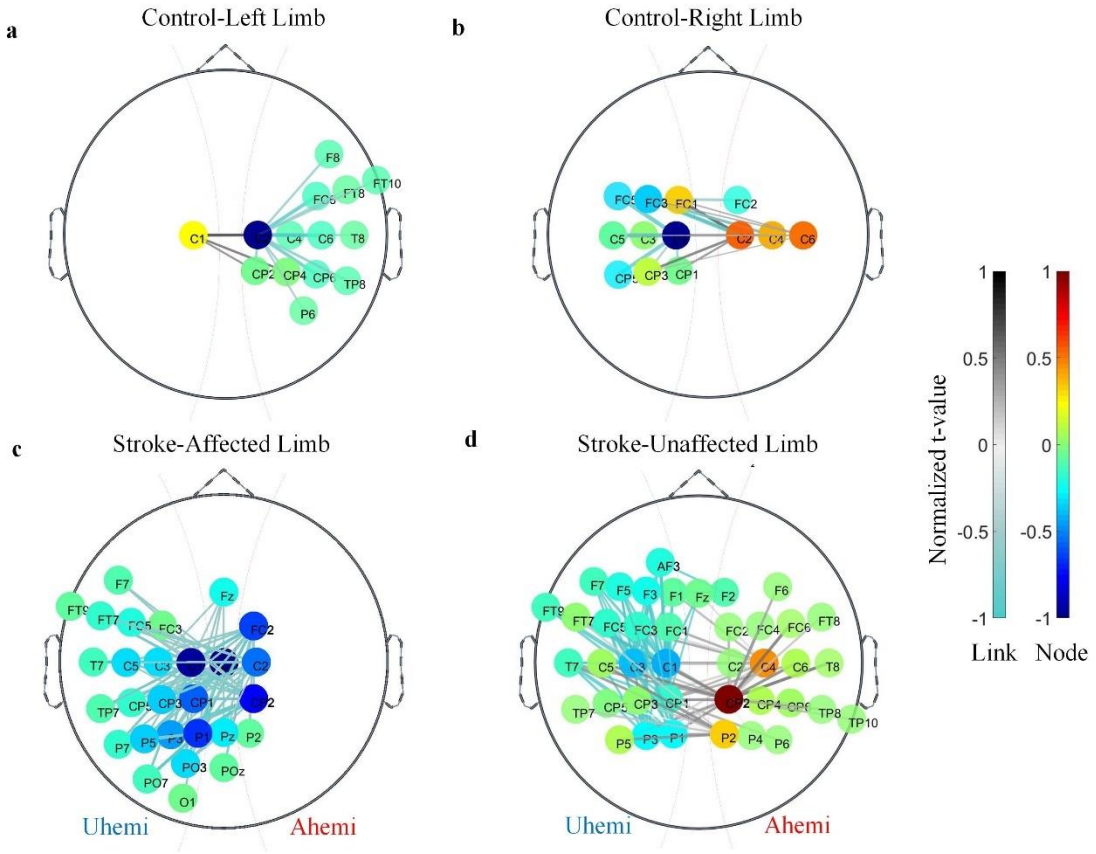

Figure 2-4. The SFC topography when implementing fabric stimulation to both groups. The stroke-affected and -unaffected limbs denoted the respective left and right limbs. Uhemi and Ahemi denoted the respective unaffected and affected hemispheres.

As aforementioned, the SFCs possessed a narrower area in the ipsilateral than the contralateral hemisphere reflecting the specular comportment of hemispheric lateralization within the SFC pattern noted upon stimulating the left forearm. Similarly, a contralateral reduction and an ipsilateral rise were displayed in the average SFC intensity in both hemispheres upon simulating the right forearm, as shown in Figure 2-4b. Partial distribution in the central-parietal areas was observed in CP5 while comprehensive distribution focused upon the S1 region (CP1, CP3, FC1, FC2, FC5, C3, C4, C5) and the central cortical region (FC3, C1, C2, C6) via the five clusters of SFCs. Of the 13 channels on the topography, nine of them were contralateral channels leading

to a 69% hemispheric lateralization degree. The average SFCs intensity for the respective ipsilateral and contralateral channels was +21.64 and -1.84.

In reaction to the fabric stimulation, the SFC topography structure was more amalgamated in the stroke group comparing with the unimpaired group. The average intensity of the SFC changed and a greater number of brain areas were active in the two hemispheres upon the implementation of stimulation to the stroke-affected forearm, contrasting with the hemispheric lateralization displayed in the unimpaired participants, as portrayed in Figure 2-4c. The occipital (O1), temporal (TP7, T7), frontal (FT7, FT9, F7, Fz), and parietal (POz, PO7, P5, P7) regions were partially covered while the majority of the somatosensory (Pz, Cz, P1–P3, C1–C3, CP1¬–CP3, C5, PO3, FC2, FC3, FC5, CP5) region was covered by the nine clusters of connections possessed by the SFC in relation to distribution. In 28 out of 62 channels, four of them were contralateral channels leading to a 14% hemispheric lateralization degree. The average SFCs intensity of the ipsilateral channels was -211.55 and the average SFCs intensity of contralateral channels was -14.46.

The control group displayed fewer active brain areas and stronger hemispheric lateralization regarding the SFC distribution in comparison with the stimulation to either limb in post-stroke individuals, as demonstrated in Figure 2-4d. Nonetheless, both groups demonstrated a contralateral reduction and an ipsilateral increase reflected by the average SFC intensity within both hemispheres. The controls displayed a narrower coverage in comparison to the stroke group where the parietal (P5, P6), frontal (FT7–FT9, Fz, F1–F3, AF3, F5–F7), sensorimotor (P1–P4, FC1–FC6, C1–C6, CP1¬–CP6), and temporal (TP10, TP7, TP8, T7, T8) regions are covered by the 10 clusters of connections possessed by the SFC. Of the 40 channels on the SFC topography, 21 are contralateral channels leading to a 53% hemispheric lateralization degree. The average

SFC intensity of the ipsilateral channels was +54.20 and the same parameter of the contralateral channels was -52.35.

2.3.2 Brain networking properties after stroke

2.3.2.1 Large-scale properties

As illustrated in Figures 2-5a–c, the networking brain structure at the large scale, represented by E_{loc}, E_{glo}, and SW, was compared regarding the fabric stimulation to distinct limbs within each group. As seen in Figure 2-5a, there was small-world characteristics ($SW > 1$) during the stimulation to both limbs in both groups. No significant SW change was observed regarding the different limbs after stroke. There was significant rise regarding local efficiency E_{loc} and global efficiency E_{glo} in the affected limb in comparison to the unaffected limb after stroke (paired t-test; E_{loc}: P= 0.009, effective size (EF)=0.54; E_{glo}: P= 0.006, EF=0.56). Moreover, no significant differences regarding the large-scale features were observed between the limbs in unimpaired participants.

2.3.2.2 Intermediate-scale properties

As seen in Figure 2-5d e and f, the intermediate-scale networking brain structure, represented by the density of intra- (K_{inter}) and the density of inter-hemispheric (K_{inter}) FC, was compared between distinct limbs in each group. In comparison to the unaffected limb, the post-stroke affected limb demonstrated a significant higher interdensity K_{inter} (EF=0.375, P = 0.038, paired t-test). Conversely, the interdensity K_{inter} demonstrated no significant difference between limbs in unimpaired participants (paired t-test, P>0.05). For the intradensity K_{intra}, no significant variance in either hemisphere was found between the different limbs after stroke (paired t-test, P>0.05). In the controls, the contralateral hemisphere demonstrated a significant higher K_{intra}

during the fabric stimulation to the Rlimb (or Llimb) than the Llimb (or Rlimb) (paired t-test, Lhemi: P= 0.006, EF= 0.81; Rhemi: P=0.002, EF=0.63).

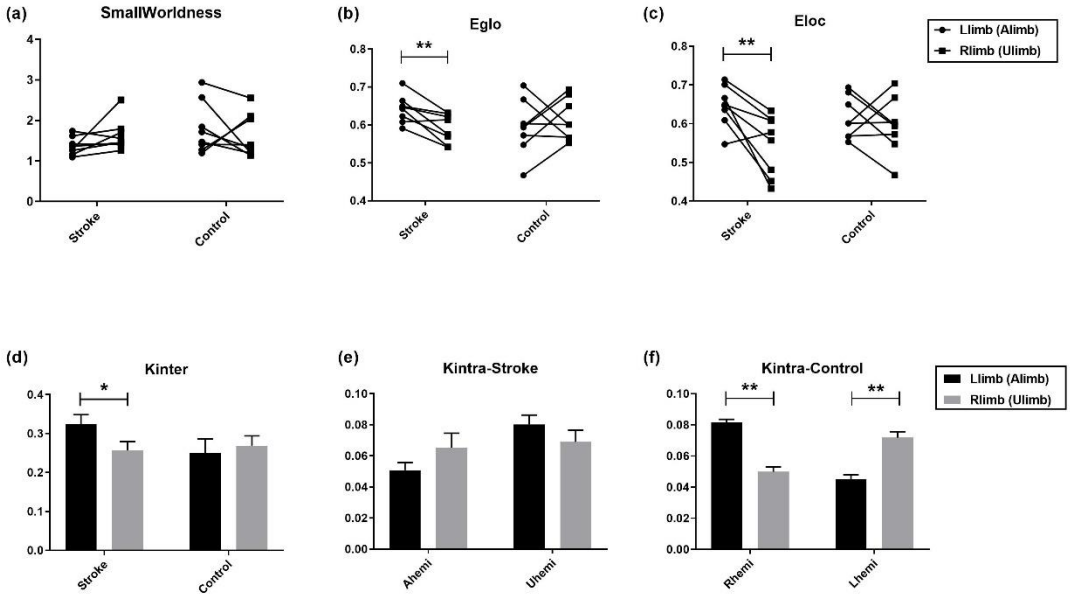

Figure 2-5. Networking brain structure measured at large and intermediate scales in both groups. The error bar denoted standard deviations.

2.3.2.3 Small-scale properties

Regarding the stroke group, as shown in Figure 2-6a, solely the ipsilesional somatosensory region displayed significant variance in terms of the interdegree D_{inter} between the different limbs (P<0.05, paired t-test with FDR correction,). The stroke-affected forearm demonstrated significantly lower interdegree D_{inter} in P2 but significantly higher interdegree D_{inter} in CP2, C2, and FC2 in comparison to the unaffected forearm during the fabric stimulation (P<0.05, 0.29<EF<0.50). Moreover, solely the ipsilesional S1 region (CP2, C4) demonstrated significant variance in terms of the intradegree D_{intra}, when the affected forearm being stimulated, compared to the unaffected forearm during the stimulation (P<0.05; C4: EF=0.36, C6: EF=0.29).

Regarding the unimpaired participants, significant changes in intradegree D_{intra} and interdegree D_{inter} presented symmetric distribution over the two hemispheres when comparing the between fabric stimulation to different forearms, as shown in Figure 2-6b (paired t-test with FDR correction, P<0.05). The left forearm during the stimulation demonstrated significant lower interdegree D_{inter} in FC1, FC3, CP1, CP3, and C2 but significant higher interdegree D_{inter} in CP2, CP4, and CP1 (P<0.05, 0.21<EF<0.29), compared to the right limb during the stimulation. Moreover, significant lower intradegree D_{intra} was observed in the somatosensory regions (P7, CP3, C1, C3, C5, FC3), but significant higher intradegree D_{intra} was found in the parietal (P8) and somatosensory (CP6, CP4, C2, C6) areas in the opposite hemisphere during the stimulation to the left forearm in comparison to the right forearm (P<0.05, 0.14<EF<0.36).

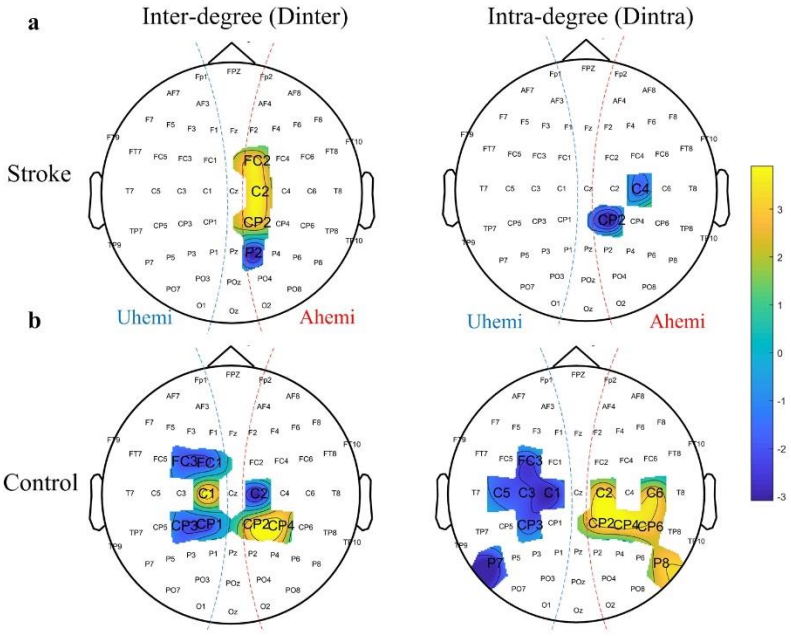

Figure 2-6. Statistical comparison on the small-scale networking brain structure between both forearms within each group. T-values in the statistical comparison were denoted by the color scheme.

2.4 Discussion

The cortical responses in tactile sensation induced by a piece of cotton fabric in chronic stroke patients and unimpaired controls were examined by analyzing the EEG-based FC and the networking structure in the brain. In results, increased local and global efficiencies and interhemispheric connectivity, additional involvements of neighboring brain areas, and altered hemispheric lateralization in the networking brain structure characterized the cortical rearrangement in response to fine tactile stimulation following a stroke.

2.4.1 Post-stroke Alteration of Hemispheric Lateralization

For the hemispheric lateralization degree, as shown in Figure 2-4, the control participants attained values of 69% and 92% for the Rlimb and Llimb stimulation respectively, while the stroke group attained values of 53% and 14% for the unaffected forearm and affected forearm respectively following fabric stimulation in the SFC topography. The changes in the SFC intensity post-stroke were consistent with the altered hemispheric lateralisation in SFC re-distribution. Specifically, the contralateral reduction and ipsilateral elevation were observed when implementing the stimulation on the unaffected limb and both limbs in the controls, while both hemispheres experienced decreased intensities of SFC when implementing the stimulation to the stroke-affected limb. These SFC topologies suggested a reorganized brain structure from the lesional to non-lesional side when implementing the fabric stimulation to the affected forearm after stroke. In line with prior works regarding motor functions [97], the neural regeneration and plasticity working upon the intact contralesional hemisphere could generate the compensatory effect to the ipsilesional hemisphere in the tactile sensation after stroke. The establishment of new synapses with denervated neurons and the germination of new collaterals by surviving axons proximal to

denervated areas could be catalysed by stroke-induced damaged neurons [98]. The neuron regeneration occurred at distinct brain areas that had prior anatomical connectivity with the damaged area [99]. The moulding of neuroplastic processes following a stroke and compensatory motions linked to motor impairments are facilitated in large part by the contralesional cortex, as per multiple prior works. Following stroke-induced sensory impairments, the contralesional hemisphere could enact equivalent compensatory effects [97]. These findings demonstrated that the tactile impairments in the sensorimotor rehabilitation could be ascertained via the SFC analysis in this work.

As demonstrated in Figures 2-6 and 2-5e–f, the intradegree D_{intra} and the intradensity K_{intra} validated the redistributed SFC pattern following a stroke in the changed functional structure of the cortical connectivity. As Figures 2-6b and 2-5f portray, the somatosensory area was the prime location for the increased contribution to tactile sensation in the contralateral limb in comparison to the ipsilateral limb in the unimpaired group, implying hemispheric lateralisation. In the control subjects, the fine tactile stimulation to the left and right limbs occurring in the somatosensory area was indicative of SFC symmetry. Deactivation in ipsilateral S1 and overactivation in the contralateral S1 area were induced by the right median nerve stimulation or distinct sensory stimuli on the right hand, such as coolness, pressure, vibrotactile, and warmth, per prior fMRI results [100] [101] [102]. The EEG patterns in the process of transient sensory stimulation in the unimpaired group demonstrated similar cortical activation patterns to those in fMRI.

As shown in Figures 2-6a and 2-5e, the stimulation of the affected forearm in comparison to the unaffected forearm stimulation demonstrated significantly reduced FC within the ipsilesional S1 area which, in turn, confirmed the altered hemispheric

lateralisation despite no significant changes in the hemispheric scale of the stroke group. The deactivated ipsilesional S1 area within the reorganised brain following a stroke could be linked to the asymmetric SFC pattern, per these findings [33]. The transient sensory stimulation provoked the deactivated ipsilesional S1 after stroke, in comparison with unimpaired participants, demonstrating heightened intra-hemispheric FC in ipsilesional S1 as assessed by fMRI. Moreover, when a sponge was used to stimulate the skin, the unimpaired patients' cerebral responses were different, with the contralateral S1 region becoming overactive as part of a symmetrical activation pattern [100]. These results revealed that the transient fabric stimulation to the chronic stroke participants generated the deactivation of the ipsilesional S1 area with asymmetric connectivity patterns.

2.4.2 Broader SFC topological distribution after stroke

Broader SFC topological distribution related to the involuntary attention was found in the fabric stimulation after stroke (Figure 2-4). As an exogenous attention, the involuntary attention could be triggered by short-term stimulus, while the endogenous attention could be triggered in goal-directed tasks with a person’s voluntary intention [103]. The involuntary attention related to the tactile sensation tasks could be attracted in the experiment settings. It was because that the fabric stimulation could be the only exogenous inputs to the participant whose cognitive processes and active mental tasks was asked to be minimized. Meanwhile, the visual and audio interferences was also suppressed via earplugs and an eye mask in the experiment settings. In the results, broader SFC topological distribution was found, including not only the temporal, but also the frontal as well as parieto-occipital areas in fine tactile sensation by either forearm after stroke, particularly in the affected side, while a SFC topological distribution focused on somatosensory area was found in the fabric stimulation to either

forearm in the controls. The temporal, parieto-occipital, as well as frontal areas were belonged to dispersed attentional networks [104]. These results revealed the recruitment of additional neural networks for involuntary attention in the fine tactile impairments after stroke, contributing to compensating impaired somatosensory related cortical areas as in motor tasks [105].

The compensatory effects from the attentional neural networks implemented in the neuro-regeneration after stroke, in line with the compensatory effects from the contralesional side of the brain in post-stroke fine tactile impairments [99]. The dispersed attention networks went through the neuro-regeneration process and show restored synaptic connection after stroke because they are nearby parts of the somatosensory region [106]. As focal attention participants in various cognitive, motion, or study activities [103], our findings demonstrated that the involuntary attention related higher-level mental functions could compensate the lower-level touch sensation impairments on the stroke survivors. In rsfMRI results, involvements of FC among attentional and somatosensory areas were found in the restoration of tactile functions after stroke, where the FC from the attentional areas had a significant correlation with the tactile discrimination test scores [34] [14]. Nonetheless, little has been done on neurological evaluation of the attentional distraction attracted by the fine tactile stimulation. Our results demonstrated the compensation from dispersed attentional areas to the somatosensory areas in fine tactile sensation after stroke.

2.4.3 Post-stroke enhanced interhemispheric FC

The interhemispheric connectivity presented significant differences at the somatosensory area, without significant difference at the hemispheric scale when comparing the stimulation to right and left limbs in unimpaired participants (Figure 2-5 and 2-6). The stroke group presented a significant enhancement in the

interhemispheric connectivity mainly over ipsilesional somatosensory regions when the affected forearm was stimulated, in comparison with the unaffected limb. This increase of interhemispheric connectivity could be related to the interhemispheric imbalance and the enhanced resting-state interhemispheric FC at the chronic stage after stroke [107] [108]. The fMRI studies on post-stroke motor functions found interhemispheric over-inhibition from contralesional to ipsilesional primary motor area [107] [100]. The resting-state interhemispheric connectivity gradually recovered at the sub-acute stage and even increased to a higher level at the chronic stage compared to the unimpaired persons [72] [108]. The results of this study also revealed that the FC alteration in fine touch after stroke was influenced by interhemispheric connectivity over somatosensory regions with ipsilesional hemisphere. Given the crucial function of interhemispheric connection in interhemispheric mutual control, this was caused by the compensatory shift from the lesional to the non-lesional side of the brain, which would then result in changes of hemispheric lateralization as revealed by the SFC re-distribution [109]. Prior research on unimanual motions in the unimpaired suggested that interhemispheric connectivity promoted the hemispheric lateralization through corpus callosum, where activities in contralateral hemisphere was inhibited, contributing to the interhemispheric information transfer in touch discrimination tasks [110] [111]. In resting-state fMRI studies, the interhemispheric FC experienced a compensatory neuroplastic processes during the motor restoration [72] [108] [109]. Our results revealed that the post-stroke compensatory neural mechanisms of transient fine tactile sensation were also accounted for interhemispheric connection over somatosensory regions within the ipsilesional hemisphere.

2.4.4 Enhanced cortical efforts after stroke

The networking brain structures in post-stroke fine tactile sensation still possessed segregation and integration abilities after stroke [112] [113]. This was revealed by the no significant difference in smallworldness ($SW > 1$) between the groups (Figure 2-5). Nonetheless, the fine touch sensation of the afflicted limb had a stronger propensity of the brain network to integrate distinct regions through intra- and inter-group FC following stroke [35], which was revealed by the significant higher global and local efficiencies than the unaffected limb after stroke. The presence of dense internal and external connections between sets suggests that the brain network automatically separated into sets of nodes [112]. A working memory study found improved cortical efficacy after the recruitment of additional brain regions, implying an efficient but uneconomical networking structure. Therefore, the significant increase of global and local efficiencies in fabric stimulation after stroke was related to the regeneration of connections in the compensation from the contralesional side of the brain and additional networks in fine tactile sensation after stroke. Especially in the case of motor deficits, functional deficits following a stroke revealed no definitive conclusion with respect to the alterations in local and global efficiency. The compensation from the contralesional side of the brain and the further involved attentional areas are potential determinants of the increased cortical activity when experiencing the fine tactile sensation after stroke, per the results of this paper examining local and global efficiency.

2.4.5 Limitation

Despite this work validated the functional significance of brain network metrics by recruiting unimpaired participants as the control group, there was the lack of correlation analyses on FC indices with clinical scores in this work. This was mainly due to the low sensitivity of current clinical assessments on fine tactile sensation given the subjective nature of sensory perception and low-resolution of clinical scales [11].

Another limitation that the stroke lesion was inaccessible in this work, due to the low-spatial resolution of EEG. In future works, a longitudinal study on the fine tactile impairments with multi-modal neuroimaging of both EEG and fMRI will be conducted to identify the evolution of the FC indices contributed by the stroke lesion per se and the compensatory processes after the stroke onset. We will also investigate the altered FC patterns in fine tactile impairments in individuals with cortical stroke to demonstrate the generalizability of the proposed fabric stimulation and FC indices in current study.

2.5 Periodic Summary

This study examined post-stroke changes in connectivity among cortical regions provoked by fine tactile stimulation in chronic stroke patients through the EEG-based functional connectivity analysis. Enhanced local and global efficiencies, additional involvements of other brain areas, increased interhemispheric FC, and altered hemispheric lateralization in the networking brain structure characterized the change in FC when implementing fine tactile sensation following a stroke, per the findings. In SFC topology, involuntary attention from dispersed attention networks and the contralesional compensation were revealed when implementing the stimulation to the stroke-affected side in comparison with stroke-unaffected side and the unimpaired group. The compensatory effects from the contralesional side of the brain and the attentional areas associated with involuntary attention in fine tactile stimulation could contribute to the enhanced local and global efficiency for the enhanced cortical activities after stroke.

Table 2-1. Recruited participants' demographic data.

Group	No. of participants	Stroke types, Hemorrhage / ischemic	Affected side, left/right	Gender, male/ female	Age (years, mean±std)	Min/Max years after stroke
Stroke	8	2/6	4/4	7/1	60.8±7.2	10/28
Control	8	-/-	-/-	3/5	57.8±12.1	-/-

Table 2-2. Stroke participants' clinical scores.

Clinical assessment	FMA full motor score	FMA shoulder/ elbow	FMA wrist/ hand	FMA sensory	ARAT	FIM	MAS elbow	MAS wrist	MAS finger
Score (mean± std)	44.38± 16.70	29.55± 9.60	14.95± 7.28	1	29.28± 18.35	65.43± 1.98	1.12± 0.56	0.87± 0.64	0.79± 0.51

CHAPTER 3

PATHWAY-SPECIFIC CORTICO-MUSCULAR COMMUNICATION ON POST-STROKE MOTOR COMPENSATION FROM PROXIMAL UPPER LIMB TO FINE MOTOR CONTROL OF DISTAL FINGERS

3.1 Introduction

Permanent sensorimotor deficits was commonly observed after stroke [30]. Motor compensation to the impaired muscles/joints with abnormal muscular patterns, e.g., muscle weakness, spasticity, and muscle discoordination, are gradually formed after stroke, particularly at the chronic stage, to improve independence in activities of daily livings [97] [114] [115]. Despite its useful to accomplish specific daily tasks, the compensation could decrease the range of motion in a joint, change the inter-joint motions, and exacerbate the long-term chronic pain after stroke [116]. These functional changes in motor compensation could dominant the neuroplastic processes in post-stroke recovery, resulting in maladaptive neuroplastic processes [117]. Nonetheless, the motor compensation has been misinterpreted as motor improvements in clinical assessments [118, 119]. The brain rearrangement in motor compensation, in particular the precise movement in distal hand and wrist joints, was poorly understood [114, 116].

The manifestation of neuroplastic processes on post-stroke motor functions was observed as a bidirectional alteration that impacted not only the efferent (descending) corticomuscular pathway, but also the afferent (ascending) corticomuscular pathway [12] [120]. These were caused by the reliance of both motor commands and sensory feedback in the closed-loop neuromuscular systems in voluntary movements [121].

Specifically, the fine motor control demand accurate and refined synchronization between motor and multisensory and systems [122]. Research into neuroplastic processes in the context of compensatory movements after stroke has typically investigated in terms of either the central or peripheral nervous system in isolation or the coherent neural activity that occurs between these two systems [123] [124]. Compensation in the peripheral motor system can manifest as disproportionate muscular activity in the proximal UE in distal movements [44]. Cortical rearrangement regarding the proximal elbow-shoulder compensation to distal hand motions in the central motor system can foster hyperexcitability in the unaffected hemisphere [125]. This was a consequence of the bilateral anatomical configuration of corticospinal innervation regarding the proximal should-elbow joints [126] [127]. Cortical restructuring included diminished spatial resolution in muscular discoordination and region-specific overexcitation in the relevant hemisphere, including the premotor cortex (PMC) over the ipsilesional hemisphere [119] [128]. Transcranial magnetic stimulation (TMS) research suggested that there was post-stroke enhancement of ipsilateral motor projections as a consequence of proximal muscle compensation in the paretic UE. This inhibited the motor restoration in the distal UE [129] [130]. Overall, these works revealed the presence of cortical restructuring or musculoskeletal disarray in motor compensation in post-stroke individuals. The neuroplastic mechanisms regarding the reorganized sensorimotor cortex and disco-ordinated muscles during compensatory motions are yet unknown. There was a lack of the research into bidirectional corticomuscular communication regarding the proximal UE during the distal hand movements. There was also limited information about the neuroplastic processes in the impaired motor precision in post-stroke individuals. Therefore, the

bidirectional corticomuscular communication in post-stroke proximal compensation to precise control of the distal fingers still needs to be investigated.

The directional neural interaction among cortical and muscular oscillations can be detected using directed cortico-muscular coherence (dCMC). Specifically, the pathway-specific (descending and ascending cortico-muscular pathways) communication within the closed-loop neuromuscular system can be detected with the dCMC between based on the neural recordings of EEG and EMG signals, which has been investigated in both post-stroke and unimpaired participants [131] [132]. Neuroimaging techniques of TMS somatosensory-evoked potential (SEP) was adopted to detect changes in descending and ascending cortico-muscular interactions in post-stroke individuals [44]. However, TMS and SEP TMS and SEP primarily examined the static characteristics of corticomuscular circuits when the participant was in a resting-state [44]. This imposes limitations on the exploration of altered post-stroke voluntary motor control. Conversely, dCMC that relies on EEG and EMG in voluntary movements had the capacity to gauge the motor commands and sensory feedback dynamically [40], due to the high time resolution of EEG and EMG among neuroimaging devices. Hence, it was possible to examine post-stroke pathway changes related to motor compensation and impaired motor precision. Earlier dCMC research examined the implications of dCMC in unimpaired subjects when conducting the isotonic contraction of the abductor pollicis brevis (APB) [41, 44]. The results indicated that there was increased sensitivity in relative values of descending and ascending dCMC when compared with CMC. Further dCMC studies examined dCMC in leg muscles with impaired reduced motor precision in respect of balance in unimpaired individuals during walking and standing [133]. The findings indicated a significantly raised descending dCMC during imbalanced walking or standing. Additionally, during

balance-perturbed standing, there was a discernible increase in the descending dCMC to muscles of the medial gastrocnemius for precise movements. Furthermore, the ascending dCMC from the extensor carpi radialis (ECR) to the S1 was responsible for enabling precise movements during the wrist movements [134]. In addition, the SMA could participate in gennerating the descending motor commands on the wrist movements [134]. These works indicate that dCMC can detect pathway-specific corticomuscular communication during active motor control. Nevertheless, the bidirectional corticomuscular communication was only identified in the agonist muscle after stroke. The bidirectional corticomuscular communication in motor compensation has not investigated yet. This was a consequence of the lack of dCMC measurement when multiple muscles are in coordination. There was limited information about dCMC in impaired motor precision after stroke because of inadequate information about dCMC configurations in peripheral movement stabilization. Bridging these gaps would render it possible to improve rehabilitation strategies designed to remedy maladaptive neuroplastic processes, thereby promoting more effective long-term recovery. The objective of this study was to examine pathway-specific corticomuscular communication in proximal elbow-shoulder compensation to distal finger movements with precise control after stroke, which was evaluated using dCMC in the four UE muscles, namely: the extensor digitorum (ED), the flexion digitorum (FD), the biceps brachii (BIC) and the triceps brachii (TRI).

3.2 Methods

The pathway-specific CMC in elbow-shoulder compensation to the precise finger movements was investigated in stroke participants using dCMC analyses. Using current recordings of EEG and EMG signals, isometric finger extension was examined in stroke patients on both sides as well as in the dominant side of the control participants. The

current EEG and EMG were then split into unstable movements and stable movements in line with EMG stability for the dCMC evaluation in precise motor control. The dCMC phase was subjected to linear regression analysis in order to determine the conduction delay in both ascending and descending paths.

3.2.1 Subject Recruitment

This study was approved by the same ethical committee as in Chapter 2 (No.: HSEARS20170502002; HSEARS20190119001). The control and stroke participants were required to satisfy the same criteria as in the Chapter 2. Meanwhile, the stroke participants should have moderate-to-severe UE motor impairments ($15 < \text{FME-UE} < 45$, where the maximal FME-UE is 66) [21] [135] [137]. There were no gender requirements because CMC is independent of gender [44]. Fourteen stroke subjects were selected for inclusion in the study, in addition to the eleven (age-matched, $P>0.05$, independent t-test) control participants. The participants' demographic data and stroke participants' clinical scores are summarized in the respective tables 1 a and b. The unimpaired participants only included individuals with dominant (right) limbs. However, either left or right hemiplegia, the non-affected side could be considered as the dominant side in the post-stroke participants in respect of the habitual adaptation during the chronic post-stroke stage (≥10 years, table 1 a) [49]. The written consent on the experiment purpose was obtained from all subjects prior to the commencement of the research as in the Chapter 2.

3.2.2 Experimental setup and protocol

In a quiet environment, participants took up a comfortable seated position in front of a computer screen. In order to make sure that the force output plane was orthogonal to gravity, the forearm to be tested was fixed onto a horizontal slab and kept in a neutral

position, as shown in Figure 2-1(A). A robotic orthosis was worn onto the hand for a stable joints angles as follows: the wrist straight at 0°, the thumb metacarpophalangeal (MCP) at 180°, the thumb interphalangeal (PIP) at 165°, and the remaining digits' MCP and PIP joints at 135°. The 64-channel EEG cap was worn onto the subject to record the EEG signal of 21 channels from the sensorimotor cortex (C1-6, CPZ, CP1-6, FC1-6, FCZ, and CZ). For EMG recordings, a total of pairs of electrodes were applied to the muscular bellies of ED and FD regarding finger motions and TRI and BIC regarding elbow motions. One EMG electrode on the olecranon was used as reference (all electrode-skin impedance < 5 kΩ). After the amplification, a 50 Hz notch filter and a band-pass filter of 2-100 Hz for EEG and of 10-250 Hz for EMG were used to process the signals. Using a self-programmed visual interface, as in Figure 2-1(B), the target contraction range of 10%–30% isometric maximum voluntary contraction (iMVC) was denoted by the blue cursors and the real-time contraction level in accordance with the normalized levels of EMG activation. The acquisition devices and configuration as well as the visual feedback interface was detailed in [125].

The experiment commenced with instructions to the participants to conduct the following iMVC test as in [125]. The EMG_{base} and EMG_{max} for each muscle comprised 0% iMVC and 100% iMVC, respectively. The EMG_{base} and EMG_{max} in the ED were employed to compute the desired contraction range (10%-30% iMVC) (the color gradient, Figure 3-1(B)). Subsequently, participants performed finger extensions at 20% iMVC for 35-s, during which the limbs were positioned as in Figure 3-1(A). Finger extensions were employed due to the fact that extensor impairment tends to be more extensive there than in UE flexors following a stroke [138]. The choice of a contraction level targeted at 20% iMVC was based on the conclusion that contraction levels <50% iMVC can produce obvious CMC with beta bands (13–35 Hz), in addition

to averting muscle fatigue. Moreover, this contraction level was deemed realistic for stroke patients [41] [125]. Furthermore, fine motor control has a closer relationship with lower-level contractions than is the case with higher-level contractions because it necessitates greater effort and cognitive focus on lower force output [59, 139]. When performing the task, the participants were required to keep the red pointer at the midline to generate the desired 20% iMVC, with the permissible fluctuation within the blue pointers to generate the acceptable range of 10%-30% iMVC, as in Figure 3-1(B). A 3-s initiation period was adopted in order to make sure that participant achieved the printer range prior to the 35-s sustaining contraction. Each participant had to perform 5 repetitive trials accompanied by a 2-min intertrial resting state. EEG and EMG were collected when the participant conducting the 35-s movement. The participants were required to limit body movements and facial expression in addition to ensuring that they remained awake. Furthermore, participants were asked to avoid active mental tasks when engaged in the target movement. We also monitored the muscle fatigue upon completion of teach test, in respect of the EMG mean power frequency (MPF). Identical experiment protocols were adopted for the two groups.

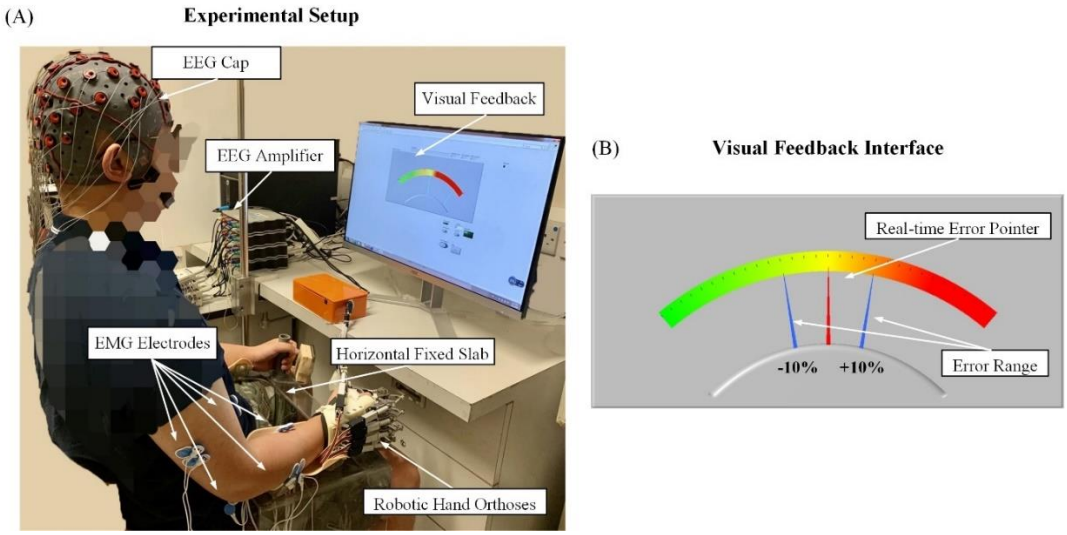

Figure 3-1 (A) Experimental setup of dCMC evaluation; (B) Visual feedback interface for real-time motion control. [125].

3.2.3 EEG and EMG processing

3.2.3.1 Data preparation

Figure 3-2 outlines EEG/EMG processing pipeline employed in this study. These accord with Fieldtrip and EEGLAB toolbox processes and adhere to current approaches [140, 141]. The signals were firstly down-sampled to 1000 Hz, wherein only the initial 30-s EEG and EMG data were kept in order to standardize the signal length and safeguard stability. A notch filter (50 Hz) and a band-pass filter (5-80 Hz) were performed on EEG. This was completed through the application of independent component analysis (ICA) [92], to eliminate artifacts cause by ocular motions. In addition, a 10 Hz high-pass filter and a 50 Hz notch filter were conducted on EEG. A visual examination was performed on the EEG and EMG in order to remove segments and channels that possessed excessive motion artifacts, e.g., body movements and muscle activities, related to facial expression. The data length was 120-150 seconds per person. Subsequently, EEG and EMG were divided into epochs of 1024 point/epoch without overlap [43].

Figure 3-3 shows the EMG spectra EEG spectra during finger extension in representative participants, where EEG was from C3 channel in the affected/control UE and from C4 in the unaffected UE. There was an evident peak in beta band in the control participant, while no peak was found in the stroke participant. EMG with the highest amplitude was changed from ED to BIC muscle in the affected UE of the stroke participant, in comparison the unaffected limb after stroke and the control limb.

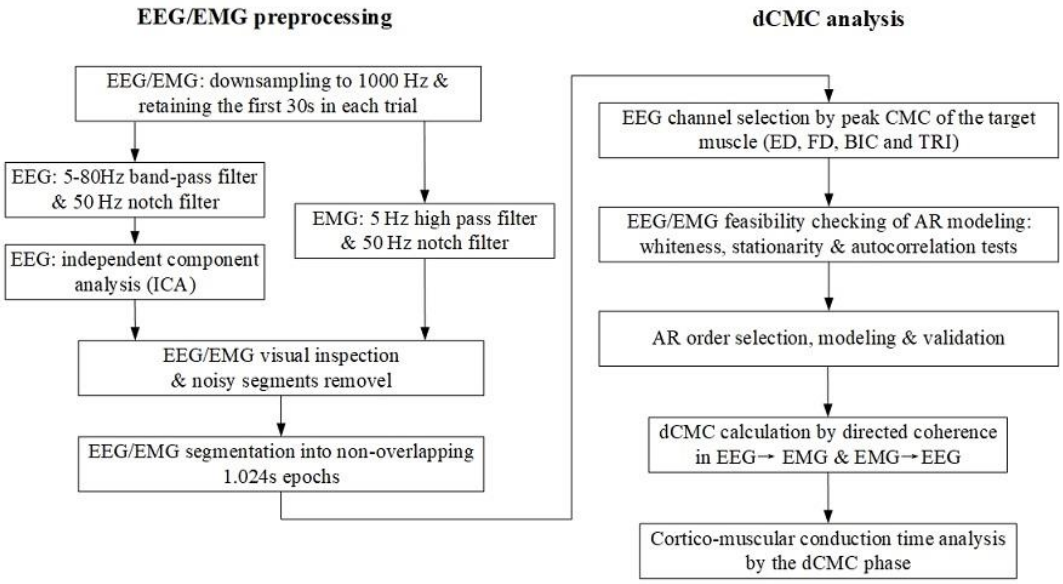

Figure 3-2 Signal processing flow chart.

3.2.3.2 EEG channel selection by peak CMC

The peak CMC in the beta band (13–35 Hz) [43, 142] was calculated regarding a target EEG channel over the sensorimotor cortex and a target muscle in the subject, according to the follows:

$$CMC_{ij} = \frac{|S_{ij}(f)|^2}{S_{ii}(f) * S_{jj}(f)} \tag{3-1}$$

where $S_{ii}(f)$ and $S_{jj}(f)$ are the autospectra of EEG i and EMG j, respectively. $S_{ij}(f) = < x_i(f) x_j^*(f) >$ is the EEG and EMG cross-spectrum. Meanwhile, * is the complex conjugate, $< >$ is the expectation. The $x_i(f)$ and $x_j(f)$ are the complex Fourier transforms of $\hat{x_i}(f)$ and $\hat{x_j}(f)$, respectively. The confidence level was determined as follows:

$$CL_{(\alpha\%)} = 1 - P^{\frac{1}{N-1}} \tag{3-2}$$

where P is the significance level (0.05 in this study), N is the number of epochs ($N \in [164,175]$ in this study), $CL(\alpha\%)$ represents the coherence confidential limit

($CL(\alpha\%) \in [0.0170, 0.0182]$ in this study). The coherence was considered to be significant if it is higher than the CL. The EEG channel with peak CMC of target muscleS was obtained and applied to subsequent dCMC calculation in each subject. Figure 3-3(C) shows the representative CMC topographies regarding ED when conducting finger extension by the 2 participants, where the color in each channel encodes the peak CMC within beta band. In terms of distribution, the peak CMC channel was observed in the contralateral hemisphere for each limb. However, in terms of CMC strength, the affected limb presented a lower CMC value in the peak channel and a weakened hemispheric lateralization ($CMC_{contralateral\ hemisphere}/CMC_{ipsilateral\ hemisphere}$) than the unaffected limb after stroke and the unimpaired subject.

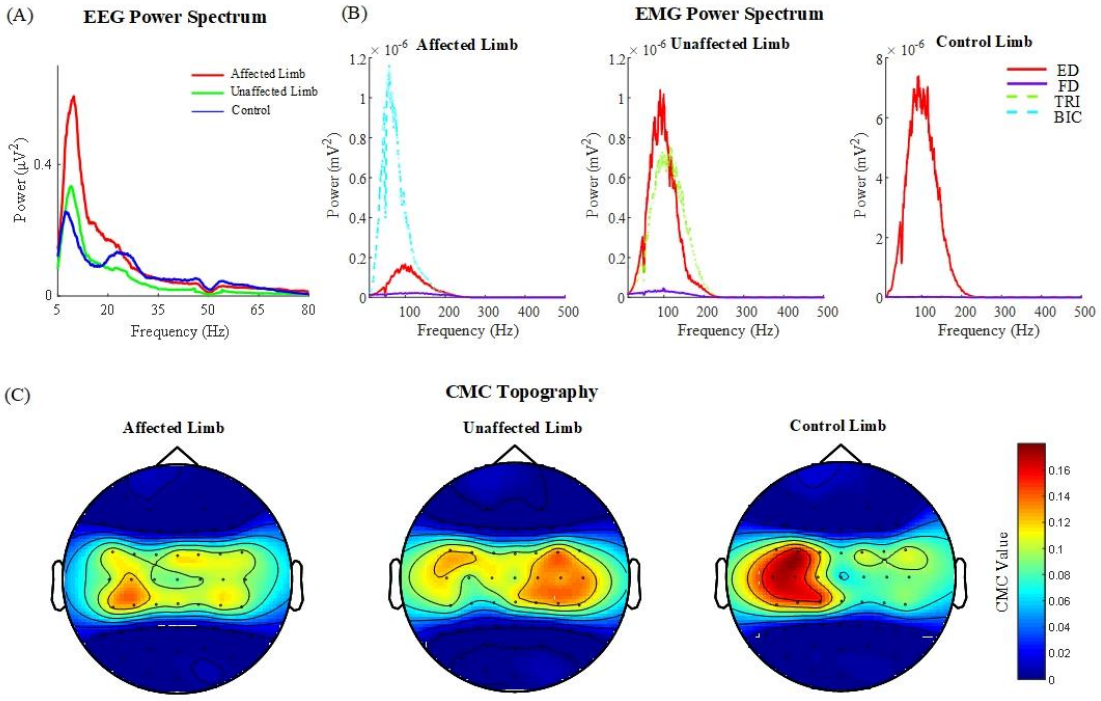

Figure 3-3 EEG (A) and EMG (B) power spectra and the topographies of CMC (C) for the ED muscle when conducting the finger extension in representative participants.

EEG was from the C3 channel in the affected and the control limbs and from the C4 channel in the unaffected limb.

3.2.3.3 dCMC analysis

The dCMC indicates a pathway-specific cortico-muscular contribution to voluntary movement between motor areas and desired muscles, which was measured with directed coherence in accordance with autoregressive (AR) modeling [44, 143]. The dCMC was calculated between the EEG signal of peak CMC and the EMG signal from a target muscle [44, 142]. The dCMC is based on AR-model wherein the AR simulates bidirectional signal exchanges with a graphic that depicts the frequency content and phase shift (delay). In the AR modeling, EEG $X_{EEG}(t)$ and EMG $X_{EMG}(t)$ signals, were represented as $X(t) = (X_{EEG}(t),\ X_{EMG}(t))^T$, as indicated in the following equation [133]:

$$X(t) = \sum_{\tau=1}^{p} A(\tau)X(t-\tau) + E(t) \qquad (3\text{-}3)$$

where $E(t)$ represents the residual vector of the white noise, $A(\tau)$ indicates the 2×2 matrix of model coefficients ($A(0) = I$, the identity matrix), τ signifies the time delay, and k indicates the model order. An appropriately high model order of $k = 60$ was chosen for a 0.5-Hz spectral resolution. It could also contribute to sufficiently estimate the corticomuscular conduction delay [134], wherein multiple information criteria were employed in respect of the model order series from 1 to 80, as per [133]. The EEG and EMG signals in the AR modeling were normalized for unit variance [134] [144]. In addition, Welch's method was employed to determine the power spectra that characterized the initial EEG and EMG signals, which were compared with the signals obtained from AR modeling [134, 145].

$$X(f) = A(f)^{-1}E(f) = H(f)E(f) \qquad (3\text{-}4)$$

where the transfer function possessed by the system $H(f)$ and the residual $E(f)$ were secured by z-transforming the equation (3-3) into $A(z)X(z) = E(z)$, i.e., $X(z) = A^{-1}(z)E(z) = H(z)E(z)$, where $z = e^{i2\pi f\Delta t}$ (the imaginary part is i, frequency point is denoted as f the and the time resolution is denoted as Δt) (27, 28). The dCMC value from EMG to EEG is computed as the following equation [143]:

$$dCMC_{EEG\leftarrow EMG}(f) = \frac{|H_{12}(f)H_{12}^{*}(f)C_{22}|}{|H_{12}(f)H_{12}^{*}(f)C_{22}+H_{11}(f)H_{11}^{*}(f)C_{11}|} \qquad (3\text{-}5)$$

wherein $H_{12}(f)$ denotes the item in 1st row and 2nd column in $H(f)$, indicating the information transfer in EMG to EEG. $H_{11}^{*}(f)$ denotes the impact of the EEG on itself and "*" signifies that the complex conjugation. C_{11} and C_{22} represent noise contributions to the EEG and EMG. The significant level of dCMC was estimated with the surrogate data (P<0.05) [44, 133]. The surrogate data here was secured through a random realignment of the EEG and EMG phase structure (1000 repetitions), the purpose of which was to reduce the presence of false positives [146].

The pathway-specific corticomuscular conduction delay were evaluated in accordance with the dCMC phase [44], as followings:

$$\theta(\mathrm{f}) = \arg\left(\mathrm{H}_{12}(\mathrm{f})\right) \qquad (3\text{-}5)$$

where the argument for the complex number is denoted as arg (), and $H_{12}(f)$ comprises the item in the $H(f)$. The conduction delay from EMG to EEG, $T_{EEG\leftarrow EMG}$, was the beta-band phase delay as $T_{EEG\leftarrow EMG} = \Delta\theta_{EEG\leftarrow EMG}(f)/2\pi\,\Delta f$ [44]. Specifically, the time was estimated as the beta-band slope of the phase-frequency plot $\theta_{EEG\leftarrow EMG}(f)$, in accordance with the linear fitting approach [44, 147]. This process was also used to determine the conduction delay in the reverse direction $T_{EMG\leftarrow EEG}$.

3.2.4 dCMC of precise motor control

In respect of the pathway-specific CMC in precise motor control, the dCMC was examined in stable and unstable movements during sustained muscle contractions [148]. The concurrent EEG and EMG signals for each test were divided according to the median EMG stability, to further extract the randomly presented less-stable EMG [148]. Figure 3-3 presents the EMG segments during finger extensions. This was shaped by the poor motor precision at post-stroke distal UE, as indicated previously on the unimpaired (53). All five trials were used (retaining the first 140 s for consistent length in each trial), which was subdivided into 5-s data segments [148], thereby creating 28 segments for each participant. EMG stability in each segment was determined using the following equation:

$$EMG\ Stability = 1 - \frac{SD(EMG_{envelope})}{Mean(EMG_{envelope})} \quad (3\text{-}8)$$

where SD represents the standard deviation. Based on the EMG stability median, a total of 28 segments were classified into the stable movement (14 segments) and the unstable movement (14 segments) with the respective high and low EMG stability. Subsequently, the dCMC was determined segment-by-segment and averaged across segments for the stable and unstable movements. Figure 3-4 shows the EMG envelope of the ED in representative subjects. The EMG signal was less stable in the affected limb with the unstable segments randomly presented over the 30 s when comparing to the unaffected limb and the controls.

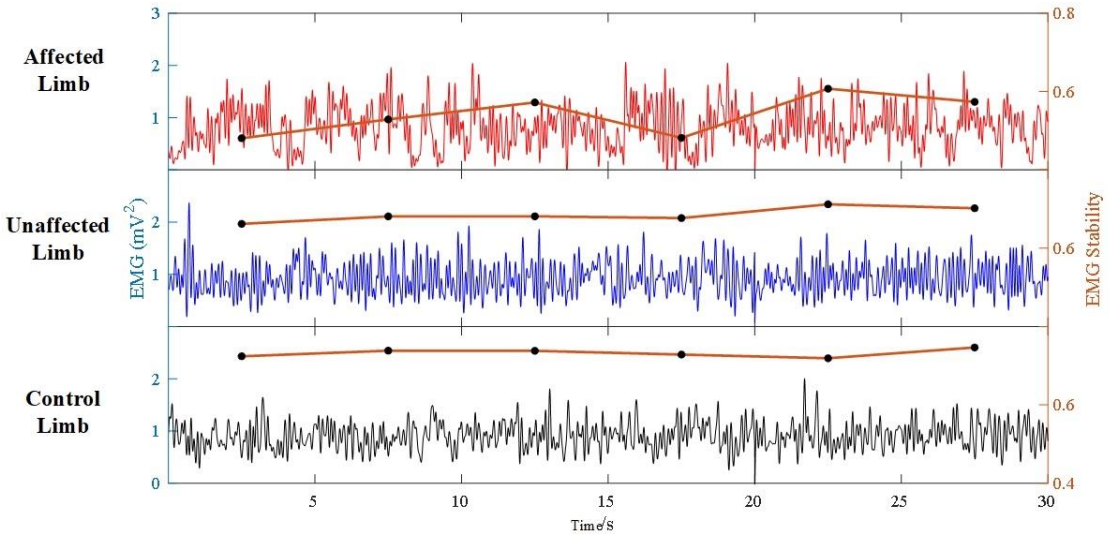

Figure 3-4 EMG envelope from the ED muscle in representative participants.

3.2.5 Statistical analysis

The dCMC, the conduction delay and the EMG stability, were checked and made sure to obey the normal distribution through the Shapiro-Wilk test of normality. Firstly, intragroup comparisons regarding dCMC strength was performed by a two-way Analysis of Variance (ANOVA) for different corticomuscular pathways and muscles with each limb group. Secondly, a paired t-test on dCMC was performed to evaluate the dCMC distinction between corticomuscular pathways. Thirdly, a one-way ANOVA on dCMC among different muscles was conducted with either Dunnett's T3 (unequal variance) or the Bonferroni post hoc test (equal variance) [149, 150]. In inter-group comparisons, the dCMC among the three limbs were compared in each corticomuscular pathway using one-way ANOVA with either Dunnett's T3 or the Bonferroni post hoc test according to equal/unequal variance. The same statistical comparison was performed for inter-group comparisons on EMG stability and dCMC. Finally, a two-way ANOVA on the conduction delay was performed regarding different limb and muscles. Finally, the one-way ANOVA was used to compare the conduction delay in different muscles and in different limb groups, respectively. Statistical significance was

set at 0.05, 0.01 and 0.001. All statistical calculations in the study were performed using SPSS 24.0 (2016).

3.3 Results

3.3.1 dCMC spectra in different muscles

Figure 3-5 shows dCMC spectra in both groups when performing the precise control on finger extensions. For the stroke-affected UE, the significant descending dCMC peaks were found in TRI, FD, and BIC but not in ED. In addition, significant ascending dCMC peaks in both distal muscles were observed with a larger ascending dCMC in the ED muscle compared to FD in affected limbs. However, they were not present in the BIC and TRI muscles. There was no evident descending predominance (a larger descending dCMC peak than the peak of the ascending dCMC) in the ED. However, the descending predominance was evident in the TRI, FD, and BIC muscles when conducting finger extension by the affected limbs. Significant descending dCMC peaks were evident in all muscles of the stroke-unaffected limb. The significant ascending dCMC peak in the stroke-unaffected limb was reported in the TRI and FD as well as the BIC, but not in ED. The descending predominance in the unaffected limb was found at both distal muscles and TRI rather than the BIC. The muscles in the unimpaired participants limbs presented with significant peaks in both pathways when conducting the fine control of finger extension. Meanwhile, all the muscles had descending predominance. Unlike the stroke-unaffected limb and the controls, the stroke-affected limbs displayed clear ascending predominance only in ED and clear descending predominance in FD, BIC as well as TRI.

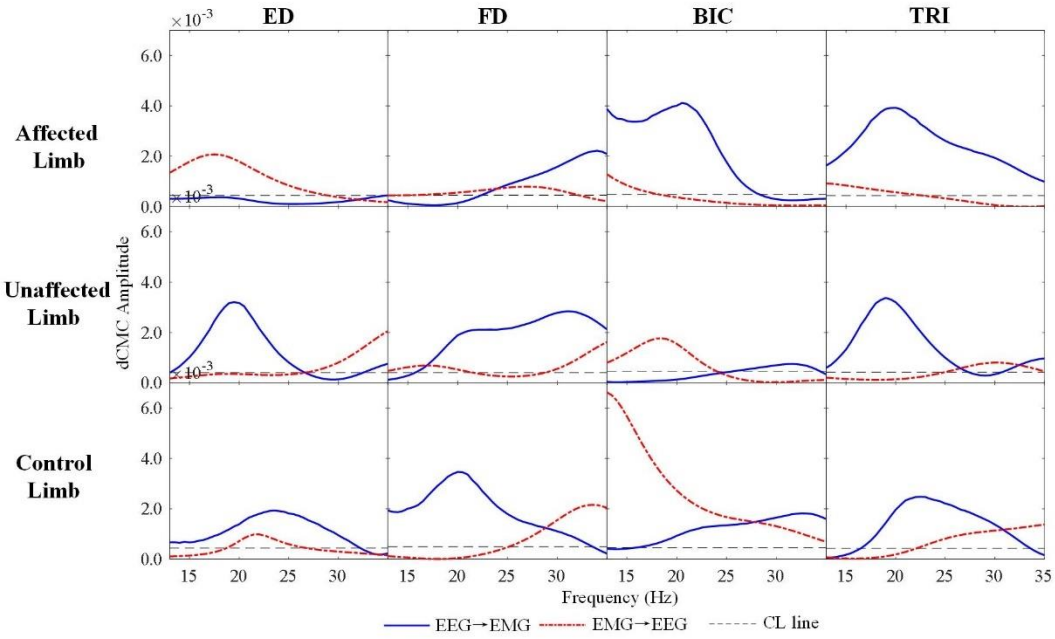

Figure 3-5 Representative dCMC spectra when conducting the finger extension in both groups.

3.3.2 dCMC strength

Figure 3-6 displays the dCMC in both groups when conducting finger extension. A significant descending predominance in the UE (2-way ANOVA; P<0.01, EF=0.07, main effect of the pathway factor) and a significant dCMC distinction among four muscles were found in stroke-affected limb (2-way ANOVA; P<0.05, EF=0.08, main effect of the muscle factor). Significant interaction effects between factors of the pathway and muscle were also observed in the affected UE (2-way ANOVA; P<0.05, EF=0.07). This descending predominance was further reported in TRI and BIC muscles (paired t-test; P<0.05, EF=0.23 for BIC; EF=0.23 for TRI), but not in the FD and ED muscles (P>0.05). Significant decrease of the descending dCMC was reported in the FD and ED when compared with the BIC (1-way ANOVA; P<0.01, EF=0.21).

A significant descending predominance was also reported in unaffected UE (2-way ANOVA; P<0.001, EF=0.15, main effect of the pathway factor), which was further

spotted on the TRI and FD (paired t-test; P<0.05, EF=0.50 for FD and EF=0.27 for TRI). There was no significant variation of dCMC among the four muscles (P>0.05). The interaction regarding factors of the pathway and muscles was not significant (P>0.05).

The unimpaired participants presented the significant descending predominance (2-way ANOVA; P<0.001, EF=0.15, main effect of the pathway factor). This descending predominance was further spotted on distal muscles, FD and ED (paired t-test; P<0.05, EF=0.50 for ED, EF=0.64 for FD), but was not on TRI and BIC (P>0.05). No significant dCMC differences were reported among the four muscles or significant interaction between the factors (P>0.05).

For inter-group dCMC comparison, the descending dCMC had significantly smaller value in ED in the affected limb than was the case in the unaffected limb and the limb (1-way ANOVA; P<0.05, EF=0.18). The affected FD displayed a reduced dCMC in descending pathway in comparison with FD in unaffected UE and the controls, albeit an insignificant trend (P>0.05). For proximal TRI and BIC, there was no significant inter-group difference of descending dCMC (P>0.05). There was no significant difference for the ascending dCMC for both factors (P>0.05).

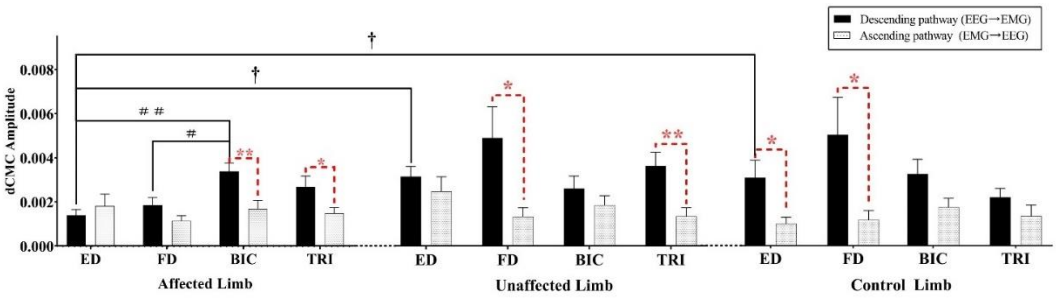

Figure 3-6 dCMC values of the UE muscles when conducting the finger extension in both groups. The error bar denoted the standard deviation.

3.3.3 Stable and unstable movements-related dCMC

Figure 3-7 depicts dCMC and EMG stability during the unstable and stable finger movements. During unstable movements, the stroke-affected UE had significantly smaller EMG stability at ED and FD (1-way ANOVA; P<0.001, EF=0.18 for FD and EF=0.34 for ED), without significant distinction of EMG stability on TRI and BIC (P>0.05), in comparison with the stroke-unaffected UE and the controls. Figure 3-7(B) shows that ED and FD had significantly larger ascending dCMC in affected limbs than control limbs (1-way ANOVA; P<0.05, EF=0.20 for FD and EF=0.29 for ED). The affected TRI muscle presented a significant larger ascending dCMC compared to both post-stroke unaffected limb and the controls (1-way ANOVA; P<0.01, EF=0.26). Figure 3-7(C) shows that the affected BIC had significant larger descending dCMC than the controls (1-way ANOVA; P<0.05, EF=0.17). The affected TRI had significant larger descending dCMC than both post-stroke unaffected limb and the controls (1-way ANOVA; P<0.05, EF=0.17).

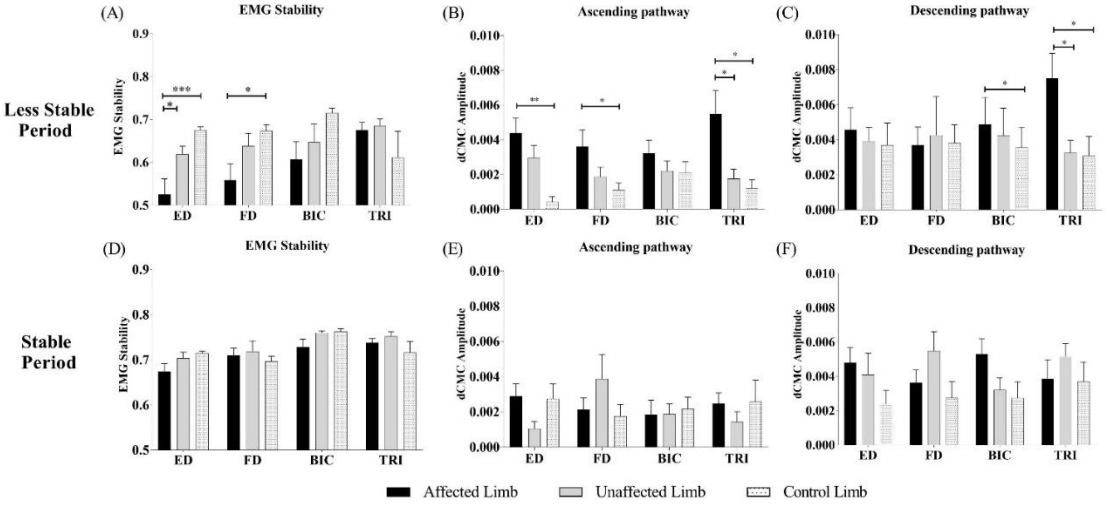

Figure 3-7 EMG stability and the descending and ascending dCMC values when conducting fine control of finger extensions at stable and unstable periods in both groups. The error bar denoted the standard deviation.

3.3.4 dCMC phase delay

The corticomuscular conduction delay is presented in Figure 3-8(A). In respect of the conduction delay for descending control, no significant distinction was found among three limbs (2-way ANOVA; P<0.01, EF=0.10, main effect of the group factor). A significantly extended conduction delay for descending control was found to ED in affected limbs than was the case with both unaffected and control limbs (1-way ANOVA; P<0.05, EF=0.19). In Figure 3-8(B) for the descending precedence (the descending conduction delay < the ascending conduction delay), the descending precedence was found in only 34% of the stroke participants in affected ED but in 67% of stroke participants in unaffected ED. Conversely, 80% of participants in the unimpaired group exhibited descending precedence in ED. Other three muscle displayed comparatively small differences (<20%) for descending precedence among UE groups.

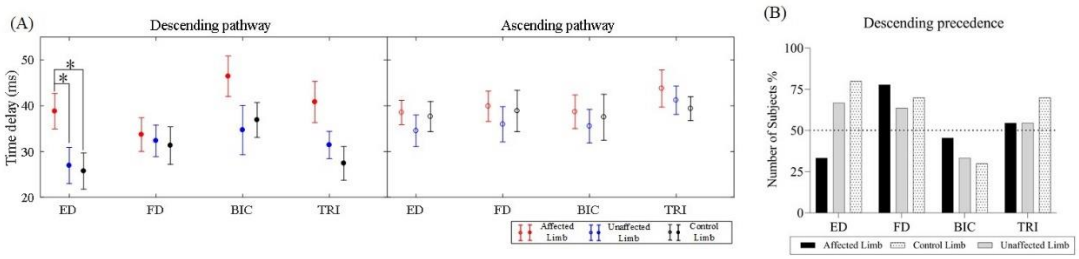

Figure 3-8 (A) Pathway-specific corticomuscular conduction delay. (B) The percentage of participants with descending precedence in each group.

3.4 Discussion

This study investigates pathway-specific neuroplastic processes in post-stroke proximal compensation to the fine control of distal finger extensions. This was achieved using comparative dCMC evaluation between the sensorimotor areas and ED, FD, BIC, and TRI muscles. According to the findings, the proximal compensation to distal finger movements with impaired motor precision exhibited shifted predominance from the

distal fingers to proximal elbow-shoulder joints in the descending control, excessive sensory feedbacks in distal UE in the ascending pathway for precise control, and extended conduction delay for descending control to the ED.

3.4.1 Post-stroke alteration of descending predominance

The post-stroke dCMC had the relocation of the motor control from the distal fingers to proximal upper limb in descending pathways when conducting finger extension in the affected side. In the results, the affected distal UE displayed reduced descending dCMC and shifted descending predominance from finger extensors towards the proximal UE for compensatory movements. Results pertaining to dCMC revealed that descending control to ED and FD was significantly decreased compared to the affected BIC. Affected limbs displayed the descending predominance in elbow-shoulder muscles BIC and TRI. Conversely, the descending predominance was in ED and FD in the controls (Figure 3-6). The dCMC configurations observed in the unimpaired participants demonstrated the efficacy of the dCMC metrics employed in the current study [134]. In previous works, comparable results regarding descending predominance was found in voluntary contractions, including wrist extensions [134], the finger flexions [46], and the imbalanced leg movements [133]. Descending and ascending pathways transfer motor commands and peripheral sensations, respectively, in voluntary muscular contractions [121, 122]. In respect of affected limbs, the changes reported in this study might be a consequence of maladaptive neuroplastic processes in efferent pathways arising from post-stroke “learned disuse” [119]. The flexors and extensors exert excitation and inhibition to each other in oppositional manner for antagonism within the corticomuscular system in the unimpaired persons [151] [152]. Reduced descending control to hand-wrist movements revealed the denervation of corticospinal tracts with the reduced monosynaptic neural connections to target muscles

after the emergence of post-stroke brain lesions [43] [153]. Furthermore, the shifted predominance from the hand-wrist to elbow-shoulder segment in the descending control could be attributed to the cortical reorganization, such as interhemispheric disinhibition and competition within the unimpaired hemisphere [119] [128]. The hand-wrist and proximal arms were found to have competitive interaction over the ipsilesional sensorimotor cortex [154]. Hence, our findings demonstrated that the proximal muscles gained more descending control when conducting finger extension by the paretic UE. This was principally the consequence of the diminished ispilesional inhibition and counterbalance to the contralesional hemisphere.

Descending predominance changes were observed in the post-stroke unaffected side in this study (see Figure 3-6). The findings indicated that the post-stroke unaffected side exhibited the descending predominance in TRI and FD, compared to the descending predominance in ED and FD in the controls, although no significant dCMC difference compared to the unimpaired participants. This indicated an shifted descending predominance in post-stroke unaffected limbs from ED to TRI, which was possibly caused by the disinhibited M1 in the unaffected hemisphere with a lack of inhibition on the proximal upper limb in hand movements [4] [155]. The paretic side after stroke has been the subject of considerable research. Conversely, little research has been done into the non-paretic side after stroke. Previous research on the post-stroke unaffected side primarily focused on peripheral kinematics or EMG activities. For example, the dexterity measured by kinematics was damaged in both elbow-shoulder and hand and wrist joints in the non-paretic UE during dynamic UE movements [156] [157]. The findings of this study suggested that functional alterations in the post-stroke unaffected limb had shifted descending predominance to the synergistic extensor TRI when conducting finger extension.

3.4.2 Excessive sensory feedbacks in post-stroke fine motor control

Excessive sensory feedbacks in the ascending pathway were found in the distal muscles for the precise control to the unstable finger extension. In the results, the unstable movement revealed that the affected ED and FD had a significant reduction of EMG stability, but a significant increase of ascending dCMC and on significant changes of the descending dCMC, compared to unimpaired participants (see Figure 3-7). The reductions in EMG stability indicated the post-stroke impairments of the precise control of finger movements, resulting in unstable movements. A significant correlation was reported between the force precision and EMG stability during sustained muscle contraction, as per [59, 148]. Moreover, the post-stroke excessive ascending feedbacks without descending changes indicated that the impairments of the precise motor control could be a consequence of the impaired sensorimotor recalibration in the closed-loop neuromuscular system when a person trying to stabilize the peripheral muscles. In the unimpaired persons, the descending motor control can reach a desired level through the comparison of anticipated and actual levels of the sensory reafferent information, e.g., tactile and proprioceptive sensations, in motor activities [158]. The findings on post-stroke excessive sensory feedback measured by the ascending dCMC were consistent the increased sensory thresholds measured by traditional clinical assessments, due to the functional sensory deficiency. It also indicated the failure of calibrating the descending motor commands using the afferent information due to the impaired cortical sensorimotor integration between the somatosensory areas and the ipsilesional hemisphere, as detailed later in Chapter 4. Moreover, existing research into stroke individuals found comparable inverse relationships between fine motor performance and corticomuscular communication in different muscles [59, 139]. Existing research into stroke participants has indicated that impaired corticomuscular communication

exacerbated unstable leg motions [40] [120]. Bao et al. reported a comparable unidirectional ascending enhancement in post-stroke individuals, rather than the bidirectional enhancement in unimpaired participants, during the pedaling assisted by NMES compared to the pure passive or active pedaling without NMES assistance [40]. Our results revealed that post-stroke impaired motor precision had properties of unidirectional augmentation, i.e., the enhanced ascending feedbacks, as a result of the impaired sensorimotor recalibration.

3.4.3 Extended descending cortico-muscular conduction delay

The conduction delay in the controls in this study, when compared to existing research into dCMC phase delay, provided additional confirmation of the efficacy of the dCMC measurement for pathway-specific neural interaction [44][148]. The conduction delay (Figure 3-8) related to the ED at the post-stroke unaffected side and the controls' dominant side accorded within the range of 20-40 ms in previous works into the unimpaired individuals[44] [148].

The descending conduction efficiency regarding the affected hand and wrist joints was significantly reduced in the ED. Moreover, there were no significant changes in the FD. According to the findings, the stroke-affected ED muscle (~38.8 ms) experienced significantly extended conduction delay in the descending corticomuscular pathways and significantly diminished persons possessing descending precedence (46%), in comparison with the stroke-unaffected side and the controls, whereas the FD revealed no significant changes among different limbs (Figure 3-8). In respect of the ED, comparable findings related to the reduced conduction efficiency was found with CMC [43] or TMS [153] in post-stroke individuals as a consequence of the reduction in fast pyramidal corticospinal tracts from the ipsilesional side of the brain. These related to the inadequate motoneurons firing in accordance with time summation mechanisms at

the spinal level [159] [160]. No significant changes in conduction efficiency in the antogaonist FD could be caused by flexor adaptation to the routine force production and diminished inhibition from upper motor neuron in post-stroke weakened antagonism [139] [161] [162], irrespective of the sparse spinal tracts and the reduced descending motor control, as per the ED [162] [163]. The dCMC evaluation in this study indicated the inefficient conduction to the ED in descending corticomuscular pathways when conducting the post-stroke finger extensions.

The findings in this work demonstrated that the pathway-specific CMC could be a potential diagnostic and prognostic biomarker as the therapeutic target for long-term neurorehabilitaion of fine motor functions and compensatory movements after stroke. In future works, a longitudinal study from the subacute to chronic phase after stroke will be conducted to investigate the dCMC patterns contributed by stroke lesion per se and maladaptive neuroplasticity following a stroke.

3.5 Periodic Summary

This study examined post-stroke pathway-specific corticomuscular communication in proximal compensation to distal finger movements with impaired precision through dCMC analyses. The study findings indicated that the post-stroke proximal compensation to distal finger movements experienced shifted predominance from the distal fingers to proximal UE in descending control, enhanced sensory feedbacks from distal fingers for precise control, and extended conduction delay in descending control to the ED. Shifted predominance from the hand-wrist to elbow-shoulder joints for the descending control in the affected limb was found in BIC and TRI, compared to the ED and FD in the controls. Pathway-specific CMC for precise control exhibited significantly enhanced sensory feedbacks from ED, without significant changes to the descending control in unstable movements. This was due to the impaired sensorimotor

recalibration in precise control to the affected distal UE and shifted controlling resources to the proximal joints in descending pathways.

Table 3-1 a. Recruited participants' demographic data.

Group	No. of participants	Stroke types, hemorrhage/ ischemic	Affected side, left/right	Gender, male/ female	Age (years, mean±std)	Min/Max years after stroke
Stroke	14	7/7	7/7	3/11	56.5±9.5	10/28
Control	11	-/-	-/-	3/8	50.6±16.8	-/-

Table 3-1 b. Clinical scores of the stroke participants.

Clinical assessment	FMA full motor score	FMA shoulder/ elbow	FMA wrist/ hand	ARAT	FIM	MAS elbow	MAS wrist	MAS finger
Score (mean± std)	44.38± 16.70	29.55± 9.60	14.95± 7.28	29.28± 18.35	65.43± 1.98	1.12± 0.56	0.87± 0.64	0.79± 0.51

CHAPTER 4

INTEGRATED SENSORIMOTOR EVALUATION OF CORTICAL REARRANGEMENT AFTER STROKE WITH SENSORY-/MOTOR-LEVEL NEUROMUSCULAR ELECTRICAL STIMULATION (NMES) AND ELECTROENCEPHALOGRAPHY (EEG)

4.1 Introduction

A combination of sensory and motor deficits affects approximately 80% of stroke survivors [31] [164]. Post-stroke individuals frequently experience spasticity, weakness and dis-coordination of the musculature, as well as somatosensory abnormalities, issues which have a negative impact on their autonomy to perform routine daily activities [12] [15]. It has been established that sensorimotor integration is a key factor in the functional restoration following a stroke; the accurate coordination of multisensory and motor information is necessary in order to achieve a stable posture and to perform fine motor skills [121]. Additionally, the functional (or behavioral) alterations and the neurological adaptions following cortical repair are mutually potentiating in the ongoing neuroplastic process of sensorimotor deficit reparation and remodeling [97]. Although sensorimotor integration has been emerged in stroke rehabilitation and shown promise to enhance the recovery process [18][164], there is little research to date which has studied the efficacious and integrated assessment of both sensory and motor deficits from either functional or neurological perspectives after stroke. Techniques routinely used in the clinical setting to evaluate patients' progress are frequently weighted in favor of motor rather than sensory functions [11]. Nevertheless, inefficacious or

prejudiced assessments could mislead diagnostic and therapeutic decisions, and thus, restrict the outcome of therapeutic initiatives. This may arise as a result of the varied presentations of deficits seen in stroke survivors and the absence of consistent patterns of sensorimotor recovery [9] [11]. Sensory deficits have been associated with a lower level of motor function and functional prognosis [18], e.g. diminished tactile discrimination led to higher latency times for task performance, such as pinch grip, despite an improvement in muscle strength following therapy. [8]. Thus, efficacious and integrated sensorimotor assessments would be valuable in rehabilitation programs for stroke survivors.

Contemporary techniques for the assessment of sensorimotor function include conventional clinical evaluations; simple parameters of behavioral adaptations following a stroke are broadly utilized by practitioners. Nevertheless, the majority of these are notably prejudiced towards motor skills; the evaluation of sensory deficits generally lack depth and complexity, and are used in clinical work sparingly [9]. Just under a quarter of occupational and physical therapists indicated in a cross-sectional survey that they performed somatosensory evaluations with standardized parameters in their routine practice. Approximately three-quarters of these therapists utilized interview or the observation of motor tasks as a measure of sensory abilities, or even overlooked the evaluation of sensory functions altogether [9]. Furthermore, the reliability and reproducibility of conventional clinical tests have been queried owing to the absence of neural identification [11]. One commonly utilized evaluation method is the Fugl-Meyer assessment (FMA) which comprises a straightforward ordinal scale to describe the degree of deficit, i.e., 0 = ‘absent’, 1 = ‘impaired’, and 2 = ‘normal’. This is often completed using simple visual and manual examination, which potentiates clinical data subjectivity and lack of resolution [165]. The absence of control of

sensorimotor stimulation during conventional clinical evaluations has additionally exacerbated the low subjectivity of the testing results, particular in relation to sensory assessments [11]. Instances of this are the commonly conducted two-point discrimination and monofilament assessments; these could be influenced by differences in the examiner's manual strength of application of the tactile stimulant [11]. Thus, efficacious and integrated sensorimotor assessments with controlled sensorimotor stimulation, together with neurological parameters with objectivity and which are equally weighted towards the evaluation of both sensory and motor deficits, are clearly underrepresented in the clinical arena.

In addition to clinical evaluations, neurological deficits can be detected and assessed objectively by visualizing the cortical reorganization that has occurred following a stroke, using a range of neuroimaging and neurophysiological methods, e.g., fMRI, PET and EEG [165] [166]. The latter, in contrast to fMRI and PET, amongst others, is relatively inexpensive and able to recognize transient cortical activities during the performance of sensorimotor tasks with a temporal sensitivity of milliseconds [75] [167]. Thus, EEG can be employed to document post-stroke task-centric cortical reorganization in relation to both sensory and motor deficits; the arising data encompass changed cortical activation and disruption in connectivity via the analysis of event-related desynchronization (ERD), synchronization (ERS) and functional connectivity (FC) [37] [78] [168]. To date, there has been limited work pertaining to the use of EEG in effective and integrated sensorimotor evaluations of cortical reorganization following a stroke, essentially owing to the absence of a suitable model for patients with such a heterogeneity of deficits. The majority of earlier research on EEG has been performed in the context of either sensory or motor assessment; motor execution (ME), motor imagery (MI) and fabric stimulation paradigms have been applied in isolation

[168] [169]. In terms of an integrated sensorimotor evaluation approach, we studied changes in corticomuscular pathways, i.e., descending motor control and ascending sensory feedback, through the analysis of directed corticomuscular coherence (dCMC) between EEG and electromyography (EMG) signals. This was applied in the context of hand dexterity during a task of finger extension in stroke survivors [10]. Decreased descending motor control, enhanced ascending sensory feedbacks, and extended descending conduction delays were identified within the agonist ED during the fine motor control after stroke. Nonetheless, sensorimotor assessments founded on dCMC may not demonstrate complete generalization to individuals who have suffered a stroke and who have a range of deficits since in those with significant functional loss, such fine motor skills could be too challenging [169]. Additionally, the corticomuscular interplay measured by dCMC relates to particular corticomuscular pathways rather than the reorganization of the cortex, i.e. the changed cortical activation and disruption, in connectivity observed in sensorimotor loss [170] [171]. Furthermore, there are few data pertaining to the relationship between the neurological alterations observed by neuroimaging techniques and the variations of the functional behavior recognized in relation to sensorimotor tasks in stroke survivors. In particular, there is an absence of research which has looked at the relationship between the patterns of cortical reorganization in relation to sensorimotor functionality and associated clinical scores. The requisite for a generalizable EEG-based integrated sensorimotor assessment in combination with behavioral evaluations for the sensorimotor evaluation of cortical reorganization in stroke survivors was therefore recognized.

An integrated sensorimotor method, neuromuscular electrical stimulation (NMES) offers regulatable stimulation intensities. This permits a target muscle to receive selective sensory (sensory-level NMES) and motor (motor-level NMES) inputs via the

depolarization of relevant subcutaneous sensory and motor nerve cells via electric currents [69] [70]. These tests have been utilized in patients post stroke, and who have a variety of neurological deficits. As it is a non-invasive investigation and relatively inexpensive, sensory- and motor-level NMES can be utilized both in clinical institutions and in patients' residences [69] [70]. A combination of sensory-level NMES and single-channel EEG has been employed in order to examine the ascending sensory pathway integrity, a process referred to as SEP assessment [172]. A number of researchers have also studied the cortical neuromodulatory influence of NMES, predominantly by evaluating the impact of varying NMES values in unimpaired populations without neurological deficits [69] [70] [173]. A range of intensities and doses of NMES on alpha- and beta band ERD patterns were appraised by Insausti et al. following hand-wrist extensor stimulation, which involves the muscles, ED and ECU [69]. When contrasted against sensory-level NMES, motor-level NMES led to notably increased ERD in relation to the sensorimotor cortex in the contralateral hemisphere. This was ascribed to the suppressive and enhancing influences of sensory- and motor-level NMES cortical neuromodulation, respectively. [173]. Motor-level NMES-induced ERD trends related to those seen with active as opposed to passive knee extensions; this finding suggested the potential to use EEG and motor-level NMES to assess voluntary motor skills. There are few studies which have evaluated cortical neuromodulation of sensory-/motor-level NMES in individuals who have suffered stroke. In one stroke survivor, clear ERD patterns were identified by Qui et al. during motor-level NMES; these were absent during passive movements [173]. However, these researchers failed to conduct a comparison between populations, either with respect to knee extension induced by NMES or passive movement, or between subjects who were normal neurologically and stroke survivors. When considered in combination,

these previous findings indicate that NMES has the potential to produce identifiable EEG patterns that are associated with sensorimotor functions. There is little information relating to the application of both sensory- and motor-level NMES and EEG for integrated sensorimotor eevaluation of cortical reorganization following a stroke. This is undoubtably a consequence of the void in knowledge pertaining to changed cortical neuromodulator activities as a result of sensory-/motor-level NMES. Overcoming this gap in knowledge would add to the development of an efficacious and integrated sensorimotor evaluation which could facilitate clinical diagnostic abilities and positively influence therapeutic planning in the rehabilitation of stroke survivors. The aim of this study, therefore, is to evaluate an integrated sensorimotor evaluation of cortical reorganization through the analysis of the neuromodulatory influences of sensory-/motor-level NMES based on EEG signals post stroke.

4.2 Methods

The integrated sensorimotor evaluation of cortical rearrangement after stroke was investigated by analyzing stimulation intensity, cortical activation, and cortical connectivity during sensory-/motor-level NMES in comparison with the unimpaired controls. First, sensory- and motor-level NMES were applied to the hand-wrist extensors, i.e., ED and ECU, at both sides of stroke and unimpaired groups with synchronized EEG recordings from the whole brain. The sensory-/motor-level NMES intensities were then compared between the groups (stroke vs unimpaired) to evaluate behavioral changes in sensorimotor impairments after stroke. To assess neurological changes in the post-stroke Cortical rearrangement, the time-frequency and spatial-temporal features of the NMES-induced cortical neuromodulation were investigated using the EEG-based ERD and ERS analyses in both groups. Hemispheric lateralization in the NMES cortical neuromodulation was also quantified, using the laterality index

(LI) in the ERD/ERS topographies, i.e., LI-ERD/ERS, across different stimulation periods. In addition, correlation analyses of the clinical scores and the significantly changed ERD/ERS features after stroke were performed to identify the relationships between cortical rearrangement patterns and behavioral changes related to sensorimotor impairments after stroke. Finally, cortical interaction in the NMES-induced neuromodulation was investigated using FC analyses of EEG signals during and after sensory-/motor-level NMES.

4.2.1 Subject recruitment

This study was approved by the same ethical committee as in Chapter 2 (No.: HSEARS20210123005). The same inclusion criteria as Chapter 3 was used in this study. Meanwhile, the stroke participants should have moderate sensory impairments, with the "light touch" and "position" items ≤ 1 in the sensory sub-scale of the FMA. We recruited a total of 35 participants with 15 stroke survivors and 20 age-matched ($p>0.05$, independent t-test) unimpaired persons as the control group. The participants' demographic data and the stroke participants' clinical scores are summarized in the respective Tables 4-1 a and b. The written consent on the experiment purpose was obtained from all subjects prior to the commencement of the research as in the Chapter 2.

4.2.2 Experimental design

4.2.2.1 Experiment setup

The participant seated comfortably in a quiet room (temperature: 18–20 °C and relative humidity: 60%±5%) [168]. Figure 4-1 A shows the experimental setup. A support bracket was used to place the forearm to reduce friction with the table during hand-wrist movements, and the other forearm was resting on a cushion. The hand and wrist

joints were standardized to make sure the movement direction orthogonal to gravity during the stimulation [10] [125]. The electrical stimulation to the hand-wrist extensors was delivered by a self-made programmable neuromuscular stimulator [56]. The NMES output had varied pulse width ranging of $0 \sim 200$ μs, constant inter-pulse interval of 25 ms and amplitude of 80 V. It generated a train of square pulses of 5-s one cycle, as in our previous work [56]. Whole-brain EEG signals were acquired from a 64-channel EEG cap with the same acquisition and amplification setup as in the Chapter 2. A self-programmed LabVIEW visual interface was adopted to synchronously trigger the stimulation and the corresponding marker (Square wave with a duration of 1.5-ms) onto the EEG signals at each NMES onset, according to the experiment timing (as detailed later in ***Experiment protocol***). The visual interface was used to control and monitor the start, end, and timing of each trial.

4.2.2.2 Experiment preparation

The NMES electrodes (5×5 cm^2, PALS Neurostimulation Electrodes; Axelgaard Manufacturing Co., Ltd.) were attached to the common area of the muscle bellies of the ED and ECU, i.e., ED-ECU, in both arms for the extension in hand and wrist joints [56]; the ECU and ED were recruited together because of their narrow and anatomically close muscle bellies [49, 174]. The ECU-ED was selected because of the typically delayed and poor recovery in the hand-wrist joint compared with the proximal elbow and shoulder joints in the UE after stroke [97] [168]. It was commonly observed that the UE extensors were more severely impaired than the flexors and impeded by the inappropriate flexor activation during voluntary movements after stroke [138, 168]. The skin preparation was conducted with abrasive gel and alcohol pads to reduce the electrode-skin impedance before the electrode attachment [138, 168]. The position of NMES electrodes was standardized as previous works [69]. The position of the NMES

electrodes was further confirmed by verifying that the movement plane was orthogonal to gravity during the NMES-induced full extension of the hand and wrist, because hand-wrist rotation, i.e., circumduction, could occur if electrodes were positioned inappropriately [69].

4.2.2.3 Experiment protocol

At the beginning of the experiment, the sensory- and motor-level NMES intensities were identified individually on both arms with the limb positioned as shown in Figure 4-1 A. Stimulation intensity was controlled by varying the NMES pulse width (0–200 μs) in steps of 2 μs during a 5-s stimulation period, with other NMES parameters kept constant (see the Experiment setup above for details). Figure 4-1 B shows the identification of sensory- and motor-level NMES intensities according to the perceptual, motor, and pain thresholds in each participant [69] [70]. The sensor-level NMES intensity was defined as the median value between the perceptual and motor threshold, while the motor-level NMES intensity was the highest non-painful level with full extension hand-wrist, i.e., 2 μs below the pulse width of the pain threshold, which was typically used for sensorimotor rehabilitation after stroke [69] [70] [49]. The perceptual, motor, and pain thresholds were identified by asking the participant to verbalize their sensation and by observing their corresponding initial reaction or motion during the 5-s stimulation when the NMES pulse width was increased with steps of 2-μs from 0-μs, as follows: (1) perceptual threshold: initial “tingling” sensation in the forearm; (2) motor threshold: initial twitching of the wrist or fingers; (3) pain threshold: initial painful sensation after the full hand-wrist extension (i.e., a range of motion ≥ 60° from the natural position, with the palm orthogonal to the table) [69]. The same procedure was used to identify the sensory- and motor-level NMES intensities on both arms.

These sensory-/motor-level NMES intensities were recorded for each participant and kept constant throughout the experiment.

The sensory- and motor-level NMES were randomly delivered to the participant in a total of 64 cycles (4 cycles × 4 trials × 2 NMES levels × 2 arms). Figure 4-1 C shows the timing of one trial. Four cycles of NMES with a duration of 5 s per cycle were delivered to the hand-wrist extensors in each trial. There was a preparation period of 20 s at the beginning of each trial and an interval of 25-s after each NMES cycle. The subject was asked to keep quiet but not fall asleep throughout the trial [168]. Inter-trial rest periods of 5 min were provided to avoid fatigue [168]. EEG signals were continuously recorded throughout the experiment. Procedures were identical on both arms of all participants; none of them reported painful, thermal, or any uncomfortable sensations throughout the experiment. EEG signals were monitored in real-time to inspect and immediately make up for any trials with large motion artifacts or EMG activities due to possible body movements and facial expressions, to ensure constant signal quality.

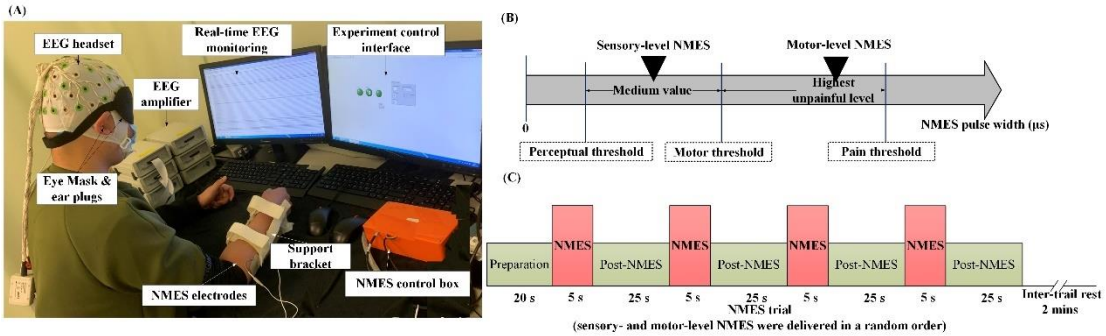

Figure 4-1. (A) Experiment setup. (B) Identification of sensory- and motor-level NMES intensities according to the perceptual, motor, and pain thresholds determined for each participant. (C) Experiment timing of an NMES trial.

4.2.3 EEG analysis

4.2.3.1 EEG preprocessing

Figure 4-2 shows the main procedures of the EEG signal processing. The recorded EEG signals were first preprocessed using the same procedures as the Chapter 2. The EEG was also notch filtered at 40 Hz to remove the noise from the neuromuscular stimulator. The EEG channels near the peripheral border and bilateral ears (Fp1–2, Fpz, O1–2, Oz, F7–8, T7–8, P7–8, TP7–10, PO7–8, and FT9–10) were discarded to avoid the unstable EEG gel contacts, and the remaining 42 EEG channels were included in further analyses, as practiced previously [40]. We flipped the EEG electrode positions along the mid-sagittal plane in stroke participants with right hemiplegia to enable a group analysis with higher statistical power, as in previous studies [168] [35]. Finally, data segmentation was performed according to each NMES onset to obtain EEG segments of 30 s on the NMES cycles containing the three conditions, i.e., immediately before the NMES onset ([-5, 0] s), during the NMES ([0, 5] s), and immediately after the NMES [5, 25] s. In total, we obtained 480 segments from the affected/unaffected side of the stroke group ($N = (N_{\text{Sensory−level NMES}} + N_{Motor-level\ NEMS)} \times N_{subject}$, where $N_{\text{Sensory−level NMES}} = N_{Motor-level\ \text{NMES}} = 16$ and $N_{subject}$ =15) and 640 segments from the left/right side of unimpaired participants ($N_{\text{Sensory−level NMES}} = N_{Motor-level\ \text{NMES}} = 16$ and $N_{subject} = 20$). The EEG analyses followed the latest updates and instructions of the Fieldtrip and EEGLAB toolboxes [140] [141].

4.2.3.2 ERD/ERS analysis

Alterations in cortical neuromodulatory effects induced by NMES in the time-frequency and spatial-temporal domains after stroke were investigated using ERD and ERS analyses, representing the respective cortical activation during the stimulation (i.e., power attenuation) and cortical recovery after the stimulation (i.e., power enhancement)

[37] [78] [169]. ERD/ERS analyses were typically adopted to identify cortical sensorimotor responses in stroke and unimpaired participants during motor imagery and motor execution tasks in the literature [37] [169]. Here, ERD/ERS was calculated for the 30-s EEG segments of the NMES cycles based on the event-related spectral perturbation (ERSP) analysis [176]. The strength of ERD and ERS was proportional to the respective negative and positive ERSP values [169] [176]. The ERSP at the frequency f and time t was defined as the normalized time-frequency spectrum by the mean spectrum across the 5-s baseline period, i.e., immediately before the NMES onset ([-5, 0] s), which was calculated as follows [176] [140]:

$$ERSP(f,t) = \frac{S_{NEMS}(f,t) - \mu_{Baseline}(f)}{\sigma_{Baseline}(f)} \quad (4\text{-}1)$$

where the time-frequency spectrum $S_{NEMS}(f,t)$ was obtained by the wavelet transform on the 30-s EEG segment, and then the average was taken across all segments in sensory-/motor-level NMES [140]. The Morlet wavelet was adopted with $f \in$ [3, 80] Hz, $t \in$ [-5, 25] s, and a number of cycles of 15 controlling the time-frequency resolution [177]. The $\mu_{Baseline}(f)$ and $\sigma_{Baseline}(f)$ are the respective mean and standard deviation of the $S_{NEMS}(f,t)$ across the baseline period ([-5, 0] s) at the frequency f. The unit of ERSP is std., by definition [177]. The ERD/ERS was the mean EPSP over the specific time-frequency window, as follows [176]:

$$ERD/ERS = \frac{1}{K}\sum_{f\in F}\sum_{t\in T} EPSP(f,t) \quad (4\text{-}2)$$

where F is the frequency band, e.g., alpha and beta bands ([8, 30] Hz), and T is the time window, e.g., [0, 5] s for ERD and [5, 25] s for ERS. K is the total number of time-frequency bins within the time-frequency window F and T.

The time-frequency distribution of the NMES-induced cortical neuromodulation was analyzed using ERSP and ERD/ERS in the C3/C4 channel contralateral to the stimulation side (i.e., C3 and C4 for the respective stimulation to the right and left limbs). The C3/C4 channel was selected because it typically presented significant cortical sensorimotor responses in stroke and unimpaired individuals during tactile sensation and motor tasks [168] [10]. For the time-frequency window in the C3/C4-ERD/ERS calculation, the frequency band F was the theta ([4, 8] Hz), alpha ([8, 12] Hz), beta ([13, 30] Hz), and gamma ([31, 80] Hz) band, and the time window T was [0, 5] s for ERD and [5, 25] s for ERS. The C3/C4-ERSP and C3/C4-ERD/ERS were calculated on both sides of all individuals in both groups (i.e., in the stroke-affected, stroke-unaffected, control-left, and control-right limbs) to identify possible ERD/ERS differences related to hand asymmetry in unimpaired participants and altered movement strategies in the stroke-unaffected limb [10].

The spatial-temporal distribution of the NMES-induced cortical neuromodulation was analyzed through the ERD/ERS topographies across different stimulation periods. The ERD topographies were calculated based on the EEG recordings during the NMES (i.e., [0, 5] s). The ERS topographies were calculated based on a non-overlapping moving time window of 2 s on the EEG after the NMES (i.e., T =[5, 7] s, [7, 9] s, [9, 11] s, [11, 13] s, [13, 15] s, [15, 17] s, [17, 19] s, [19, 21] s, [21, 23], and [23, 25] s), to demonstrate the dynamic process of cortical recovery after stimulation, as reported previously on motor execution after stroke [169]. All topographical analyses in the current study were performed on the EEG data from the stroke-affected and control-right limbs within the alpha and beta bands (F =[8, 30] Hz). It was because the stroke-affected and control-right limbs presented significant differences in terms of both behavioral and neurological properties, as indicated by sensory-/motor-level NEMS intensities and

C3/C4-ERD/ERS, without significant differences among the stroke-unaffected, control-right, and control-left limbs (as detailed later in the Results).

The hemispheric lateralization in the spatial-temporal distribution of the NMES-induced cortical neuromodulation was further quantified by the laterality index (LI), based on the ERD/ERS topographies across different periods, i.e., LI-ERD/ERS, in the stroke-affected and control-right limbs. The LI was used to measure hemispheric asymmetries in topographical changes after stroke, as in previous fMRI and EEG studies [168] [33]. The LI value was proportional to the dominance of the contralateral hemisphere in NMES neuromodulation, where $LI > 0$ and $LI < 0$ represented the respective contralateral and ipsilateral dominance. The LI was calculated as follows:

$$LI = log_{10} \left| \frac{ERD/ERS_{contralateral}}{ERD/ERS_{ipsilateral\,\&\,midline}} \right| \quad (4\text{-}3)$$

where $ERD/ERS_{contralateral}$ and $ERD/ERS_{ipsilateral\,\&\,midline}$ are the mean ERD/ERS values in the contralateral sensorimotor area and in the ipsilateral sensorimotor area and the midsagittal plane, respectively [178].

4.2.3.3 Functional connectivity estimation

The altered cortical interaction in NMES neuromodulation after stroke was investigated using the FC among cortical areas in sensory-/motor-level NMES, to identify the altered cortical contribution from other areas to the sensorimotor area in the networking brain structure[33] [168] [179]. The FC was estimated by the imaginary coherence (ImCoh), as Chapter 2 [84]. The ImCoh was calculated with Equation 2-1. The ImCoh spectra were calculated using a time window of 2 s with 50% overlap (0.5-Hz frequency resolution) based on the EEG during ([0, 5] s) and after the NMES ([5, 15] s) within alpha and beta bands [8, 30] Hz), because most significant changes in cortical activation,

as measured with ERD/ERS, after stroke occurred within the time-frequency window of [0, 15] s and [8, 30] Hz (as detailed in the Results).

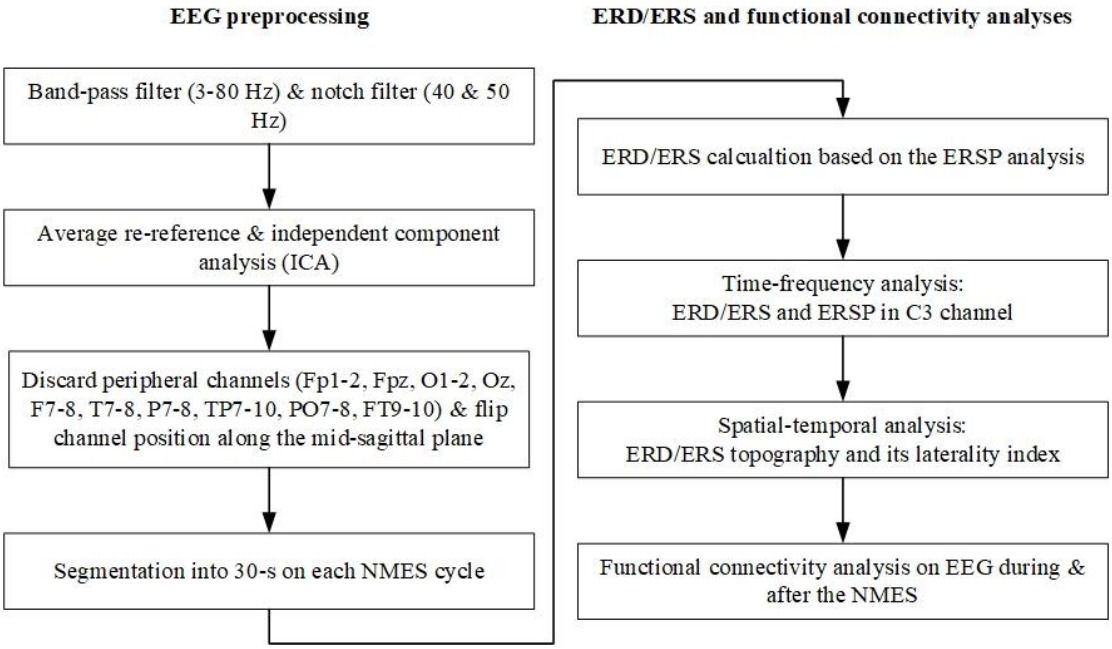

Figure 4-2. Electroencephalography (EEG) signal processing flow chart.

4.2.4 Statistical analysis

The Shapiro-Wilk test of normality was used to verify the sensory- and motor-level NMES intensities, the C3/C4-ERD/ERS, and the LI values on ERD/ERS topographies (i.e., LI-ERD/ERS) all followed a normal distribution ($p>0.05$). The stroke-affected, stroke-unaffected, control-left, and control-right limbs were compared to investigate possible functional and neurological differences related to hand asymmetry in unimpaired participants and altered movement strategies in the stroke-unaffected limb. First, comparisons of sensory-/motor-level NMES intensities among the four different limbs were conducted using one-way ANOVA with Bonferroni post hoc tests, to identify behavioral changes in the sensorimotor impairments after stroke. To assess neurological changes in sensorimotor impairments, comparisons of C3/C4-ERD/ERS in each frequency band (theta, alpha, beta, and gamma bands) were conducted using

two-way mixed ANOVA with the limb (i.e., stroke-affected, stroke-unaffected, control-left, and control-right limbs) and stimulation (sensory- and motor-level NMES) as factors. Then, one-way ANOVA and paired t-tests were performed for the limb and stimulation factors, respectively, with the Bonferroni method for the multiple comparison correction. In addition, an inter-group comparison of the LI-ERD/ERS across different periods was performed between the stroke-affected and control-right limbs using paired t-tests to evaluate altered hemispheric lateralization after stroke. Furthermore, inter- and intra-group comparisons of ERD/ERS topographies were conducted using the cluster-based permutation test for the respective differences between the subject groups and between the NMES levels, to identify altered cortical activation after stroke [180]. The same inter- and intra-group comparisons were conducted on the FC topographies using the cluster-based permutation test, to identify altered cortical contributions from other areas to the sensorimotor area after stroke. The cluster-based permutation test was adopted as it has been reported to be suitable for multiple comparison corrections on EEG topographies with multiple channels, e.g., 64 channels in the whole brain, based on nonparametric statistics [85] [180].

Spearman's correlation analyses were used to identify the relationship between the cortical rearrangement patterns and the behavioral changes in sensorimotor impairments after stroke. The correlation analysis was firstly performed between the clinical scores (FMA wrist/hand, MAS-wrist, and MAS-finger) and the sensory-/motor-level NMES intensities in the stroke-affected limb. It was then, performed between the clinical scores and the ERD/ERS features, i.e., the LI-ERD and LI-ERS in motor-level NMES and the LI-ERD and the C2&Cz-ERS (mean ERS in C2 and Cz channels across the [5, 15] s) in sensory-level NMES. The FMA wrist/hand (FMA-W/H), MAS-wrist, and MAS-finger were selected because they were typically adopted as the primary

outcome measures in sensorimotor rehabilitation after stroke [48] [181]. The level of statistical significance was the same as the Chapter 3.

4.3 Results

4.3.1 Increased sensory-/motor-level NMES intensities after stroke

Figure 4-3A shows the sensory-/motor-level NMES intensities in both arms of the stroke and control participants. Table 4-2a lists the NMES intensities with the statistical results. Significant increases in both sensory- and motor-level NMES intensities in the post-stroke affected limb were observed compared to the unaffected limb and both limbs of the controls ($p<0.001$; EF=0.32 for the sensory-level NMES, EF=0.50 for the motor-level NMES; 1-way ANOVA). In contrast, sensory- or motor-level NMES intensities exhibited no significant differences among the unaffected limb and the left and right limbs of unimpaired participants (1-way ANOVA).

Figure 4-3B shows the significant correlation between the clinical scores and sensory-/motor-level NMES intensities. Table 4-2b lists the detailed correlation coefficients and possibilities between the clinical scores and sensory-/motor-level NMES intensities. A strong positive correlation was found between the motor-level NMES intensities and the MAS-wrist scores ($r=0.727$, $p<0.01$). The motor-level NMES intensities also exhibited a significant positive correlation with the MAS-finger scores ($r=0.697$, $p<0.01$), but no significant correlation with the FMA-W/H scores ($r=0.136$, $p>0.05$). The sensory-level NMES showed a significant negative correlation with the FMA-W/H scores ($r=-0.612$, $p<0.05$) and a significant positive correlation with the MAS-finger scores ($r=0.563$, $p<0.05$), but no significant correlation with the MAS-wrist scores ($r=0.442$, $p>0.05$).

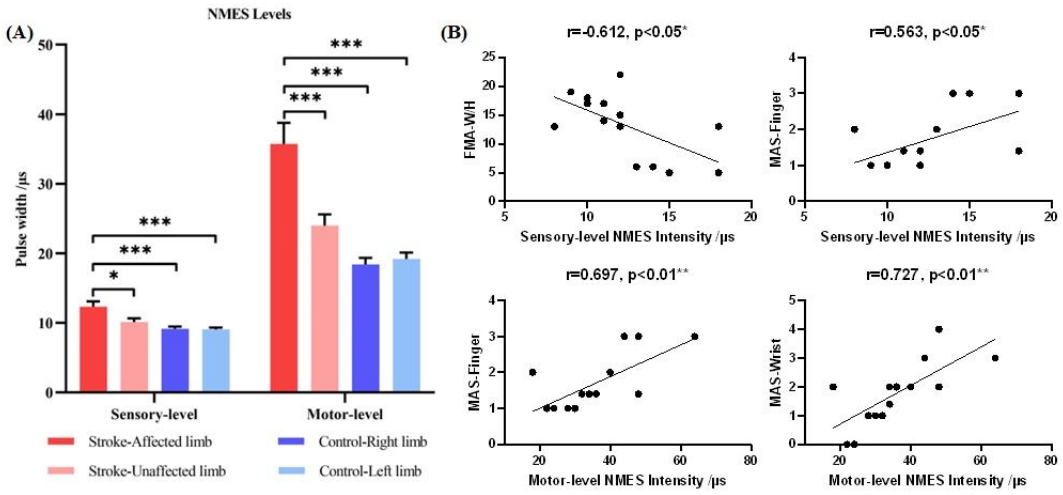

Figure 4-3. (A) Sensory-/motor-level NMES intensities in both limbs of both groups. (B) Significant correlation between the intensities of sensory-/motor-level NMES and clinical scores in the stroke-affected limb.

4.3.2 ERD/ERS changes in sensory-/motor-level NMES after stroke

4.3.2.1 Time-frequency distribution of cortical activities in NMES after stroke

Figure 4-4A shows the C3/C4-ERD/ERS in different frequency bands when sensory-/motor-level NMES was applied to the four stimulated arms. Both alpha and beta bands exhibited a significant decrease in ERD and a significant increase in ERS in the stroke-affected limb than the control-right limb during the sensory-/motor-level NMES ($p<0.05$, main effect of the stimulated limb; 2-way ANOVA). In contrast, the theta and gamma bands exhibited no significant ERD/ERS differences for the different limbs or different NMES levels ($p>0.05$). Specifically, the alpha-band ERD had a significant decrease in the affected limb compared to the controls during the sensory-/motor-level NMES ($p<0.05$, EF=0.12, main effect of the stimulated limb; 2-way ANOVA). A significant decrease in alpha-band ERD was further observed in the affected limb compared to both limbs in the controls during the motor-level NMES ($p<0.05$, EF=0.27, 1-way ANOVA), but no significant alpha-band ERD differences were found among the

four limbs during the sensory-level NMES ($p>0.05$). As for the different NMES levels, the control-right limb exhibited a significantly higher alpha-band ERD during the motor-level NMES than the sensory-level NMES ($p<0.05$, EF=1.07, paired t-test), while the stroke-affected, stroke-unaffected, and control-left limbs exhibited no significant alpha-band ERD differences between NMES levels ($p>0.05$).

The beta-band ERD had significant decreases in the stroke-affected limb compared to the control-right limb during the sensory-/motor-level NMES ($p<0.01$, EF=0.17, main effect of the stimulated limb, 2-way ANOVA). The significantly decreased beta-band ERD was further observed in the stroke-affected limb, compared to the control-right limb, during the motor-level NMES ($p<0.05$, EF=0.23, 1-way ANOVA), but no significant differences were found among the four limbs during the sensory-level NMES ($p>0.05$). As for the different NMES levels, both right and left limbs in the controls presented a significantly higher beta-band ERD during the motor-level NMES than the sensory-level NMES ($p<0.05$, EF=1.08 for the left limb and EF=1.42 for the right limb, paired t-test), while the stroke group presented no significant differences between NMES levels in either limb ($p>0.05$).

The alpha-band ERS was significantly increased in the stroke-affected limb compared to both left and right limbs in unimpaired participants after the sensory-/motor-level NMES ($p<0.05$, EF=0.11, main effect of the stimulated limb, 2-way ANOVA). The significant increase in alpha-band ERS in the stroke-affected limb compared to both limbs in the controls was further observed after the motor-level NMES ($p<0.05$, EF=0.21, 1-way ANOVA), but there were no significant alpha-band ERS differences among the four limbs after the sensory-level NMES ($p>0.05$). There was also no significant alpha-band ERS differences between the sensory- and motor-level NMES in any limbs ($p>0.05$).

The beta-band ERS was significantly increased in the stroke-affected limb compared to the control-right limb after the sensory-/motor-level NMES ($p<0.05$, EF=0.14, main effect of the stimulated limb, 2-way ANOVA). The significantly increased beta-band ERS in the stroke-affected limb was further observed after the motor-level NMES ($p<0.05$, EF=0.21, 1-way ANOVA), but there were no significant beta-band ERS differences among the four limbs after the sensory-level NMES ($p>0.05$). There was also no significant difference in beta-band ERS between the sensory- and motor-level NMES in any limbs ($p>0.05$).

Figure 4-4B shows the mean time-frequency distribution of cortical activities in the C3/C4 channel, i.e., the mean C3/C4-ERSP, across all participants in each group during the sensory- and motor-level NMES. In both limbs of the controls and the stroke-unaffected limb, a remarkable ERD within alpha and beta bands was observed during both sensory- and motor-level NMES. The ERD presented a more widespread time-frequency distribution during motor-level NMES compared to the sensory-level NMES. In contrast to the controls and the stroke-unaffected limbs, the affected limb exhibited weakened ERD during the motor-level NMES, enhanced ERS after the motor-level NMES, and no obvious ERD differences between the sensory- and motor-level NMES within the alpha and beta bands. Although the unaffected limb also exhibited increased alpha- and beta-ERS compared to the controls immediately after the sensory-/motor-level NMES mainly in 5–10 s, the change was more short-lived than that in the affected limbs, which was observed in 5–20 s.

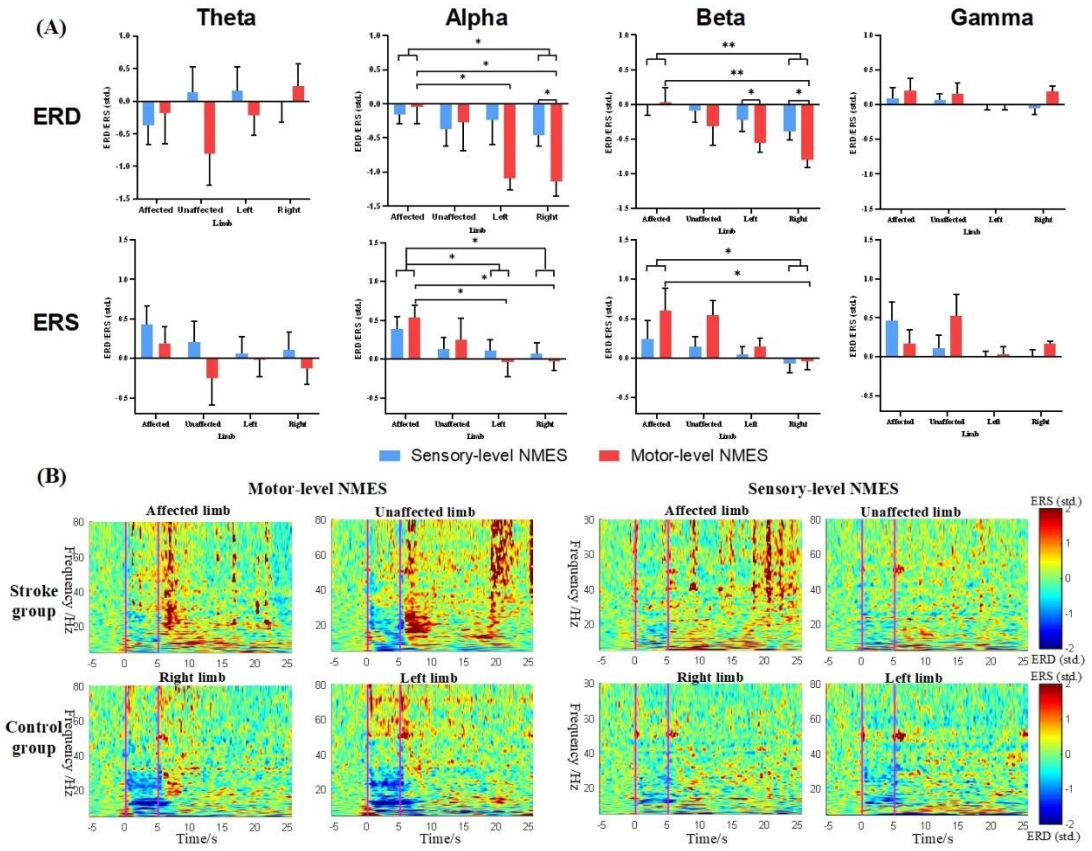

Figure 4-4. (A) C3/C4-ERD/ERS during the sensory-/motor-level NMES in both groups. The error bar denoted the standard deviation. (B) Time-frequency distribution of the cortical activities in the C3/C4 channel in the sensory-/motor-level NMES in both groups.

4.3.2.2 Spatial-temporal distribution of cortical activities in NMES after stroke

Figure 4-5 shows the ERD/ERS topographies in the stroke-affected and the control-right limbs, in addition to the corresponding inter-group (stroke-affected vs control-right limbs) and intra-group (sensory-level NMES vs motor-level NMES) statistical comparison ($p<0.05$, cluster-based permutation test), where the significant ERD/ERS changes were labeled with the channel name. The motor-level NMES post-stroke highlighted a redistributed ERD from the contralateral to the ipsilateral hemisphere and a redistributed ERS from the ipsilateral to the contralateral hemisphere, compared to

the controls. Specifically, a shifted ERD hotspot, i.e., the peak value of the mean ERD, from the contralateral to the ipsilateral sensorimotor area, after stroke was found both during (0–5 s) and within the 2 s immediately following the motor-level NMES (5–7 s). A significantly reduced ERD after stroke was observed in bilateral sensorimotor areas during the motor-level NMES (i.e., 0–5 s in the timeline, with significant changes at channels of FC1 2 6, C1 3 4 6, CP1 3 4 6). The significant reduction in ERD after stroke still occurred in the contralateral sensorimotor area within the 2 s immediately following the motor-level NMES (5–7 s: FC1 3, C3 5, CP1 3 5), where the hand-wrist joint spontaneously moved backed to the natural position after the NMES-induced extension. During the 2–6 s after the motor-level NMES (7–11 s in the timeline), a significant ERS increase in the contralateral hemisphere and a significant ERS decrease in the ipsilateral hemisphere after stroke were observed (7–9 s: C1 3 5, CP1 3 4 5, P4 5; 9–11 s: FC2, C1 3, CP2 5, Pz 2 4 5). These significant ERS changes were maintained during the 6–12 s after the motor-level NMES (11–17 s), where the contralateral increase and ipsilateral decrease in ERS occurred within 6–8 s and 8–12 s after the motor-level NMES, respectively (11–13 s: AF4, FC2, P2, PO4; 13–15 s: Fz, FC3, Cz 1 3; 15–17 s: Fz, C1 3, CP1 3). The significant inter-group ERS difference occurred within 12 s after the motor-level NMES (5–17 s).

Sensory-level NMES after stroke exhibited a disappearance of ERD but a significant enhancement of ERS, mainly in the Cz and C2 channels of the central area. The ERD disappearance was observed in the stroke-affected limb compared to the controls both during and within the 2 s immediately after the sensory-level NMES (0–5 s and 5–7 s). A significant reduction in ERD in the ipsilateral hemisphere was found during the sensory-level NMES after stroke (0–5 s: C2 4 6, CP4 6). The significant ERS increase occurred mostly in the Cz and C2 channels, i.e., the central area, and partly in the

contralateral frontal areas after the sensory-level NMES (5–9 s: Cz, C2, F3, F5, FC5; 9–11 s: FC2 and Cz; 11–13 s: Cz and C2; 13–15 s: Cz, C2, F6). The significant inter-group ERS differences occurred within 10 s after the sensory-level NMES (5–15 s).

The intragroup comparison yielded significant changes in the cortical discrimination between the motor- and sensory-level NMES after stroke, i.e., a redistribution from the contralateral to the ipsilateral hemisphere during the NMES and additional recruitment of contralateral sensorimotor and ipsilateral frontal areas after the NMES, compared to the controls. Specifically, the significantly higher ERD in the motor-level NMES than the sensory-level NMES occurred in the contralateral hemisphere in the controls (0–5 s: FC1, C1 3 5, CP1 3 5, Pz 1 3, PO3; 5–7 s: FC1 3, C1 3, CP3) but in the ipsilateral hemisphere in the stroke group (0–5 s: C2, CP2 4; 5–7 s: Cz, CPz, CP2) during and within the 2 s after the motor-level NMES. Meanwhile, the controls exhibited a significantly higher ERS in the bilateral frontal area within 2 s immediately after the motor-level NMES compared to the sensory-level NMES (5–7 s: AF3 and AF4), while no significant ERS differences were observed in stroke participants. Furthermore, the unimpaired participants exhibited a significantly higher ERS, mainly in the ipsilateral hemisphere, during the 6–14 s after the motor-level NMES than that after the sensory-level NMES (11–13 s: AF4, Fz, F4, FC2; 13–15 s: FC2, Cz, C2; 15–17 s: F2, FC6, C6; 17–19 s: FC6 and C6). In contrast to unimpaired participants, the stroke group exhibited the significantly higher ERS in the contralateral sensorimotor and ipsilateral frontal areas during 6–12 s after the motor-level NMES than that after the sensory-level NMES (11–13 s: FC3, C1 3, CP1 3, P2; 13–15 s: C1, CP1, F4 6, FC6; 15–17 s: AF4, Fz, F4 6, FC4 6). No significant intragroup ERS differences were found in either group in the 2–6 s after the sensory-level NMES (7–11 s). The intra-group ERS differences occurred within 12 s and 14 s after the NMES in the respective stroke and control participants.

Figure 4-6 shows the ERD/ERS laterality index in the sensorimotor area when the sensory-/motor-level NMES was applied to the affected limb of the stroke group and the right limb of the control group. During the motor-level NMES (0–5 s, Figure 4-6 A), the significant change in ERD lateralization from the contralateral to the ipsilateral sensorimotor area after stroke was indicated by a significant decrease in the LI, from LI>0 to LI<0, in the stroke-affected limb compared to the controls ($p<0.05$, EF=1.08, independent t-test). In the 2–10 s after the motor-level NMES, significant changes in ERS lateralization from the ipsilateral to the contralateral sensorimotor area after stroke were indicated by a significant increase in the LI, from LI<0 to LI>0, in the stroke-affected limb compared to the controls ($p<0.05$, EF=1.17 in 7–9 s, EF=0.73 in 9–11 s, EF=0.69 in 11–13 s, EF=0.20 in 13–15 s, independent t-tests). There was no significant change in the LI-ERD/ERS after stroke within 0–2 s and 10–20 s after the motor-level NMES (i.e., 5–7 s, 15–25 s, $p>0.05$). During the sensory-level NMES (0–5 s, Figure 4-6 B), significant changes in ERD lateralization from the contralateral to the ipsilateral sensorimotor area after stroke were indicated by a significant decrease in the LI, from LI>0 to LI<0, in the stroke-affected limb compared to the controls ($p<0.05$, EF=0.89, independent t-test). There was no significant change in the LI-ERD/ERS after stroke within any period after the sensory-level NMES ($p>0.05$).

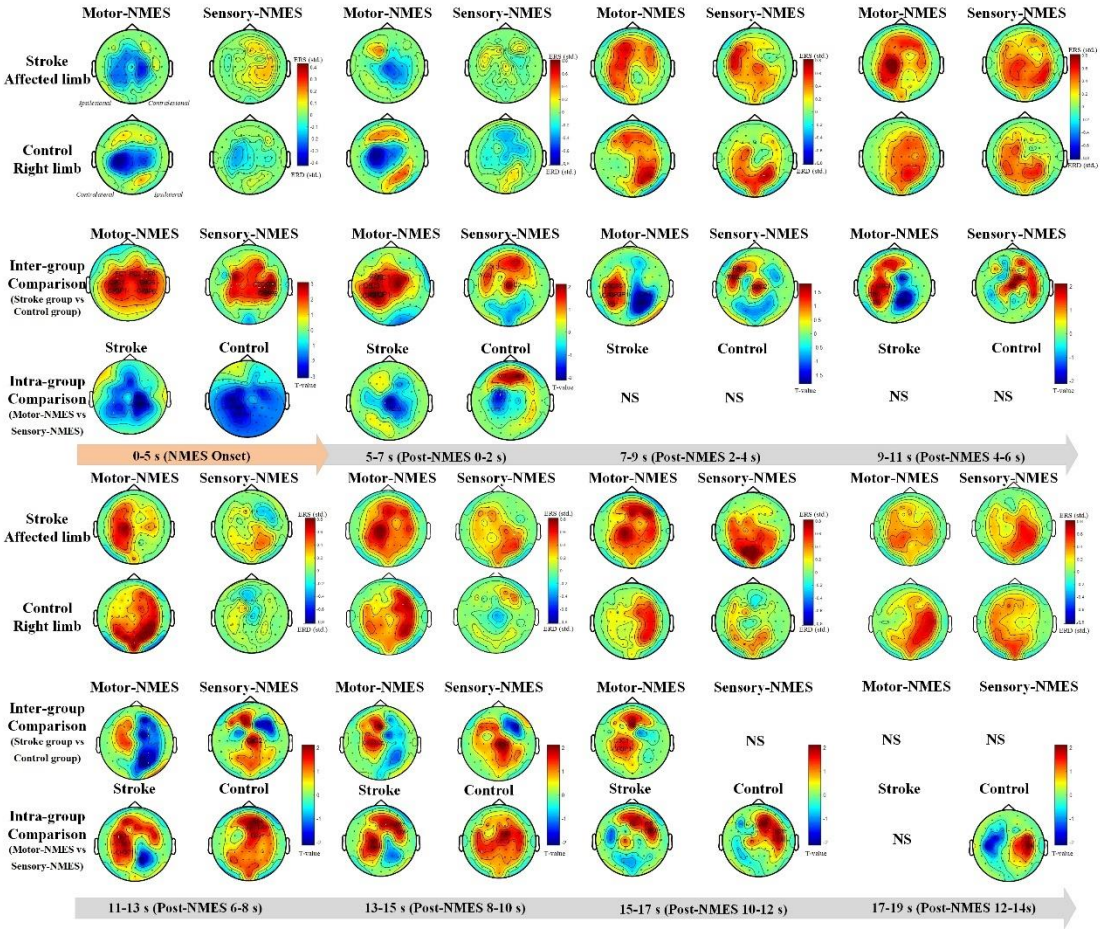

Figure 4-5. ERD/ERS topographies when sensory-/motor-level NMES was implemented in the affected limb of the stroke group and in the right limb of unimpaired participants. EEG channels with significant changes in the statistical comparison were denoted by the corresponding channel names.

4.3.2.3 Correlation between ERD/ERS features and sensorimotor impairments

Figure 4-7 shows the significant correlation between the clinical scores and the significantly changed ERD/ERS features after stroke, i.e., the LI-ERD and LI-ERS in motor-level NMES and the LI-ERD and the Cz&C2-ERS in the sensory-level NMES. The FMA-W/H scores exhibited a significant positive correlation with the LI-ERD during both sensory- ($r=0.609$, $p<0.05$) and motor-level NMES ($r=0.682$, $p<0.01$), but no significant correlation with either the LI-ERS after motor-level NMES ($r=-0.178$,

p>0.05) or the Cz&C2-ERS after sensory-level NMES (r=0.169, p>0.05). The MAS-wrist scores showed a significant negative correlation with the LI-ERD during the motor-level NMES (r=-0.641, p<0.05) and a significant positive correlation with the LI-ERS after the motor-level NMES (r=0.609, p<0.05). No significant correlation of the MAS-wrist scores was found with either the LI-ERD during the sensory-level NMES (r=-0.138, p>0.05) or the Cz&C2-ERS after the sensory-level NMES (r=0.411, p>0.05). Furthermore, the MAS-finger scores only showed a significantly positive correlation with the LI-ERS after the sensory-level NMES (r=0.578, p<0.05), but no significant correlation with either the LI-ERD/ERS during the motor-level NMES (r=0.387 for LI-ERD and r=0.265 for LI-ERS, p>0.05) or the LI-ERD during the sensory-level NMES (r=-0.006, p>0.05).

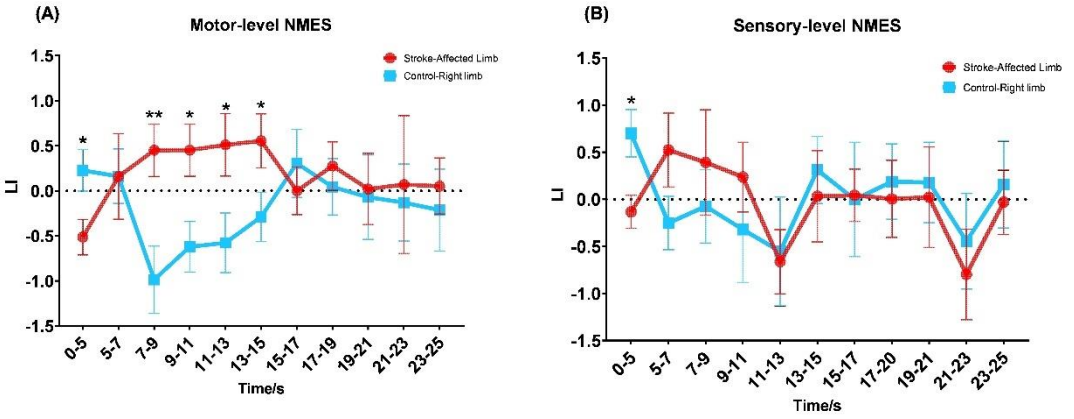

Figure 4-6. LI of ERD/ERS in the sensorimotor cortex when sensory- (A) and motor-level (B) NMES were implemented in the affected limb of the stroke group and in the right limb of unimpaired participants.

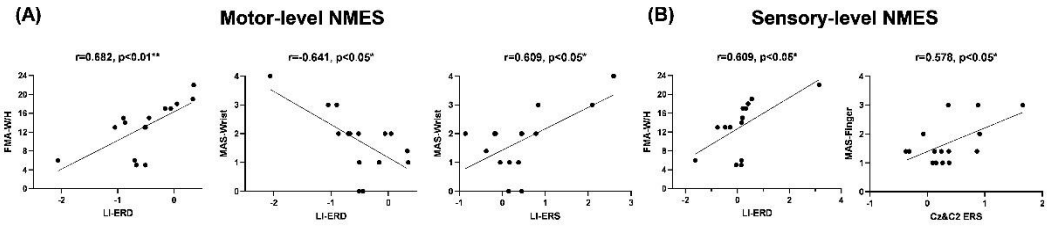

Figure 4-7. Significant correlation between the clinical scores and ERD/ERS features after stroke ($p<0.05$, Spearman's correlation), i.e., LI-ERD and LI-ERS in motor-level NMES (A), and the LI-ERD and C2&Cz-ERS in sensory-level NMES (B).

4.3.3 Functional connectivity changes in sensory-/motor-level NMES after stroke

Figure 4-8 shows the significant changes in functional connectivity after stroke during and after the sensory-/motor-level NMES (inter-group comparison between the stroke-affected and control-right limbs, $p<0.05$, cluster-based permutation test). The FC topographies highlighted significantly weakened FC after stroke from the central sensorimotor area to the contralateral, i.e., ipsilesional, hemisphere throughout both sensory- and motor-level NMES. Significantly enhanced FC after stroke occurred over the central sensorimotor area, mainly connecting with the dorsolateral prefrontal cortex during the sensory-level NMES, with the ventrolateral prefrontal and superior temporal areas after the motor-level NMES, and with the posterior parietal and inferior occipital areas after the sensory-level NMES; no significant FC enhancement was observed during the motor-level NMES ($p>0.05$). Specifically, during the motor-level NMES, significantly weakened FC after stroke was observed, all centering on the sensorimotor (Cz, C2, CPz, CP1, CP2) and somatosensory association (P1, P2, Pz) areas and connecting with the contralateral hemisphere, while no significant FC enhancement was found ($p>0.05$). In terms of connection intensity (i.e., t-values), the FC centers over the sensorimotor and somatosensory association areas exhibited the weakest connection (i.e., with the negative peak of the summed t-values) among all channels, with the following summed t-values: -79.3 at CPz, -61.6 at C2, -59.8 at CP2, -55.8 at Pz, -53.8 at Cz, -52.0 at CP1, -46.2 at P1, and -38.1 at P2.

During the sensory-level NMES, significantly weakened FC after stroke centering on the sensorimotor (Cz, C1, C2, CP1, CP2) and somatosensory association (Pz) areas was

also found, connecting mostly with the contralateral hemisphere and partly with the ipsilateral somatosensory association area. Meanwhile, there was significantly enhanced FC after stroke over the sensorimotor and somatosensory association areas, centering mainly on the dorsolateral prefrontal cortex (AF3 and AF4) and partly on the premotor (FC3) and somatosensory association areas (P1 and P2). In terms of connection intensity, the FC centers over the sensorimotor and somatosensory association areas (i.e., Cz, C1, C2, CP1, CP2, and Pz) exhibited the weakest connection among all channels, with the following summed t-values: -73.9 at C2, -56.0 at CP2, -53.1 at Cz, -36.4 at CP1, -35.4 at Pz, and -25.9 at C1. The FC centers over the prefrontal area (AF3 and AF4) exhibited the strongest FC (positive peak of the summed t-values) among all channels, with the summed t-values of -29.2 at AF3 and 23.7 at AF4.

After the motor-level NMES, significantly weakened FC after stroke centering on the sensorimotor area (C1, C2, CP1, CP2) was still observed, connecting mostly with the contralateral hemisphere and partly with the ipsilateral frontal and prefrontal areas. The sensorimotor and somatosensory association areas after stroke exhibited significantly enhanced FC centering on the ventrolateral prefrontal cortex (F5 and F6) and superior transverse temporal areas (C5). In terms of connection intensity, the FC centers over the sensorimotor area (C1, C2, CP1, CP2) exhibited the weakest connection among all channels, with summed t-values of -49.4 at CP2, -42.7 at C1, -34.5 at C2, and -24.9 at CP1. The FC centers over the transverse temporal (C5) and frontal (F5) areas exhibited the strongest connections among all channels, with summed t-values of 27.6 at C5 and 21.1 at F5.

After the sensory-level NMES, significantly weakened FC after stroke centering on the sensorimotor (C1, C2, CP1, and CP2) and somatosensory association (P1 and P2) areas was found to be connected with the contralateral hemisphere, while the sensorimotor

and somatosensory association areas exhibited significantly enhanced FC centered on the bilateral posterior parietal and inferior occipital areas (PO3, PO4, P5, and P6). In terms of connection intensity, FC centers over the sensorimotor and somatosensory association areas exhibited the weakest connection among all channels, with the following summed t-values: -36.5 at CP2, -28.4 at C2, -28.3 at P2, -27.0 at C1, and -21.7 at CP1. The FC centers over ipsilateral parietal (P5) and parietal-occipital areas (PO3) exhibited the strongest connection among all channels, with summed t-values of 34.5 at P5 and 36.9 at PO3.

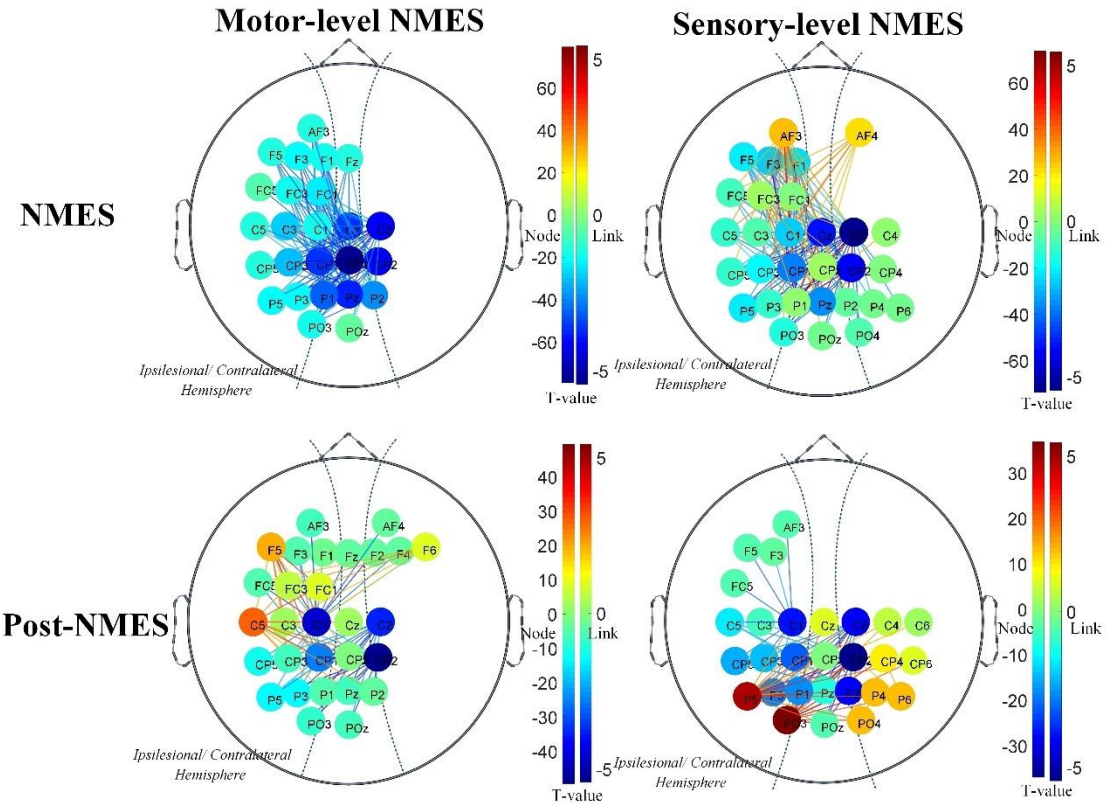

Figure 4-8. Significant FC changes during sensory-/motor-level NMES after stroke. Only EEG channels, i.e., nodes, with significantly changed FC between the stroke and control participants were plotted. The t-value in the statistical comparison was denoted by the color scheme on the links and nodes.

4.4 Discussion

The combined sensorimotor assessment of cortical reorganization following a stroke was examined in the study using the analysis of the neuromodulatory influences of sensory-/motor-level NMES based on EEG signals. Two groups were studied, one encompassing stroke survivors and the other encompassing unimpaired control subjects. A comparison of stimulation intensities and EEG-derived ERD/ERS and FC in sensory-/motor-level NMES was made between the two cohorts in order to appraise behavioral and neurological alterations of the post-stroke reorganization of the cortex in sensorimotor deficits. It was demonstrated that in the stroke subjects, sensory- and motor-level NMES intensities were elevated. These were related to voluntary motor performance and spasticity as determined by hand-wrist joint clinical scoring systems. During sensory-/motor- level NMES, several alterations in ERD/ERS and FC were revealed, suggestive of the changed cortical activation and connectivity patterns seen following a stroke and during cortical reorganization. The latter was additionally associated with functional behavior differences as evidenced by clinical score parameters for the hand-wrist joint.

4.4.1 Increased sensory/motor-level NMES intensities after stroke

In the stroke cohort, sensory- and motor-level NMES intensities were utilized as an immediate behavioral parameter for an integrated sensorimotor assessment carried out using regulated stimulation of sensory and motor nerve cells. Compared to the unaffected limb and both limbs of the controls, the affected stroke limb displayed a rise in sensory- and motor-level NMES intensities (Figure 4-3A). Motor-level NMES intensity was positively related to wrist/hand spasticity (MAS-wrist and finger). Sensory-level NMES was negatively associated with voluntary motor performance (FMA-W/H), but the intensity of sensory-level NMES was positively linked with hand spasticity (MAS-finger) (Figure 4-3B). The collected data showed that the behavioural

alterations associated with both sensory and motor deficits in the hand and wrist joints following a stroke could be evaluated using sensory- and motor-level NMES intensities. Although the depolarization of sensory axons contained within a mixed nerve bundle was possible with the use of varying NMES formulations for touch, vibration, pricking pain and temperature sensations [182] [183], earlier electro-tactile research has shown that in the current experiment, tactile sensation was conscripted through the Pacinian corpuscle and Merkel disc mechanoreceptors [183] [184]. The subjects did not verbalize any symptoms of discomfort during the trials, and so the rise in sensory-level NMES intensity noted in stroke survivors implied that for sensory perception to occur, enriched sensory afferents were necessary, principally through the recruitment of dermal tactile receptors. Conventional clinical appraisals have demonstrated equivalent elevations in thresholds for sensory perception in individuals following a stroke. Examples include an extension of the minimal discernible distance on the two-point discrimination test and the larger required diameter in order to positively respond to the monofilament test [185] [186]. The identified relationship between voluntary motor performance and spasticity (clinical scores of FMA-W/H and MAS-finger) in this study is in keeping with earlier work which has demonstrated that attenuated motor skills following stroke were associated with sensory deficits [12]. Diminished awareness of the body and the lack of certainty regarding peripheral functionality, such as muscle activation, proprioception and direction of motion, have been recognized following extended motor performance fortified by visual compensation in stroke subjects with somatosensory deficits [15]. Spasticity following a stroke has also been associated with numbness in relation to light touch, proprioceptive and thermal sensations [15]. However, when motor-level NMES was applied, conscription of motor units occurred through both immediate recruitment of efferent pathway motor neurons and also

following the secondary conscription of tracts in the corticospinal columns [70] [187]. The latter reflected the activation of afferent pathway sensory receptors which encouraged sensorimotor integration. Thus, the motor-level NMES intensity rises seen in the current work implied that compared to controls, in stroke survivors, activation of both motor and sensory neurons was amplified in order to achieve a full range of hand-wrist extension, essentially as a result of cortical sensorimotor integration deficits. These observations are referred to subsequently in 4.4.3 Altered cortical connectivity in sensory/motor-level NMES after stroke. The positive association of motor-level NMES intensity spasticity (MAS-wrist/finger) was not unexpected, as in stroke survivors, UE extension is generally hindered by the rise in muscle tone linked with spasticity of the flexors [138]. Frequently, an enduring involuntary contraction was present in the latter, caused by diminished reciprocal inhibition from the opposing extensor muscles [161]. Such observations substantiated the use of the hand-wrist extensor muscles as the subjects of the integrated sensorimotor evaluations as they are generally subject to a higher degree of deficit in comparison to the flexor musculature [168] [138]. Additionally, in subjects (n=2) with marked sensory deficits, e.g. FMA-wrist/hand light touch =0, a sensory stimulation was felt prior to the first twitch of the muscle following the application of sensory-level NMES; there was no overlapping of the NMES intensity perceptual and motor thresholds. The FMA sensation evaluation only offered one strength of stimulation as applied by hand, and was measured in a straightforward ordinal scale where 0=anaesthesia, 1=hypoaesthesia, and 2=normal. Thus, the clinical assessments are unlikely to be sufficiently sensitive to identify modest changes in sensory impairments in stroke survivors. When judged against clinical scoring systems conventionally used for appraisal in clinical practice, the sensory-level NMES applied in the present work offered a stimulation that could be regulated, had a

high resolution and exhibited a high degree of sensitivity for efficacious sensory evaluations in this patient population.

4.4.2 Altered ERD/ERS in sensory/motor-level NMES after stroke

The feasibility of the motor-/sensory-level NMES for the integrated sensorimotor evaluation was demonstrated by the consistent ERD/ERS findings in the control group as in previous works, where the ERD patterns in motor-level NMES was similar to those in the voluntary movements without significant correlation with those in passive movements [173]. It indicated that both motor and somatosensory systems in the closed-loop sensorimotor network were activated by the motor-level NMES, which recruited motor units on target muscles not only by the direct activation of descending motor neurons, but also by the indirect activation of corticospinal tracts via the activation of ascending sensory neurons through the cortical sensorimotor integration [69].

In comparison with the controls, the time-frequency and spatial-temporal ERD/ERS during motor-level NMES indicated a notable redistribution of ERD from the contralateral to the ipsilateral hemisphere during stimulation (0–5 s), and a redistribution of ERS in the alpha and beta bands in the stroke-affected limb during stimulation (5–15 s). These results are illustrated in Figure 4-4, 5 and 6. A decline in ERD with elevated ERS was additionally seen in the ipsilesional hemisphere of stroke survivors compared to the controls. In this cohort, the identified redistribution trends of ERD and ERS were significantly correlated to voluntary motor performance, i.e., LI-ERD and FMA-W/H, and spasticity, for instance, i.e., LI-ERD/ERS and MAS-wrist (Figure 4-7). The results implied that the combination of motor-level NMES and EEG had the potential for the assessment of reorganization of the cortex in stroke survivors with motor deficits. These were evidenced by changes in the dominance of the

hemispheres not only during stimulated cortical activation but also during the recovery phase of the cortex following stimulation. Diminished excitation was noted in the ipsilesional hemisphere during the stimulation, representing ERD, whereas excessive inhibition was observed following the procedure, reflecting ERS. The contralesional hemisphere demonstrated opposing findings as a result of cortical compensation [49]. When compared with the application of motor-level NMES in the current study, it has been generally challenging to attain a uniform movement pattern using targeted musculature in stroke survivors in earlier MI/ME-based assessments of motor function, owing to the marked motor loss or severe deficits, and the proximal compensation in individuals with moderate deficits [10][169]. There was even no requisite for movement in the earlier work [49]. The absence of a uniform movement in the ME/MI-based motor assessments led to inadequate excitation, both centrally and peripherally, and indistinct sensorimotor responses within the cortex [49]. The majority of MI/ME-based methods therefore obtained the redistribution of ERD and ERS within a slender time-frequency window, typically in relation to the alpha band in the second following MI/ME [188] [102] [189]. The ME of hand grasping and opening utilized by Kasier et al. could only be applied to 17/29 subjects who were suffering from residual deficits following a stroke; the remainder carried out the protocol, but only the alpha band detected any ERD/ERS redistribution [169]. Even in stroke survivors who have demonstrated significant recovery and who only have mild deficits, there is a lack of ME studies that have observed a notable decline in beta-ERD [37]. The absence of alterations in beta-ERD/ERS could imply that the reafference of the target musculature in terms of proprioception and kinesthetic for MI/ME tasks was inadequate; in unimpaired subjects, alpha- and beta-ERD reflect the efferent motor regulation and afferent sensory feedback in voluntary motion, respectively [190] [69]. In contrast to

the above research performed using MI/ME, the present motor-level NMES could be used in stroke survivors with a range of deficits; it enabled the evaluation of a standard movement with enduring activation of target musculature afferent and efferent pathways [70]. Thus, this method facilitated the assessment of the redistribution of ERD and ERS in an expanded time-frequency window in contrast to MI/ME, i.e. in both alpha and beta bands and within the 10 s following conclusion of the NMES. Although NMES only induces passive movement, the combination of motor-level NMES and EEG utilized in this study has the potential to provide an informative motor evaluation in stroke survivors than MI/ME-based evaluation.

The sensory-level NMES and EEG were exploited in order to detect the reorganization of the cortex in post-stroke sensory deficits. The acquired time-frequency and spatial-temporal ERD/ERS data during sensory-level NMES stimulation demonstrated a redistribution in ERD from contralateral to the ipsilateral hemisphere (0-5 s); following sensory-level NMES stimulation ERS was elevated in the alpha and beta bands from the C2 and Cz channels (5-15 s) in comparison to the control subjects (Figure 4-4 – 4-6). These alterations in ERD and ERS were linked with voluntary motor performance and finger spasticity, as assessed by LI-ERD and FMA-W/H, and C2- and Cz-ERS and MAS-finger, respectively (Figure 4-7). These data infer that this technique could be efficacious for the assessment of cortical reorganization of sensory deficits after stroke, and that these are evidenced by changed dominance of the hemispheres during stimulation and excessive central region inhibition following stimulation. The change in the dominant hemisphere in stroke survivors could be related to the compensatory contribution of the unaffected contralesional hemisphere, an explanation that has been proposed following work on tactile sensation [168]. In studies using fMRI, the link between this phenomenon and the natural reparation of sensory functions has been

demonstrated in the initial six-month period following a cerebral insult; a positive association was identified with tactile discrimination test scores [34]. Furthermore, in the present experiment, during sensory-level NMES, the positive relationship between the hemispheric dominance (LI-ERD) and voluntary motor performance (FMA-W/H) suggested the compensatory input to motor deficits in the presence of sensory deficits in stroke survivors, arising from the reorganization of the cortex. Despite the fact that sensory deficits could be appreciated using NMES and EEG methods by SEP, cortical reorganization could not be identified, and the extent of a post-stroke deficit could not be quantified [172]. SEP is dependent on the presence of event-related potential (ERP) constituents in a lone EEG channel in order to recognize an intact pathway, i.e. whether or not the N30 constituent was recognized as present reflected sensory loss or normality, respectively [191]. Additionally, these results could enhance the available information on the neuronal origin of spasticity seen following stroke; the excessive central regional inhibition may add to spinal cord alpha motor neuron disinhibition and the arising increased tone within the musculature; this was suggested by the positive association identified between the C2- and Cz-ERS and MAS-finger tone. Despite the fact that accrued findings from various studies have substantiated the likelihood that spasticity originates at a level above the spine with the hyperexcitation of alpha motor neurons as a consequence of impaired descending moderation, overall cortical mechanisms contributing to the condition have not been well-established [64]. In general, the ERD/ERS data from this work have implied that in stroke survivors, an efficacious and integrated sensorimotor assessment of cortical reorganization could be achieved with the application of sensory/motor-level NMES and EEG.

In this study, the stroke-unaffected limb and the control-right and control-left limbs demonstrated no changes in ERD/ERS. However, in comparison to the controls, during

motor-level NMES on the stroke-unaffected limb, a marked reduction in mean ERD and rise in mean ERS was seen in the contralateral hemisphere in alpha and beta bands, an observation equivalent to the affected limb's change in mean ERD/ERS. These findings may represent a change in cortical sensorimotor responses in the stroke-unaffected limb as a result of contralesional sensorimotor cortical disinhibition during cortical reorganization [10]. Earlier work on post-stroke motor assessments has observed changes in pathway-specific corticomuscular interactions, joint kinematics, and degrees of muscle activation in the unaffected side [10] [157]. An earlier study by the authors evaluated the fine motor skill of finger extension in stroke survivors, observing a changed trend in descending dominance, with a greater descending as opposed to ascending dCMC from the agonist ED to the synergistic brachii muscle in the unaffected limb. These data inferred that following a stroke, there could be a change in the degree of recalibration of cortical sensorimotor function influencing the descending motor patterns via sensory reafference in relation to the unaffected limb [10].

4.4.3 Altered cortical connectivity in sensory/motor-level NMES after stroke

In this study, the combined sensory-/motor- level NMES and EEG for sensorimotor assessment demonstrated diminished cortical connectivity between the somatosensory regions and the ipsilesional hemisphere in the cortical reorganization following stroke. The results emphasized the attenuated FC in stroke survivors during sensory- and motor-level NMES focusing over the somatosensory regions bilaterally and linking with the ipsilesional hemisphere (Figure 4-8). These findings were especially prominent with motor-level NMES, during which the t-value was lowest within all studied topographies. The decline in intercortical communication between somatosensory areas and the ipsilesional hemisphere suggested the reduced capacity of

the cortex for sensorimotor integration, which could also play a role in the altered ERD/ERS patterns observed in the ipsilesional hemisphere. Thus, although the rise in sensory-/motor-level NMES intensities indicated enhanced sensory inputs to the somatosensory regions following a stroke, there was an absence of this sensory data being relayed or integrated into the ipsilesional hemisphere in order to facilitate sensory perception and motor command instigation. The FC patterns was different in the unimpaired control participants. Integration within the cortical sensorimotor area could be induced by somatosensory afferents relaying data on proprioception, kinesthetic and tactile sensations during motor-level NMES, thus enabling motor output to be established and transmitted via corticospinal activation in a manner equivalent to voluntary movement [70]. The current results relating to abnormal cortical sensorimotor integration substantiate the earlier findings obtained from dCMC assessments which, in stroke survivors as opposed to controls, suggested a rise in ascending feedback in the absence of adaptations in descending regulation during the lesser stable interval of digit extension [10]. Consequent to the deficit in cortical sensorimotor integration, there was a failure to readjust the descending motor output in relation to the contrast between anticipated and the true afferent peripheral information relating to voluntary movement [10]. Such corticocortical and corticomuscular connectivity observations uniformly indicate that the abnormal sensorimotor readjustment arose in an inefficient closed-loop neuromuscular network following stroke [10].

The combined sensory-/motor-level NMES and EEG method used for the integrated sensorimotor assessment also led to the detection of cortical compensation, i.e., input from remote regions to the somatosensory areas following the cortical reorganization process after stroke. This was evidenced by the augmented FC over the somatosensory

areas. During the sensory-level NMES, this was seen through linkage with the DL-PFC (AF3, AF4); following sensory-level NMES with the posterior parietal (P5, P6) and inferior occipital regions (PO3, PO4) and after motor-level NMES, with the VL-PFC (F5, F6) and superior temporal territories (C5). Compensation within the cortex generally arose in association with the responsive regeneration of nerve cell in regions adjacent to stroke lesion; the connections between remaining nerve cells was restored, especially within the cortex in proximity to the site of vascular injury [98]. Within the present work, the sensory-level NMES was able to conscript further involuntary attention which made up for the deficits in tactile sensation in the stroke survivors; this encompassed alertness attention from the DL-PFC in the course of the stimulation as well as the spatial perception and episodic recall originating from the parietal and inferior occipital regions following the process. Involuntary attention, characterized by external attention induced by brief stimuli, could be gained owing to the reduced active mental processes and the endeavors to exclude any additional visual and audio distractions during the trials, as in earlier work on fine tactile sensation [168]. In order to complete complicated cognitive tasks, such as motor planning and abstract reasoning, focal attention derived from the DL-PFC is vital [103]; thus, the promoted FC between DL-PFC and somatosensory regions could infer that higher level attention functionality was enrolled in order to make up for the diminished tactile sensation in the sensory-level NMES following stroke. The enduring conscription of involuntary attention also occurred in stroke survivors following the stimulation, possibly in relation to spatial perception and episodic retrieval of sensory data. This was evidenced by the increased FC following sensory-level NMES to the somatosensory regions from the posterior parietal and inferior occipital areas. The latter have been described as major components giving rise to self-directed attention in relation to extrinsic triggers for

spatial attention and episodic recall of movement traces in normal subjects [193] [194]. In the current study, the increased FC following motor-level NMES reflected a rise in VL-PFC and superior temporal regions following a stroke in terms of suppressing cortical motor function, and motor re-education in the 'learner-disused' hand-wrist articulations. The VL-PFC has been determined to have the ability to supersede current motion, to revise motor plans and to learn from errors made in earlier VL-PFC functional synthesis [195]. The superior temporal region is thought to partake in the rectification of proprioception mistakes. In a fMRI study, more errors in proprioception were related to a lower level of activity in the ipsilesional temporal gyrus when completing an arm position matching activity [196]. Thus, the augmentation in FC seen following motor-level NMES in the present work could provide evidence for the potential treatment applications of NMES on post-stroke motor relearning.

This work demonstrated the effectiveness of sensory-/motor-level NMES and EEG on the measurement of both behavioral and neurological changes in the integrated sensorimotor evaluation of cortical reorganization after stroke. In future works, a longitudinal study will be conducted to investigate the prognostic values of the proposed ERD/ERS and FC metrics for predicting the clinical outcomes by monitoring the rehabilitative progress on sensorimotor functions.

4.5 Periodic Summary

The integrated sensorimotor evaluation of cortical rearrangement after stroke was investigated by analyzing the neuromodulatory effects of sensory-/motor-level NMES based on EEG signals, in comparison with the unimpaired controls. In the results, behavioral changes in the sensorimotor impairments were indicated by the significant increase in sensory- and motor-level NMES intensities in stroke participants than the controls and its significant correlation with clinical scores. Significant ERD/ERS and

FC changes after stroke visualized the ERD redistribution from the ipsilesional to the contralesional hemisphere, the ERS increases in the ipsilesional hemisphere and central areas, the weakened FC between the ipsilesional hemisphere and somatosensory areas, and the FC enhancement from other regions to somatosensory areas. These findings suggested that cortical rearrangement in sensorimotor impairments after stroke could be characterized by alterations in hemispheric dominance, cortical over-inhibition, impaired cortical sensorimotor integration, and cortical compensation, in sensory- and motor-level NMES. Notably, sensory- and motor-level NMES combined with EEG could be more informative for sensorimotor evaluations of cortical rearrangement than the previous MI/ME-based motor assessments and SEP-based somatosensory assessments, as revealed by the significant ERD/ERS changes after stroke. The post-stroke cortical rearrangement represented by the ERD/ERS changes was also significantly correlated with the behavioral changes measured by clinical scores in the hand-wrist joint. Thus, sensory-/motor-level NMES and EEG could measure both behavioral and neurological changes in sensorimotor impairments after stroke, demonstrating its effectiveness for the integrated sensorimotor evaluation of Cortical rearrangement.

Table 4-1a. Participants' demographic data.

Group	No. of participants	Stroke types, hemorrhage/ ischemic	Affected side, left/right	Gender, male/ female	Age (years, mean ± s.t.d)	Min/Max Years after stroke
Stroke	15	6/9	7/8	7/8	57±9	5/20
Control	20	-/-	-/-	11/9	46±10	-/-

Table 4-1b. Clinical scores of the stroke participants.

Clinical assessment	FMA full motor score	FMA shoulder/ elbow	FMA wrist/ hand	FMA sensory	ARAT	FIM	MAS elbow	MAS wrist	MAS finger
Score (mean± std)	34.47± 13.84	21.07± 9.84	13.2± 5.4	1	19.27±1 2.71	64.67±2 .16	1.91± 0.77	1.76± 1.09	1.69± 0.74

Table 4-2a. Sensory-/motor-level NMES intensities in both limbs of both groups.

Clinical scores \ NMES intensity	Sensory-level NMES intensity	Motor-level NMES intensity
FMA-W/H	r=-0.612, p<0.05*	r=0.136, p=0.630
MAS-finger	r=0.563, p<0.05*	r=0.697, p<0.01**
MAS-wrist	r=0.442, p=0.100	r=0.727, p<0.01**

The superscript "" denotes the significant correlation with 1 superscript for p<0.05 and 2 superscripts for p<0.01.*

Table 4-2b. Correlation between the clinical scores and sensory-/motor-level NMES intensities in the affected limbs of the stroke groups.

Group	Limbs	Sensory-level NMES intensity	Motor-level NMES intensity
		Mean±SEM	
Stroke	Affected limb	12.33±0.75	35.73±3.04
	Unaffected limb	10.13±0.51	24.00±1.61
Control	Left limb	9.05±0.29	19.20±0.89
	Right limb	9.15±0.31	18.40±0.96
One-way ANOVA P (Partial η^2)		0.000*** (0.32)	0.000*** (0.50)

The superscript "" denotes the significant inter-group difference with 1 superscript for P<0.05, 2 superscripts for P<0.01, and 3 superscripts for P<0.001.*

CHAPTER 5

CLOSED-LOOP SENSORIMOTOR REHABILITATION ASSISTED BY CMC-EMG-TRIGGERED NMES-ROBOT AFTER STROKE

5.1 Introduction

The permanent motor disability was observed in the paretic hand and wrist joints in > 80% of stroke survivors, limiting their independence in daily tasks [48]. It typically manifested as spasticity, muscle weakness, and discoordination regarding the proximal muscular compensation, mainly due to the poorer and more slowly recovering in the hand-wrist than elbow-shoulder joint after stroke [10, 97]. There was also a lack of long-term healthcare service in traditional physical therapy after being discharged from the hospital due to the professional manpower shortage of physical and occupational therapists [49]. Rehabilitation robots have been developed as an alternative strategy to assist the rehabilitation practice post-stroke with high repetition and lower costs [49]. Meanwhile, closed-loop neurorehabilitation promoting the excitation in both descending and ascending cortico-muscular pathways is the dominant force to drive functional neuroplastic processes in both central and peripheral nerve systems in post-stroke recovery [49]. It was because that the voluntary motion requires both descending motor control and ascending sensory feedbacks for precise coordination between the motor and muti-sensory systems, particularly during distal finger movements with precise control, e.g., hand dexterity and postural stabilization [59] [10]. Among the rehabilitation robots, voluntary movement-driven control and NMES (i.e., the motor-

level NMES throughout this Chapter) sensorimotor feedback have been employed as key strategies for promoting closed-loop neurorehabilitation after stroke [60].

In contrast to those with continuous passive motions (CPM), rehabilitation robots that are triggered by users' active participation have demonstrated higher efficacy [48]. However, little has been done on an effective control design engaging the voluntary motor efforts (VME) from both central and peripheral nerve systems for the closed-loop neurorehabilitation in motion practice after stroke. Current rehabilitation robots with user's voluntary inputs are mainly triggered by either the central intention or the peripheral activities in the motion practice [49]. In brain computer interface (BCI)-driven rehabilitation robots, the central-intention-triggered control strategy was adopted by detecting the movement intention, mostly via EEG in the sensorimotor cortex, during motor imagery (MI) without the requirement of motor execution (ME) [60]. For the neural mechanism, similar cortical activation patterns between MI and ME was reported in fMRI studies, e.g., activating the contralateral sensorimotor areas [61]. The BCI-MI has shown effectiveness on those with severely motor disability, e.g., persons with spinal cord injury, as it can bypass the damaged central-to-peripheral pathways [62]. However, the effectiveness of BCI-MI has been questioned in stroke rehabilitation [60]. For example, in a previous randomized control trial on subacute stroke, a similar motor outcome was achieved in participants with BCI-MI intervention compared to those with passive motion without the traditional therapies [60]. Although enhanced rehabilitation effectiveness has been reported in the MI combined with motor attempts in BCI systems, where subjects tried to move the affected limb even no active movements, the cortical compensation, e.g., the overexcitation in the contralesional side of the brain, was still failed to be inhibited with limited long-term rehabilitation effectiveness [38] [60]. On the other hand, the electromyography (EMG) has been

frequently applied in peripheral-effort-triggered robots to represent the voluntary motor efforts in target muscles with residual motor abilities after stroke [48]. The amplitude of EMG envelope could be proportional to the output force in a target muscle with robutness against the cancellation effects among discoordinated muscles and high signal-to-noise ratio compared to kinetic/kinematic signals [48]. Despite this, robotic misdrive could be triggered by the involuntary EMG due to muscular spasticity, which occurred in the passive contraction from compensatory motion in synergistic muscles or the releasing challenges following earlier contractions [63]. Despite the neural source of spasticity was largely unknown, lesions of the upper motor neurons in the cortex and/or brainstem might disinhibit the gain of many spinal reflexes (including the stretch reflexes) [64, 197]. In rehabilitation training assisted by the EMG-driven robots after stroke, unexpected motor outcomes in the proximal shoulder and elbow joints, were commonly observed despite only EMG recordings from the distal UE, e.g., hand and wrist joints in motion practice, due to the compensatory motion from the proximal to the distal UE [50]. Nonetheless, the post-stroke compensatory motion has been corrected by visual observation and manual operation, which was labor-demanding and inaccurate for invisible muscle discoordination in the precise hand control [65]. Therefore, the central-intention-triggered and peripheral-effort-triggered robots had limited effectiveness on the motor restoration in the target muscles with a lack of the inhibition cortical and muscular compensation. Effective robotic control engaging the central-to-peripheral VME in motor practice was needed for the closed-loop neurorehabilitation after stroke.

In rehabilitation robots, NMES has been combined with central-intention-triggered and peripheral-effort-triggered control strategies as the motion rewards to the voluntary inputs in motion practice after stroke [56] [70]. The NMES can provide sensorimotor

experience on target muscles by depolarizing both sensory and motor axons via electrical currents on the skin [70]. Previous neuroimaging studies reported that both efferent, i.e., descending, and afferent, ascending, pathways were activated by NMES. Motor units on target muscles was recruited in NMES not only by the direct activation of descending motor neurons, but also by the indirect activation of corticospinal tracts via the activation of ascending sensory neurons due to the cortical sensorimotor integration [69]. However, the rehabilitation effectiveness of NMES for the closed-loop neurorehabilitation after stroke was not investigated yet. This was mostly caused by a dearth of neurological assessments for the pathway-specific corticomuscular communication in NMES-assisted rehabilitation programs. Previous randomized control trials (RCT) mainly investigated the rehabilitation effectiveness of NMES from the peripheral level with traditional manual assessments [48] [60]. It was found that NMES could contribute to release spasticity, improve muscle weakness, and reduce compensatory motion related with "learned-disuse" after stroke [48]. For example, XL-HU et al. investigated the different rehabilitation effectiveness between the EMG-driven NMES-robot and EMG-driven robot for motor restoration in wrist joints after stroke [48]. It was found that the NMES-robot–assisted wrist training was more effective than EMG-driven robot, where the included NMES assistance could enhance the motor improvements in the distal UE and release the muscular co-contraction related to proximal muscular compensatory. A recent meta-analysis on BCI-driven rehabilitation systems found that BCI-driven NMES systems achieved better motor outcomes in the UE after stroke than BCI-driven robots after the training [60]. Results found that the motor improvements indicated by the pooled effect size was significantly higher in the BCI-driven NMES systems than the NMES alone and other intervention, without significant improvements in BCI-driven robots.

Despite the enhanced motor improvements by the NMES sensorimotor feedback, most rehabilitation robots still engaged VME from central nerve systems in isolation with that from the peripheral nerve system in the control design. Although a few hybrid BCI systems driven by both EEG and EMG signals were proposed [66], there was a lack of significant improvements of the efficacy in the hybrid BCI systems after stroke compared to the EEG- and EMG-driven systems. The robotic misdriving could still occurred with the involuntary EMGs in MI and MA, due to the lack of central-to-peripheral VME in motion practice. The CMC has been adopted to extract the central-to-peripheral VME with the estimation of the spectral correlation regarding EMG and EEG. It could quantify the neural synchronization between the sensorimotor cortex and target muscles in active movements [67]. For example, the attenuation and moved location of the peak CMC were connected to the impairment levels of the post-stroke motor deficiency. CMC has also been applied for neurological assessment on motor deficits in target muscles after stroke [67] [68]. In our previous work, a CMC-EMG-triggered NMES-robot system employing CMC as an indicator of central-to-peripheral VME was developed to provide guidance and assistance for active hand-wrist movement in stroke patients [49]. Our device could engage the central-to-peripheral VME in the user by the CMC-EMG-triggered control and provide sensorimotor feedbacks to the user by the NMES-robot. A pilot trial proved that our system could contribute to precise restoration on hand and wrist joints, showing inhibition on cortical and muscular compensation, and improvements of the central-to-peripheral VME among different UE muscles [49]. However, little was know on its rehabilitation effectiveness for the closed-loop neurorehabilitaion in both descending and ascending pathways after stroke. This was mostly caused by a dearth of understanding on the contribution of NMES sensorimotor feedback to the precise hand-wrist rehabilitaiton

in the CMC-EMG-triggered NMES-robot system. In other words, whether the rehabilitation effect of the CMC-EMG-triggered NMES-robot is comparable or better than CMC-EMG-triggered robot remains unknown. Therefore, the objective of this study is to investigate the closed-loop neurorehabilitation of an CMC-EMG-triggered NMES-robot and a CMC-EMG-triggered robot for the hand and wrist joints in a randomized controlled trial with a 3-month follow-up (3MFU).

5.2. Methods

5.2.1 Subject recruitment

This study was approved by the same ethical committee as in Chapter 2 with the same approval number. The stroke participants met the same inclusion criteria as the Chapter 3. This study involved a RCT with a 3MFU test. All participants were informed that they could receive a training program with either CMC-EMG-triggered NMES-robot, i.e., the NMES group, or the CMC-EMG-triggered robot, i.e., the control group. The written consent on the experiment purpose was obtained from all subjects prior to the commencement of the research as in the Chapter 2. Figure 5-1 shows the consolidated standards of reporting trials with the flowchart of the training program. Using a random number generator on Matlab (“1” and “2” denoting the respective NMES and control group), the recruited volunteers were split into two groups randomly with an equal probability.

5.2.2 Interventions

The participant in each group was given the opportunity to take part in a 20-session robotic hand training program with a weekly attendance rate of three to five [49]. Figure 5-1 shows the system setup of both groups, i.e., the CMC-EMG-triggered NMES-robot (A) and CMC-EMG-triggered robot (B), which provided guidance and

assistance for the hand-wrist motions [49]. In the system, a self-made LabVIEW control platform was employed to manage the EEG and EMG signal gathering and processing, visual guidance of the target motion, and sensorimotor feedbacks (by the NMES-robot in the NMES group and by the robot in the control group) in real-time for the closed-loop feedback control. The EEG and EMG acquisition setup was similar to the Chapter 3, except that the two-channel EMG signals were acquired from the muscle union of the extensor carpi ulnaris (ECU) and the extensor digitorum (ED), i.e., ECU-ED, and the muscle union of flexor carpi radialis (FCR) and the flexor digitorum (FD), i.e., FCR-FD, in the respective hand-wrist extension and flexion. The FCR-FD and ECU-ED were treated as muscle unions given their confined muscle bellies and close anatomical closeness [49]. In the CMC-EMG-triggered control, the central-to-peripheral VME was represented as the significant peak CMC over the sensorimotor area and the EMG activation within target range (10%-30% iMVC) in the agonist's muscle. The CMC and EMG quantified the respective cortical-originated VME and the peripheral VME in closed-loop neuromuscular systems [49], when the participant performing the 10-s target motion. The calculation of the peak CMC and the level of EMG activation was the same as the Chapter 3 [10].

For the NMES group, the NMES-robot (Figure 5-1, lower right panel) would be triggered to provide sensorimotor assistance on the target motion, i.e., trigger success, once captured the desired CAP-VME. If trigger failed, no sensorimotor assistance would be provided and the user have to repeat the current target motion in the next trial. One-channel NMES on ECU-ED was used to provide sensorimotor assistance for the hand-wrist extension, which generates square pulse and has an adjustable pulse width of 0-300 μs with other parameters kept constant at 70 V, 40 Hz), without NMES to the FCR-FD, as practiced previously [56]. The reason of one-channel NMES was that most

persons with chronic stroke can perform the hand-wrist flexion voluntarily [56]. For the control group, the only difference with the NMES group was that only robot without NMES was triggered when trigger success. For both groups, visual instruction was provided showing the real-time, the required and desired levels of EMG activation, as well as the desired motion/rest states (hand-wrist extension or flexion, or rest) (Figure 5-1, lower left panel).

In the training preparation, the participant in each group was invited to take a seat in front of the computer comfortably [49]. Then, the EEG cap and two-channel EMG electrodes on FCR-FD and ECU-ED, were prepared onto the subjects, with similar procedure as in Chapter 3 (Figure 5-1 (A)) [125]. The iMVC test was then performed on the target muscles, FCR-FD and ECU-ED, to obtain the EMG_{Max-i} and EMG_{Base-i} on each muscle with the same procedures as in Chapter 3, which could reduce bias resulted from the positioning variance of EMG electrodes in different training sessions [49]. The robotic module was worn onto the hand-wrist joint using a bracing system that applied adjustable skin pressures [49]. The testing limb was raised to a horizontal position using a hanging device to allow for gravity correction on the limb. The wrist and elbow joints were extended to of 45° and 180°, respectively, with the testing hand at a neutral position. For the NMES group only, the NMES electrodes was attached onto ECU-ED (Figure 5-1 (A), lower right panel) [56]. The NMES intensity for full hand-wrist extension was identified individually by adjusting pulse width, which was the highest tolerable level under the painful threshold without muscle fatigue during the training [56].

During the training, the participant in each group practiced the target motion, i.e., hand-wrist extension and flexion, according to the visual interface's instructions (Figure 5-1 A lower left panel). In each trial, the participant initiated the target motion within 3 s

following the start cue and held the motion for 10 s within the required contraction range [49], with the same motion requirements as in the dCMC evaluation in Chapter 3. Immediately following the 13-s motion, the motion assistance would be provided to the participant from the NMES-robot in the NMES group or from the robot in the control group, once there were desired central-to-peripheral VME levels. Otherwise, the participant would be begin to rest and repeat the motion in the next training trial as in aforementioned training setup [49]. A 10-s intertrial break and a 3-min rest every 10 trials (~ 4.6 minutes) were provided to eliminate possible muscle fatigue [49]. Muscle fatigue, as indicated by <10% MPF reduction, was monitored during the training [56], and no fatigue was found across trials.

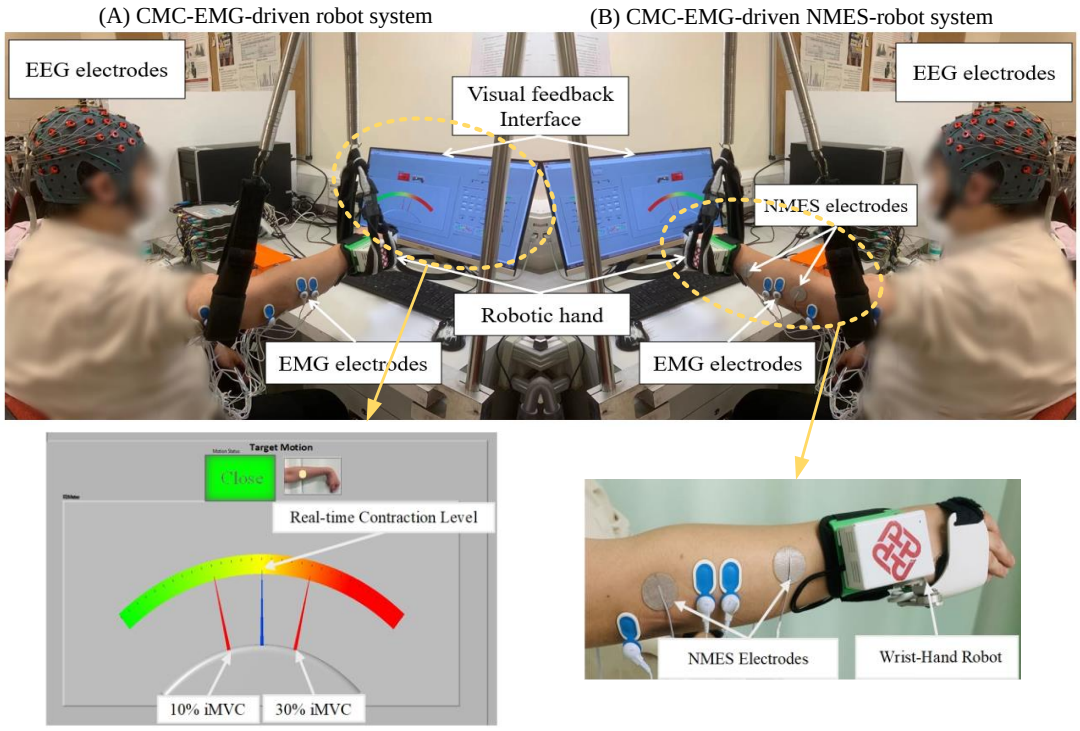

Figure 5-1 CMC-EMG-triggered robot (A) and NMES-robot (B) training systems for the recovery of hand-wrist functions.

5.2.3 Evaluation of rehabilitation effectiveness

5.2.3.1 Clinical assessments

The rehabilitation effectiveness in each participant was assessed using clinical scores, i.e., MAS-elbow, MAS-wrist, MAS-fingers [198], ARAT [22], and FMA-UE [199]. The subscales of FMA-UE (full score: 66), i.e., FMA-shoulder/elbow (FMA-S/E, 42/66) and FMA-wrist/hand (FMA-W/H, 24/66) were evaluated separately to assess the motor compensation in the UE. A blinded assessor performed a total of five times of clinical assessments, including thrice every 2-3 days in 1.5 month prior to the 1st training (Pre-training) to stabilize the baseline scores, once right following the 20th training (Post-training), and once at 3MFU. Here, the FMA was selected as the primary outcome measure [49].

5.2.3.2 CMC, dCMC, and EMG activation levels

The closed-loop neurorehabilitation effectiveness was assessed by CMC, dCMC, as well as levels of the EMG activation in hand-wrist flexion and extension with both 20% iMVC and 40% iMVC, i.e., 20% Ex, 20% Fx, 40% Ex, and 40% Fx [10] [49]. The motion scheme of 40% Ex and 40% Fx was adopted to evaluate the recovery of non-trained motions which had lower-difficulty tasks than the trained motion of 20% iMVC [49] [59]. In addition to the CMC and levels of the EMG activation, the dCMC was evaluated to further assess the closed-loop neurorehabilitation on pathway-specific corticomuscular communication post-stroke [10]. The evaluation were performed one day prior to and immediately after the 20 training sessions [49]. The evaluation setup was the same as the dCMC evaluation in Chapter 3. Different to EMG recordings from the FD and ED in dCMC evaluation, the EMG were recorded from the muscle unions of ED-ECU and FD-FCR for evaluation of hand-wrist extension/flexion in addition to the BIC and TRI. Also, the desired contraction levels in the visual interface were configured at both 20% and 40% iMVC. During the evaluation, the participant conducted the target motions in a random order [49], after the iMVC test on all muscles,

with similar procedures as the dCMC evaluation (Chapter 3). The pre-processing for raw EEG and EMG for denoising was the same Chapter 3 [49]. The calculation of CMC and levels of EMG activation were calculated based on EEG and EMG in different motions with the same procedures as in the CMC-EMG-triggered Control. The LI of CMC was estimated regarding the agonist's muscle in four motion scheme, as follows [49]:

$$LI = \frac{CMC_{ipsilesional}}{\max\left(CMC_{contralesional}, CMC_{midsagittal\ plane}\right)} \quad (5\text{-}1)$$

where $CMC_{ipsilesional}$ and $CMC_{contralesional}$ denote the peak CMC over the respective ipsilesional (e.g., FC1 FC3 FC5, CP1 CP3 CP5, and C1 C3 C5 for the right hemiplegia) and contralesional (e.g., FC2 FC4 FC6, CP2 CP4 CP6, and C2 C4 C6 for the right hemiplegia) hemispheres. The $CMC_{midsagittal\ plane}$ is the peak CMC among FCz, Cz, and CPz in midsagittal plane. Finally, dCMC was estimated based on EEG and EMG recordings in the 20% Ex, to evaluate the pathway-specific corticomuscular communication during the precise motor control [10].

5.2.4 Statistical analysis

Fisher's exact test or the independent t-test was used to compare the demographic characteristics between groups ($P > 0.05$, Table 5-1) [50]. Clinical scores, LI, dCMC, CMC, and levels of EMG activation, were checked and made sure to obey the normal distribution after the Shapiro-Wilk test of normality ($P > 0.05$). The two-way analysis of covariance (2-way ANCOVA) on the clinical scores was conducted regarding different groups (NMES and control groups) and assessment time points (pre-training, the post-training, and the 3MFU), where the pre-training assessment was used as a covariate. This could eliminate possible difference at the baseline test between NMES and control groups [50]. Then, intra-group differences of the clinical scores among

different assessment time points were evaluated in each group using the 1-way ANOVA with Bonferroni post hoc tests. The inter-group differences of the clinical scores between NMES and control groups were evaluated at the respective post-training and 3MFU using a one-way ANCOVA with the pre-assessment as a covariate. In addition to the clinical scores, one-way ANCOVA was performed on the CMC, LI, levels of EMG activation, and dCMC with the pre-training as a covariate, to evaluate the inter-group differences between NMES and control groups. We conducted paired t-test on the CMC, LI, the levels of EMG activation, and dCMC to evaluate the intra-group differences between the pre- and post-assessment in each group. The settings of statistical significance levels were the same as previous chapters.

5.3 Results

Totally, 73 participants were screened in the subsequent training (Figure 5-2). We recruited 31 participants who met the selection criteria. Among them, all participants in the NMES (n = 16) and partial control (n = 11 out of 15) groups competed the 20-session training and the 3FU assessments. Statistic information of the two groups are summarized in Table 5-1. No statistical variance was found within the NMES and control groups regarding the stroke side, gender, age, and onset time.

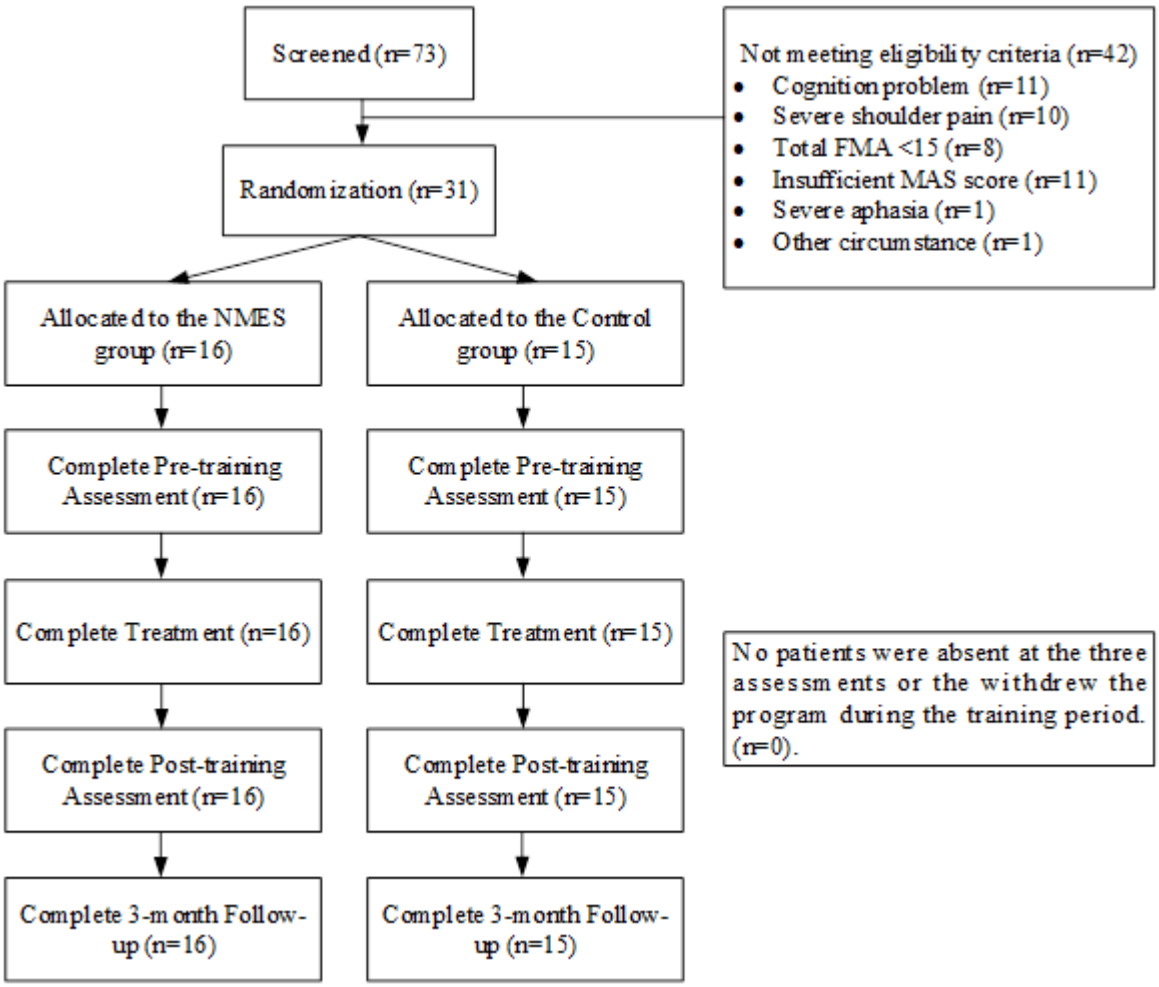

Figure 5-2 The consolidated standards of reporting trials with the flowchart of the experimental design.

5.3.1 Clinical scores

Clinical scores of FMA-W/H, FMA-S/E, ARAT, and MASs at elbow, finger, and wrist joints of participants in both groups prior to, following, and 3-month following the training are depicted in Figure 5-3. Table 5-2a and Table 5-2b shows clinical scores and the statistical results including the possibilities and effect size (EF). No significant inter-group difference was found for any of the clinical scores across the baseline assessment, i.e., pre-training, tests ($P>0.05$). Significant improvements in both the FMA-W/H and ARAT scores were found in the NMES group after the training ($P<0.05$ and $EF=0.242$ for FMA-W/H, $P<0.01$ and $EF=0.522$ for ARAT), and these augments were retained

following three months. The controls also had improved FMA-W/H and ARAT scores, but without statistical significance (P>0.05). Meanwhile, significant decreases in both MAS-finger and MAS-wrist after the training were found in participants from the NMES group at both finger and wrist joints ($P < 0.01$ and EF= 0.504 for MAS-finger, $P<0.001$ and EF= 0.597 for MAS-wrist), and these reductions were retained in the following 3 months, without significant variation for the MAS scores across the assessment time points at the elbow joint ($P > 0.05$). By contrast, mainly the MAS-wrist presented significant decreases in the control group after the training ($P < 0.01$, EF=0.296, one-way ANOVA with the Bonferroni post hoc test), which were retained in the following 3 months. At the elbow joint, we also observed significant decreases in the control group's MAS scores after the training ($P < 0.05$, EF = 0.207), but it did not maintain in the following 3 months. At the finger joint, no significant variation was observed in the controls' MAS scores across the assessment time points ($P > 0.05$). Furthermore, there were no significant variations in the FMA-S/E across assessment time points for either group ($P > 0.05$). For the inter-group comparison, the NMES group presented significantly higher FMA-W/H scores compared to the control group ($P<0.05$, EF=0.190) after the training, although it did not maintain in the following 3 months. No inter-group difference was found between the groups in FMA-S/E, MAS, and ARAT scores ($P > 0.05$).

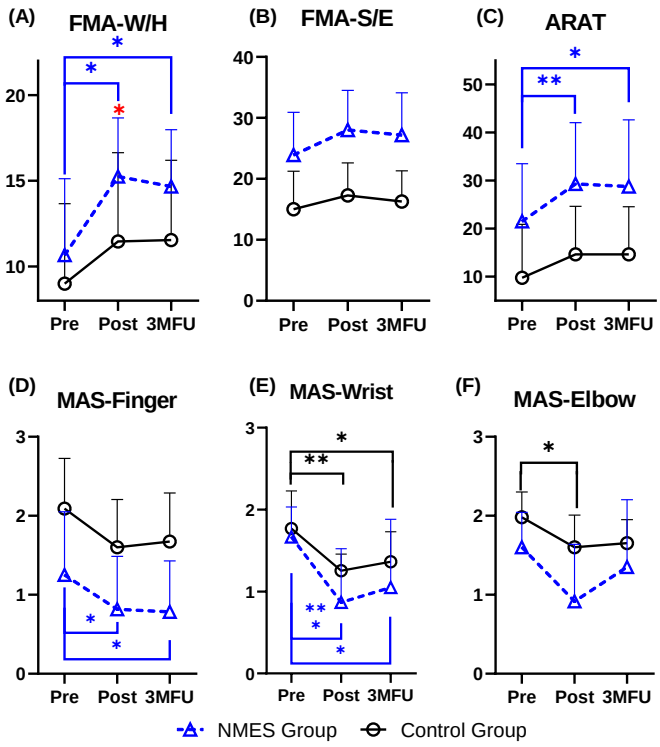

Figure 5-3 The clinical scores at each assessment in both groups. The error bar denotes the standard deviation.

5.3.2 CMC and LI

The CMC values in both groups during different motions is shown in Figure 5-4. No significant inter-group difference was found between the NMES and control groups either before or after the training during different motions ($P > 0.05$). For the intragroup comparison, a significant enhancement of CMC in ECU-ED was observed in both groups during 20% Ex after the 20-session training ($P < 0.05$, EF = 0.018 for the NMES group and EF = 0.751 for the control group, paired t-test). A significant decrease of CMC in BIC was also observed in both groups during 20% Ex ($P < 0.01$, EF = 1.053 for the control group and EF = 1.724 for the NMES group, paired t-test), but no significant change was showed in the FCR-FD and TRI in either NMES or control group after the 20-session training ($P > 0.05$). For 40% Ex, the NMES group presented a significant decrease of CMC in ED-ECU muscles ($P < 0.05$, EF = 0.971, paired t-test),

without significant changes in other three muscles after the training ($P > 0.05$). Conversely, the controls presented no significant CMC changes regarding any muscles at 40% Ex after the 20-session training ($P > 0.05$). Furthermore, there was no significant change in either NMES or control groups in hand-wrist flexion at either iMVC level ($P > 0.05$) after the training.

The LI-CMC regarding agonist's muscles in NMES and control groups during different motions before and after the 20-session training is shown in Figure 5-5. No significant inter-group differences were reported either before or after the training in different motions ($P > 0.05$). In intragroup comparison, significant LI enhancement at 20% Ex was found in both groups after 20-session training ($P < 0.05$, EF = 0.748 for the NMES group and EF = 1.071 for the control group, paired t-test). The NMES group also presented a significant LI enhancement during 40% Ex ($P < 0.05$, EF = 0.741, paired t-test), while there were no significant LI changes during hand-wrist flexion after the training ($P > 0.05$). Conversely, the controls presented no significant LI variation during 40% Ex and hand-wrist flexion at both contraction levels, following the training ($P > 0.05$).

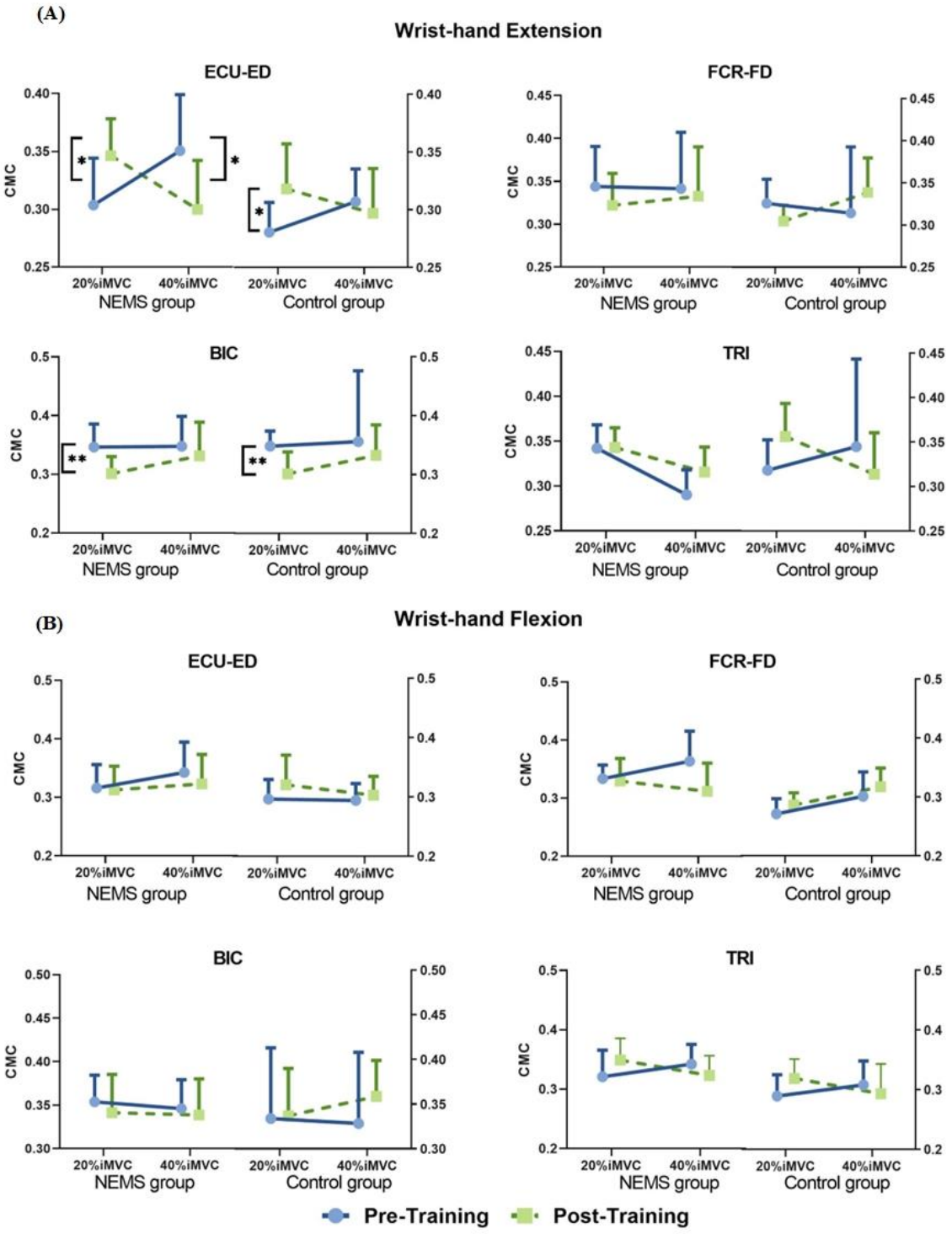

Figure 5-4 CMC at the hand-wrist extension (A) and hand-wrist flexion (B) at the hand-wrist joint in both groups before and after the 20-session training. The error bar denoted the standard deviation.

5.3.3 Evaluation by the EMG activation level

Figure 5-6 depicts the levels of EMG activation in NMES and control groups in the four motions. No significant inter-group difference in levels of EMG activation was found in any motions before the training ($P>0.05$). During 20% Ex, the level of EMG activation presented significant decreases on BIC in both groups after the 20-session training ($P<0.05$, EF= 1.007 for the NMES group and EF= 0.930 for the control group), but no significant changes in either FCR-FD or TRI in either group ($P>0.05$) following the training. During 40% Ex, the NMES group exhibited significant decreases in levels of EMG activation on UE flexors, FCR-FD and BIC ($P<0.05$, EF= 1.101 for FCR-FD and EF= 0.905 for BIC) following the training. The NMES group also had significantly smaller levels of EMG activation on FCR-FD than the control group during 40% Ex after the 20-session training ($P<0.05$). During the hand-wrist flexion, the NMES group presented significantly increased levels of EMG activation on ECU-ED at 20% Fx and significantly decreased levels of EMG activation on BIC at 40% Fx after the training ($P <0.05$, EF= 0.926 for ECU-ED and EF = 0.887 for BIC), without significant changes on other muscles ($P>0.05$). By contrast, EMG activation levels in the controls presented no significant changes during the hand-wrist extension at 40% iMVC and the hand-wrist flexion at both contraction levels following the training ($P>0.05$). No significant inter-group difference was found on the levels of EMG activation during the hand-wrist extension at 20% iMVC and the hand-wrist flexion at both contraction levels after the 20-session training ($P>0.05$).

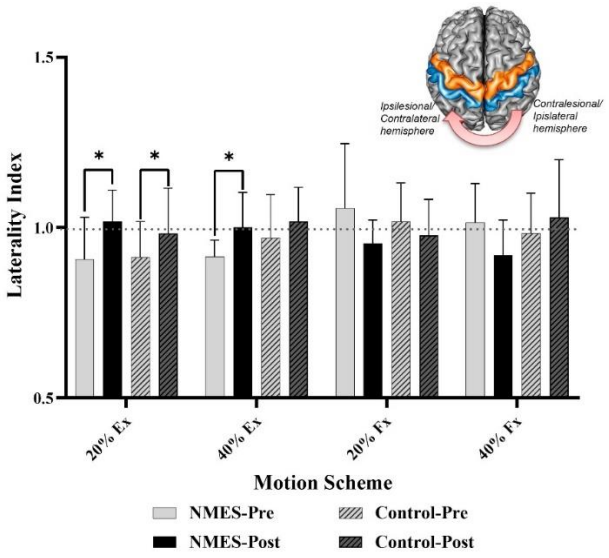

Figure 5-5 Evaluation by the LI of CMC on the agonist's muscle during different motions. The error bar denoted the standard deviation.

5.3.4 dCMC strength

The dCMC in both groups when conducting precise control to hand-wrist movements, i.e., 20% Ex, is shown in Figure 5-7. No significant inter-group dCMC difference was found either before and after 20-session training ($P>0.05$). The descending dCMC exhibited a significant decreased in BIC in both groups ($P<0.01$ and $EF = 1.724$ for the NMES group; $P<0.05$ and $EF = 0.720$ for the control group), while no significant change was found in other three muscles after the training ($P>0.05$). The only significant change in the ascending dCMC was found in ECU-ED in the NMES group with a significant increase of the ascending dCMC after the 20-session training ($P<0.05$, $EF = 1.001$). No significant changes in ascending dCMC were found in other three muscles in both groups ($P>0.05$).

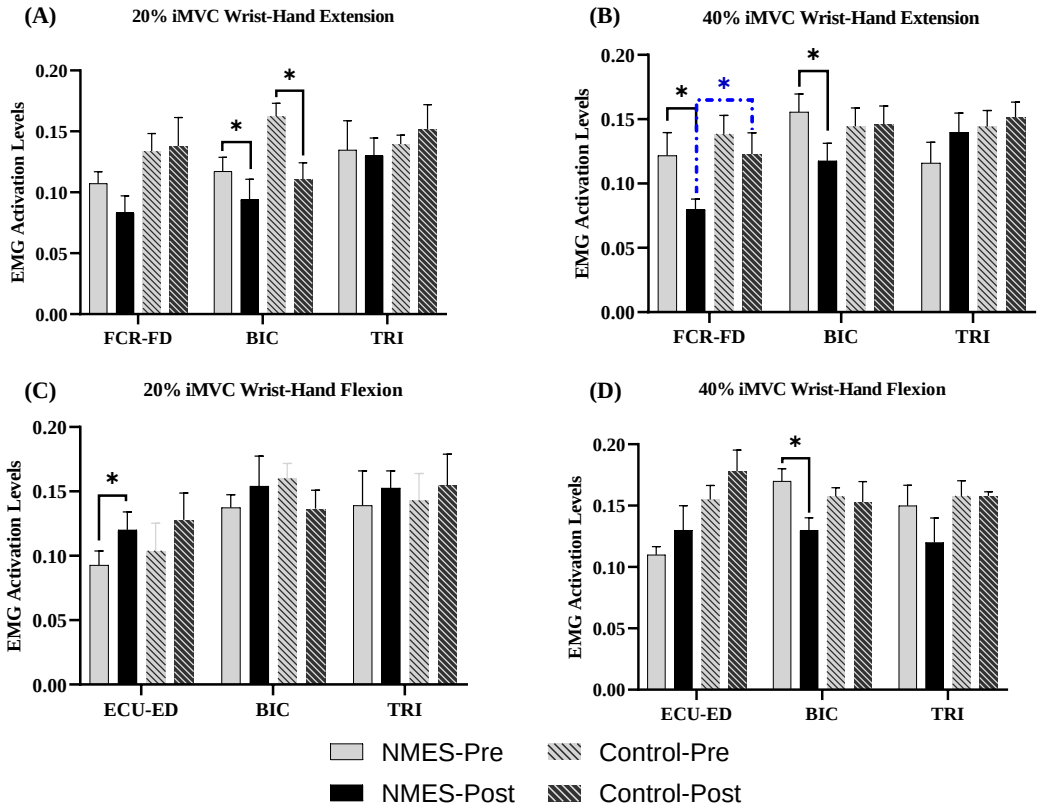

Figure 5-6 EMG activation levels in different motions. The error bar represented the standard deviation.

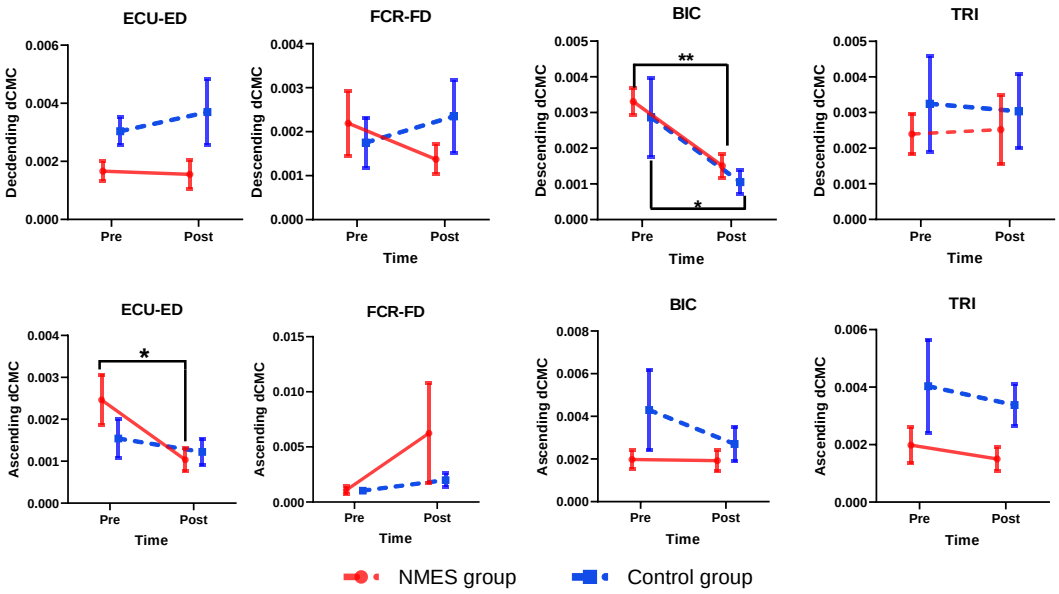

Figure 5-7 dCMC at 20% Ex in both groups. The error bar denoted the standard deviation.

5.4 Discussion

5.4.1 Motor outcome evaluated by clinical scores

The CMC-EMG-triggered NMES-robot generated better rehabilitation outcomes on improving voluntary motor functions and releasing spasticity in hand and wrist joints, particularly for the precise control to finger movements, compared to the CMC-EMG-triggered robot. In the clinical scores (Figure 5-2), significant improvements in clinical scores of FMA-W/H, ARAT, and MAS-finger were observed only in the participants of NMES group. These scores exhibited no significant variation in the control group following the training as well as the 3MFU. Meanwhile, the FMA-W/H score presented a significant larger value in the NMES group than the control group after the training, although it did not maintain after three months. Both groups presented significant release of wrist spasticity (MAS-wrist) and no significant improvements in shoulder/elbow joints (FMA-S/E) after the training. It indicated that the additional NMES assistance in the intervention could contribute to the precise movement control to hand and wrist joints after stroke [10]. Meanwhile, the CMC-EMG-triggered control inhibited the motor compensation from the proximal elbow-shoulder joint in the hand-wrist practice after stroke [49]. On the one hand, the significant improvements in both ARAT and MAS-fingers in participants from the NMES group implicated those interventions with additional NMES assistance improved the precise control to the fingers, as 16/19 sub-cores in the ARAT are related to finger motions, e.g., pinch, grip, and grasp [48]. In contrast, no improvement was found in either ARAT or MAS-finger in the control group. As precise coordination of both sensory and motor systems was required in the fine motor control, the additional finger improvements in the NMES

group could be related to the sensorimotor feedbacks of NMES [10] [168]. It was because that NMES could provide not only muscular activation, but also rich sensory experience on the desired motion, e.g., the desired muscle contraction level, the targeted muscle point, and the desired range of motion in the target joint [48]. Different from the passive stretch by robot assistance, NMES could provide similar cortical activation patterns as in voluntary movements rather than the involuntary movements even with the same range of motion. As detailed in Chapter. 4, the motor-level NMES activated both motor and somatosensory systems in the closed-loop sensorimotor network, which recruited motor units on target muscles not only by the direct activation of descending motor neurons, but also by the indirect activation of corticospinal tracts via the activation of ascending sensory neurons through the cortical sensorimotor integration [69].

Additionally, no significant changes in FMA-S/E in both groups were observed. It further demonstrated the efficacy of the control mechanism driven by CMC-EMG on inhibiting proximal compensatory motions by recruiting the central-to-peripheral VME on desired muscles, without the needs of visual observation and manual correction, as in our previous works [49].

5.4.2 Motor outcome evaluated by CMC and EMG activation levels

The NMES-robot triggered by CMC-EMG benefited the re-distribution of central-to-peripheral VME not only in the trained motions of 20% Ex, but also in the nontrained motions of 40% Ex and 40% Fx, compared to the CMC-EMG-triggered robot, enhancing the precise restoration on hand and wrist joints of the CMC-EMG-triggered control for the closed-loop neurorehabilitation. In the results (Figure 5-4, 5, and 6), both groups presented significantly improved VME distribution among UE muscles with the trained motions of 20% Ex, presenting the improved CMC in ED, decreased EMG

activation levels of BIC, as well as increased LI of CMC in ED after the training. Only the NMES group presented significantly improved VME distribution among UE muscles in the nontrained motions of 40% Fx and Ex following the training. The significant changes in the NMES group mainly included decreased CMC and increased LI in ED and decreased activation levels of BIC and FCR-FD in 40% Ex, in addition to the decreased activation levels of BIC in 40% Fx following the training. The activation levels of FCR-FD in 40% Ex decreased significantly in the NMES group than the control group following the training. These results showed that the additional NMES assistance in CMC-EMG-triggered control could contribute the motor relearning even for the non-trained motions, mainly due to the facilitated cortical sensorimotor integration via the sensory inputs on the desired motion experiences, as detailed in the next section on dCMC. In other words, the NMES sensorimotor feedback could help stroke participants exert the central-to-peripheral VME required in the control mechanism driven by CMC-EMG, thereby benefiting the precise restoration on hand and wrist joints in both trained and non-trained contraction levels, i.e., 40% and 20% iMVC [49]. The significant decreased activation levels of CMC and EMG in UE flexors, i.e., BIC and FCR-FD, in non-trained 40% Ex and Fx suggested that the NMES group achieved additional improvements in releasing the spasticity and reducing motor compensation from the proximal BIC after the training. Similarly, the LI of CMC suggested the NMES could facilitate the hemispheric lateralization from the ipsilesional to the contralesional hemisphere in the non-trained motion of 40% Ex [202]. The facilitated cortical guidance of the NMES-robot triggered by CMC-EMG implied that the activation in ipsilesional pathways could enable the re-innervation of the hand-wrist muscles [139], thereby contributing to the better motor outcomes in the NMES group as in the clinical scores.

The significant decrease in BIC in 20% EX and 40% Ex (Figure 5-6) indicated that stroke survivors presented significantly reduced compensatory movements from the proximal UE in wrist-hand extension after the training. Although BIC presented an increase in the mean EMG activation change in 20% Fx, no significant change was found. This could be related to the fact that individuals with stroke typically had more severe impairments in extensors than flexors in the UE. Meanwhile, most stroke survivors at the chronic stage preserved wrist-hand flexion in low-level force output with less compensatory movements from the proximal BIC, e.g., the flexor synergy typically occurred in high-level force output of UE movements [97] [114] [115].

5.4.3 Motor outcome evaluated by dCMC

The NMES assistance in the CMC-EMG-triggered NMES-robot facilitated the sensorimotor recalibration with the significant release of excessive ascending sensory feedbacks from the target muscle (ECU-ED) in precise control to hand-wrist extension (20% Ex), contributing to the cortical sensorimotor integration for the closed-loop neurorehabilitation. In the dCMC results, significant decrease of the ascending dCMC was only observed in the ECU-ED in the NMES group, without significant change of the ascending dCMC in the control group. Both groups exhibited significant decrease of descending dCMC in the proximal BIC muscle, without significant dCMC changes in FCR-FD and TRI muscle in either group. The reduced ascending dCMC could demonstrate that the NMES assistance could improve sensory functions after the training in the NMES group, because excessive sensory inputs were required to perceive the peripheral states after stroke, as suggested in traditional clinical assessments, dCMC measurements (Chapter. 3), and NMES measurements (Chapter. 4). The NMES assistance facilitated the sensorimotor recalibration on target muscles, ECU-ED, through the corticospinal reinnervation and cortical sensorimotor integration

for the fine motor control, where more precise motor command to target muscles could be generated due to improved sensation on peripheral states [121]. The impaired sensorimotor recalibration after stroke was observed in our previous dCMC studies [10], where the stroke participants presented a significant increase in ascending feedback without significant changes in descending control during the unstable control to fingers compared to the unimpaired controls (Chapter 3). The descending motor commands failed to be recalibrated through the desired and real levels of ascending somatosensory feedbacks in post-stroke voluntary movements, due to the impaired cortical sensorimotor integration as revealed by FC in NMES (Chapter 4). In this regard, it was found that the NMES could provide sensorimotor experience on target muscles with cortical activation patterns similar to the activation movement rather than the passive movement [173]. The enhanced cortical sensorimotor integration through the additional NMES assistance also explained the facilitated hemispheric lateralization in LI results, where significant LI increase in non-trained motion of 40% Ex exhibited only in the NMES group.

5.4.4 Future works

Although the results demonstrated the precise restoration on hand and wrist joints with inhibited motor compensation from the elbow-shoulder muscles in both groups, residual compensation from proximal UE in the controls were observed from the significant release of elbow spasticity (MAS-elbow) after the training, without significant changes after three months. This could be related to the unbalanced sample size between the control (11) and NMES groups (16). In future works, clinical assessments at 3MFU will be conducted on the additional three participants who had completed the 20 training sessions in the control group to investigate the effects of robots triggered by CMC-EMG on inhibiting the compensatory movements. In addition,

although the 20-session training program in this work demonstrated better behavioral and neurological outcomes in the NMES group than the control group, the significant enhancement in FMA-W/H scores in the NMES group than the control group after the training was disappeared at the 3-month follow-up (Figure 5-3), possibly indicating that the stroke participants did not reach their rehabilitative plateau through the 20-session training. In this regard, long-term neurorehabilitation has been a challenge due to resources constraints in healthcare systems and transportation difficulties in individuals with reduced mobility. A self-help rehabilitation device of the CMC-EMG-driven NEMS-robot system will be developed with high-integration, easy-operation, and muti-function for long-term neurorehabilitation in unconditional environment, e.g., at home-based settings.

5.5 Periodic Summary

This work compared the closed-loop neurorehabilitation effectiveness of both the NMES- and the rigid-robots, triggered by CMC-EMG for hand-wrist recovery by a randomized controlled trial with the 3MFU. We assessed the rehabilitation effectiveness of these systems with both behavioral measures of the clinical scores and neurological measures of the CMC, dCMC, and EMG activation levels, in both groups. In the results, the NMES-robot triggered by CMC-EMG exhibited better motor outcomes than the rigid-robot driven by CMC-EMG for the hand-wrist recovery following stroke. There was improved voluntary motor performance with released spasticity in the hand and wrist, re-distributed of central-to-peripheral VME among UE muscles in both trained and non-trained motions, and released excessive ascending sensory feedbacks from the target muscle through the additional NMES assistance. It was worth noting that the CMC-EMG-triggered NMES-robot facilitated sensorimotor recalibration on target ECU-ED muscles in precise control to hand-wrist extension,

contributing to the effective cortical sensorimotor integration in both trained (20% Ex) and non-trained motions (40% Ex). The additional NMES assistance in the treatment could promote the neural excitation in bidirectional corticomuscular pathways for the closed-loop neurorehabilitation after stroke.

Table 5-1 Participants' demographic characteristic.

Characteristics	NMES Group (n=16)	Control Group(n=15)	P value
Gender (male/female) [a]	11/5	13/2	0.394
Age (yrs) [b]	58.6±7.1	52.1±9.8	0.085
Times since stroke in years [b]	6.8±3.4	5.1±4.4	0.292
Stroke side (right/left) [a]	8/8	7/8	1.000
Type of stroke (ischemic/hemorrhagic) [a]	8/8	7/8	1.000

No statistical differences are found between two groups (P>0.05, independent t-test).

[a] Fisher's exact test.

[b] independent t-test.

Table 5-2a. Rehabilitation effects assessed by the clinical scores in both groups

Clinical assessments	Pre	Post	3MFU	1-way ANOVA	2-way ANCOVA		
	Mean Value (95% Confidence Interval)			P (Partial η2)	Time	Group	Time* Group
MAS-Finger (NMES group)	1.25 (0.8-1.7)	0.82 (0.44-1.20)	0.78 (0.41-1.15)	0.002** (0.504)	0.007** (0.154)	0.023* (0.085)	0.942 (0.002)
MAS-Finger (Control group)	2.09 (1.72-2.46)	1.6 (1.24-1.96)	1.67 (1.31-2.03)	0.150 (0.119)			
MAS-Wrist (NMES group)	1.67 (1.46-1.88)	0.87 (0.50-1.24)	1.05 (0.58-1.52)	0.000*** (0.597)	0.000*** (0.313)	0.096 (0.046)	0.566 (0.019)
MAS-Wrist (Control group)	1.77 (1.50-2.04)	1.25 (1.13-1.37)	1.36 (1.14-1.58)	0.005** (0.296)			
MAS-Elbow (NMES group)	1.60 (1.35-1.85)	0.92 (0.51-1.33)	1.35 (0.87-1.83)	0.065 (0.153)	0.003** (0.181)	0.208 (0.027)	0.398 (0.031)
MAS-Elbow (Control group)	1.98 (1.79-2.17)	1.60 (1.36-1.84)	1.65 (1.47-1.83)	0.031* (0.207)			
FMA-S/E (NMES group)	23.92 (19.92-27.92)	28.00 (24.30-31.70)	27.17 (23.27-31.07)	0.315 (0.068)	0.005** (0.165)	0.007** (0.117)	0.539 (0.021)
FMA-S/E (Control group)	15.03 (11.33-18.73)	17.27 (14.07-20.47)	16.27 (13.27-19.27)	0.642 (0.029)			
FMA-W/H (NMES group)	10.67 (8.17-13.17)	15.25 (13.35 - 17.15)	14.67 (12.77 - 16.57)	0.010* (0.242)	0.000*** (0.405)	0.013* (0.101)	0.301 (0.040)
FMA-W/H (Control group)	9.00 (6.20-11.80)	11.45 (8.35-14.55)	11.55 (8.8-14.3)	0.388 (0.061)			
ARAT (NMES group)	21.5 (14.7-28.3)	29.33 (22.1-36.5)	28.75 (20.9-36.6)	0.002** (0.522)	0.012* (0.138)	0.027* (0.080)	0.793 (0.008)
ARAT (Control group)	9.76 (3.17-16.3)	14.64 (8.73-20.5)	14.64 (8.77-20.5)	0.454 (0.051)			

*The superscript * indicates the significant difference with 1 superscript for P<0.05, 2 superscripts for P<0.01, and 3 superscripts for P<0.001.*

Table 5-2b. Inter-group comparison of clinical scores.

Assessment	**One-way** ANCOVA	
	Post P (Partial η2)	3MFU P (Partial η2)
MAS-Finger	0.153 (0.104)	0.050 (0.188)
MAS-Wrist	0.091 (0.143)	0.430 (0.033)
MAS-Elbow	0.191 (0.088)	0.591 (0.015)
FMA-S/E	0.058 (0.176)	0.062 (0.172)
FMA-W/H	0.048* (0.190)	0.121 (0.122)
ARAT	0.084 (0.149)	0.160 (0.101)

*The superscript * indicates the significant difference of P<0.05.*

CHAPTER 6

CONCLUSIONS

More than half stroke survivors experienced both sensory and motor impairments in the UE. Sensorimotor rehabilitation post-stroke relied on the reorganization of neuromuscular networking connectivity, i.e., cortico-cortical and cortico-muscular connectivity, in the central-and-peripheral nerves system. This work conducted four independent studies to investigate the reorganization of neuromuscular networking connectivity in sensory impairments, motor impairments, sensorimotor integration, and sensorimotor recovery after stroke.

The first study examined post-stroke changes in brain connectivity and networking structures during fine tactile sensation induced by textile fabrics through the EEG-based FC and graph theory analyses. The changes of cortical connectivity and networking structures in post-stroke fine tactile sensation had increased interhemispheric connectivity, increased cortical activities, and compensation from the unaffected hemisphere and attentional areas. These findings could provide crucial evidence for the neural reorganization of fine tactile impairments following a stroke.

The second study investigated the pathway-specific CMC in post-stroke motor compensations from the proximal UE to fine motor control of the distal fingers by dCMC analyses. The post-stroke proximal compensation to the fine motor control of distal fingers exhibited shifted descending predominance from the distal fingers to proximal UE, excessive sensory feedbacks in the precise control to distal finger extension, and extended corticomuscular conduction delay for descending control to target muscles. Notably, the impaired sensorimotor recalibration was observed with a less closed-loop sensorimotor system in the post-stroke precise control to finger

movements. These findings demonstrated the reorganization of neuromuscular networking connectivity in fine motor control following a stroke.

The third study investigated the integrated sensorimotor evaluation of cortical rearrangement following a stroke by analyzing the neuromodulatory effects of sensory-/motor-level NMES based on EEG-derived ERD/ERS and FC analyses. Results found that sensory-/motor-level NMES and EEG could measure not only behavioral, but also neurological changes related to post-stroke sensorimotor impairments, including alterations in hemispheric dominance, cortical over-inhibition, impairments in cortical sensorimotor integration, and cortical compensation. Sensory-/motor-level NMES and EEG could therefore be effective for the integrated sensorimotor evaluation of cortical rearrangement after stroke.

The fourth study compared the closed-loop neurorehabilitation of the CMC-EMG-triggered NMES-robot and the CMC-EMG-triggered robot for the hand-wrist motor restoration in a RCT with the 3MFU. Results found that the CMC-EMG-triggered NMES-robot exhibited better motor outcomes than the CMC-EMG-triggered robot for restoring hand and wrist functions after stroke. The additional NMES assistance could improve voluntary motor functions with released spasticity in the hand and wrist joints, promote the re-distribution of central-to-peripheral VME among UE muscles in both trained and non-trained motions, and release excessive ascending sensory feedbacks from the target muscle. These findings provided crucial evidence for the evolution of neuromuscular networking connectivity in the sensorimotor recovery after stroke.

In conclusion, the neuromuscular networking connectivity could be effective to evaluate the systemic neurological changes in post-stroke sensorimotor impairments and recovery.

In future works, we would like to arrange further investigations on the training effects of the CMC-EMG-triggered robot in a larger sample size.

REFERENCE

1. Feigin, V.L., et al., *World Stroke Organization (WSO): global stroke fact sheet 2022.* International Journal of Stroke, 2022. **17**(1): p. 18-29.
2. He, F., et al., *Geographical Disparities in Pooled Stroke Incidence and Case Fatality in Mainland China, Hong Kong, and Macao: Protocol for a Systematic Review and Meta-analysis.* JMIR research protocols, 2022. **11**(1): p. e32566.
3. Seitz, R.d.J., et al., *The role of diaschisis in stroke recovery.* 1999. **30**(9): p. 1844-1850.
4. Frost, S., et al., *Reorganization of remote cortical regions after ischemic brain injury: a potential substrate for stroke recovery.* 2003. **89**(6): p. 3205-3214.
5. Unnithan, A.K.A., J.M. Das, and P. Mehta, *Hemorrhagic stroke*, in *StatPearls [Internet]*. 2022, StatPearls Publishing.
6. Viktorisson, A., et al., *PRE-STROKE PHYSICAL ACTIVITY IN RELATION TO POST-STROKE OUTCOMES LINKED TO THE INTERNATIONAL CLASSIFICATION OF FUNCTIONING, DISABILITY AND HEALTH: A SCOPING REVIEW.* Journal of rehabilitation medicine, 2022. **54**.
7. Altschuler, E.L., et al., *Rehabilitation of hemiparesis after stroke with a mirror.* The Lancet, 1999. **353**(9169): p. 2035-2036.
8. Bolognini, N., C. Russo, and D.J. Edwards, *The sensory side of post-stroke motor rehabilitation.* Restorative neurology and neuroscience, 2016. **34**(4): p. 571-586.
9. Pumpa, L.U., L.S. Cahill, and L.M. Carey, *Somatosensory assessment and treatment after stroke: An evidence-practice gap.* Australian occupational therapy journal, 2015. **62**(2): p. 93-104.
10. Zhou, S., et al., *Pathway-specific cortico-muscular coherence in proximal-to-distal compensation during fine motor control of finger extension after stroke.* Journal of Neural Engineering, 2021. **18**(5): p. 056034.
11. Kessner, S.S., U. Bingel, and G. Thomalla, *Somatosensory deficits after stroke: a scoping review.* Topics in Stroke Rehabilitation, 2016. **23**(2): p. 136-146.
12. Campfens, S.F., et al., *Poor motor function is associated with reduced sensory processing after stroke.* 2015. **233**(4): p. 1339-1349.
13. Carey, L.M., T.A. Matyas, and L.E. Oke, *Sensory loss in stroke patients: effective training of tactile and proprioceptive discrimination.* Archives of

physical medicine and rehabilitation, 1993. **74**(6): p. 602-611.

14. Carey, L.M., et al., *Relationship between touch impairment and brain activation after lesions of subcortical and cortical somatosensory regions.* Neurorehabilitation and neural repair, 2011. **25**(5): p. 443-457.
15. Serrada, I., B. Hordacre, and S.L. Hillier, *Does sensory retraining improve sensation and sensorimotor function following stroke: a systematic review and meta-analysis.* Frontiers in neuroscience, 2019. **13**: p. 402.
16. Kim, J.S. and S.J.S. Choi-Kwon, *Discriminative sensory dysfunction after unilateral stroke.* 1996. **27**(4): p. 677-682.
17. Blatow, M., et al., *fMRI reflects functional connectivity of human somatosensory cortex.* Neuroimage, 2007. **37**(3): p. 927-936.
18. Meyer, S., et al., *How do somatosensory deficits in the arm and hand relate to upper limb impairment, activity, and participation problems after stroke? A systematic review.* Physical therapy, 2014. **94**(9): p. 1220-1231.
19. Sullivan, K.J., et al., *Fugl-Meyer assessment of sensorimotor function after stroke: standardized training procedure for clinical practice and clinical trials.* Stroke, 2011. **42**(2): p. 427-432.
20. Dodds, T.A., et al., *A validation of the functional independence measurement and its performance among rehabilitation inpatients.* Archives of physical medicine and rehabilitation, 1993. **74**(5): p. 531-536.
21. Charalambous, C.P., *Interrater reliability of a modified Ashworth scale of muscle spasticity*, in *Classic papers in orthopaedics*. 2014, Springer. p. 415-417.
22. Yozbatiran, N., L. Der-Yeghiaian, and S.C. Cramer, *A standardized approach to performing the action research arm test.* Neurorehabilitation and neural repair, 2008. **22**(1): p. 78-90.
23. Collin, C., D.J.J.o.N. Wade, Neurosurgery, and Psychiatry, *Assessing motor impairment after stroke: a pilot reliability study.* 1990. **53**(7): p. 576-579.
24. Ang, K.K., et al., *A Large Clinical Study on the Ability of Stroke Patients to Use an EEG-Based Motor Imagery Brain-Computer Interface.* Clinical EEG and Neuroscience, 2011. **42**(4): p. 253-258.
25. Poole, J.L., S.L.J.P. Whitney, and O.T.i. Geriatrics, *Assessments of motor function post stroke: A review.* 2001. **19**(2): p. 1-22.
26. Lincoln, N., J. Jackson, and S.J.P. Adams, *Reliability and revision of the Nottingham Sensory Assessment for stroke patients.* 1998. **84**(8): p. 358-365.

27. Stolk-Hornsveld, F., et al., *The Erasmus MC modifications to the (revised) Nottingham Sensory Assessment: a reliable somatosensory assessment measure for patients with intracranial disorders.* 2006. **20**(2): p. 160-172.
28. Winward, C.E., P.W. Halligan, and D.T.J.C.r. Wade, *The Rivermead Assessment of Somatosensory Performance (RASP): standardization and reliability data.* 2002. **16**(5): p. 523-533.
29. Dellon, A.L.J.T.J.o.h.s., *The moving two-point discrimination test: clinical evaluation of the quickly adapting fiber/receptor system.* 1978. **3**(5): p. 474-481.
30. Hu, X., et al., *Contributions of motoneuron hyperexcitability to clinical spasticity in hemispheric stroke survivors.* 2015. **126**(8): p. 1599-1606.
31. Carter, A.R., G.L. Shulman, and M. Corbetta, *Why use a connectivity-based approach to study stroke and recovery of function?* Neuroimage, 2012. **62**(4): p. 2271-2280.
32. Udupa, K. and R. Chen, *Central motor conduction time*, in *Handbook of clinical neurology*. 2013, Elsevier. p. 375-386.
33. Goodin, P., et al., *Altered functional connectivity differs in stroke survivors with impaired touch sensation following left and right hemisphere lesions.* NeuroImage: Clinical, 2018. **18**: p. 342-355.
34. Bannister, L.C., et al., *Improvement in touch sensation after stroke is associated with resting functional connectivity changes.* Frontiers in neurology, 2015. **6**: p. 165.
35. Fallani, F.D.V., et al., *Multiscale topological properties of functional brain networks during motor imagery after stroke.* Neuroimage, 2013. **83**: p. 438-449.
36. Corbetta, M., et al., *Neural basis and recovery of spatial attention deficits in spatial neglect.* Nature neuroscience, 2005. **8**(11): p. 1603-1610.
37. Gerloff, C., et al., *Multimodal imaging of brain reorganization in motor areas of the contralesional hemisphere of well recovered patients after capsular stroke.* Brain, 2006. **129**(3): p. 791-808.
38. Belardinelli, P., et al., *Plasticity of premotor cortico-muscular coherence in severely impaired stroke patients with hand paralysis.* NeuroImage: Clinical, 2017. **14**: p. 726-733.
39. Bao, S.-C., et al., *Cortico-muscular coherence modulated by high-definition transcranial direct current stimulation in people with chronic stroke.* IEEE Transactions on Neural Systems and Rehabilitation Engineering, 2018. **27**(2):

p. 304-313.

40. Bao, S.-C., et al., *Pathway-specific modulatory effects of neuromuscular electrical stimulation during pedaling in chronic stroke survivors.* 2019. **16**(1): p. 143.
41. Mima, T., et al., *Coherence between cortical and muscular activities after subcortical stroke.* Stroke, 2001. **32**(11): p. 2597-2601.
42. Fang, Y., et al., *Functional corticomuscular connection during reaching is weakened following stroke.* 2009. **120**(5): p. 994-1002.
43. Meng, F., et al., *Cerebral plasticity after subcortical stroke as revealed by cortico-muscular coherence.* IEEE Transactions on Neural Systems and Rehabilitation Engineering, 2008. **17**(3): p. 234-243.
44. Witham, C.L., et al., *Contributions of descending and ascending pathways to corticomuscular coherence in humans.* 2011. **589**(15): p. 3789-3800.
45. Laaksonen, K., et al., *Effect of afferent input on motor cortex excitability during stroke recovery.* **123**(12).
46. Gao, Y., et al., *Electroencephalogram–electromyography coupling analysis in stroke based on symbolic transfer entropy.* 2018. **8**: p. 716.
47. Winstein, C.J., et al., *Guidelines for adult stroke rehabilitation and recovery: a guideline for healthcare professionals from the American Heart Association/American Stroke Association.* Stroke, 2016. **47**(6): p. e98-e169.
48. Hu, X.-L., et al., *Wrist rehabilitation assisted by an electromyography-driven neuromuscular electrical stimulation robot after stroke.* Neurorehabilitation and neural repair, 2015. **29**(8): p. 767-776.
49. Guo, Z., et al., *Corticomuscular integrated representation of voluntary motor effort in robotic control for hand-wrist rehabilitation after stroke.* Journal of Neural Engineering, 2022. **19**(2): p. 026004.
50. Qiuyang, Q., et al., *Distal versus proximal-an investigation on different supportive strategies by robots for upper limb rehabilitation after stroke: a randomized controlled trial.* Journal of neuroengineering and rehabilitation, 2019. **16**(1): p. 1-16.
51. Luft, A.R., et al., *Repetitive bilateral arm training and motor cortex activation in chronic stroke: a randomized controlled trial.* Jama, 2004. **292**(15): p. 1853-1861.
52. Kollen, B.J., et al., *The effectiveness of the Bobath concept in stroke*

rehabilitation: what is the evidence? Stroke, 2009. **40**(4): p. e89-e97.

53. Kwakkel, G., et al., *Constraint-induced movement therapy after stroke.* The Lancet Neurology, 2015. **14**(2): p. 224-234.
54. Sirtori, V., et al., *Constraint-induced movement therapy for upper extremities in stroke patients.* Cochrane Database of Systematic Reviews, 2009(4).
55. Paci, M., *Physiotherapy based on the Bobath concept for adults with post-stroke hemiplegia: a review of effectiveness studies.* Journal of rehabilitation medicine, 2003. **35**(1): p. 2-7.
56. Rong, W., et al., *A Neuromuscular Electrical Stimulation (NMES) and robot hybrid system for multi-joint coordinated upper limb rehabilitation after stroke.* Journal of neuroengineering and rehabilitation, 2017. **14**(1): p. 1-13.
57. Krebs, H.I., et al., *Robot-aided neurorehabilitation: a robot for wrist rehabilitation.* IEEE transactions on neural systems and rehabilitation engineering, 2007. **15**(3): p. 327-335.
58. Takahashi, C.D., et al., *Robot-based hand motor therapy after stroke.* Brain, 2008. **131**(2): p. 425-437.
59. Lattari, E., et al., *Corticomuscular coherence behavior in fine motor control of force: a critical review.* Rev. Neurol, 2010. **51**(10): p. 610-623.
60. Bai, Z., et al., *Immediate and long-term effects of BCI-based rehabilitation of the upper extremity after stroke: a systematic review and meta-analysis.* Journal of neuroengineering and rehabilitation, 2020. **17**(1): p. 1-20.
61. Ang, K.K. and C. Guan, *Brain-computer interface in stroke rehabilitation.* Journal of Computing Science and Engineering, 2013. **7**(2): p. 139-146.
62. Birbaumer, N. and L.G.J.T.J.o.p. Cohen, *Brain–computer interfaces: communication and restoration of movement in paralysis.* 2007. **579**(3): p. 621-636.
63. Zhang, X. and P. Zhou, *Sample entropy analysis of surface EMG for improved muscle activity onset detection against spurious background spikes.* Journal of Electromyography and Kinesiology, 2012. **22**(6): p. 901-907.
64. Li, S. and G.E. Francisco, *New insights into the pathophysiology of post-stroke spasticity.* Frontiers in human neuroscience, 2015. **9**: p. 192.
65. Cai, S., et al., *Real-time detection of compensatory patterns in patients with stroke to reduce compensation during robotic rehabilitation therapy.* IEEE journal of biomedical and health informatics, 2020. **24**(9): p. 2630-2638.

66. Lalitharatne, T.D., et al., *Towards hybrid EEG-EMG-based control approaches to be used in bio-robotics applications: Current status, challenges and future directions.* Paladyn, Journal of Behavioral Robotics, 2013. **4**(2): p. 147-154.
67. Liu, J., Y. Sheng, and H. Liu, *Corticomuscular coherence and its applications: a review.* Frontiers in human neuroscience, 2019. **13**: p. 100.
68. Larsen, L.H., et al., *Corticomuscular coherence in the acute and subacute phase after stroke.* 2017. **128**(11): p. 2217-2226.
69. Insausti-Delgado, A., et al., *Intensity and dose of neuromuscular electrical stimulation influence sensorimotor cortical excitability.* Frontiers in neuroscience, 2021. **14**: p. 1359.
70. Carson, R.G. and A.R. Buick, *Neuromuscular electrical stimulation-promoted plasticity of the human brain.* The Journal of physiology, 2021. **599**(9): p. 2375-2399.
71. Netz, J., T. Lammers, and V. Hömberg, *Reorganization of motor output in the non-affected hemisphere after stroke.* Brain: a journal of neurology, 1997. **120**(9): p. 1579-1586.
72. Van Meer, M.P., et al., *Recovery of sensorimotor function after experimental stroke correlates with restoration of resting-state interhemispheric functional connectivity.* Journal of Neuroscience, 2010. **30**(11): p. 3964-3972.
73. Caliandro, P., et al., *Small-world characteristics of cortical connectivity changes in acute stroke.* Neurorehabilitation and neural repair, 2017. **31**(1): p. 81-94.
74. Khatri, V., R.M. Bruno, and D.J. Simons, *Stimulus-specific and stimulus-nonspecific firing synchrony and its modulation by sensory adaptation in the whisker-to-barrel pathway.* Journal of neurophysiology, 2009. **101**(5): p. 2328-2338.
75. Westlake, K.P. and S.S. Nagarajan, *Functional connectivity in relation to motor performance and recovery after stroke.* Frontiers in systems neuroscience, 2011. **5**: p. 8.
76. Schaechter, J.D., *Motor rehabilitation and brain plasticity after hemiparetic stroke.* Progress in neurobiology, 2004. **73**(1): p. 61-72.
77. Stam, C.J., G. Nolte, and A. Daffertshofer, *Phase lag index: assessment of functional connectivity from multi channel EEG and MEG with diminished bias from common sources.* Human brain mapping, 2007. **28**(11): p. 1178-1193.

78. Strens, L., et al., *Corticocortical coupling in chronic stroke: its relevance to recovery.* Neurology, 2004. **63**(3): p. 475-484.
79. Beaty, R.E., et al., *Robust prediction of individual creative ability from brain functional connectivity.* Proceedings of the National Academy of Sciences, 2018. **115**(5): p. 1087-1092.
80. Bullmore, E. and O. Sporns, *Complex brain networks: graph theoretical analysis of structural and functional systems.* Nature reviews neuroscience, 2009. **10**(3): p. 186-198.
81. da Silva, F.L., *EEG and MEG: relevance to neuroscience.* Neuron, 2013. **80**(5): p. 1112-1128.
82. Yan, J., et al., *Motor imagery cognitive network after left ischemic stroke: study of the patients during mental rotation task.* PloS one, 2013. **8**(10).
83. Philips, G.R., J.J. Daly, and J.C. Príncipe, *Topographical measures of functional connectivity as biomarkers for post-stroke motor recovery.* Journal of neuroengineering and rehabilitation, 2017. **14**(1): p. 67.
84. Nolte, G., et al., *Identifying true brain interaction from EEG data using the imaginary part of coherency.* Clinical neurophysiology, 2004. **115**(10): p. 2292-2307.
85. Maris, E., J.-M. Schoffelen, and P. Fries, *Nonparametric statistical testing of coherence differences.* Journal of neuroscience methods, 2007. **163**(1): p. 161-175.
86. Tombaugh, T.N. and N.J. McIntyre, *The mini-mental state examination: a comprehensive review.* Journal of the American Geriatrics Society, 1992. **40**(9): p. 922-935.
87. Michielsen, M.E., et al., *Quantifying nonuse in chronic stroke patients: a study into paretic, nonparetic, and bimanual upper-limb use in daily life.* Archives of physical medicine and rehabilitation, 2012. **93**(11): p. 1975-1981.
88. Singh, H., et al., *The brain's response to pleasant touch: An EEG investigation of tactile caressing.* Frontiers in human neuroscience, 2014. **8**: p. 893.
89. Moungou, A., J.-L. Thonnard, and A. Mouraux. *Using EEG (SS-EPs) to characterize the brain activity in response to textured stimuli in passive touch*. in *2015 IEEE World Haptics Conference (WHC)*. 2015. IEEE.
90. Ravandi, S.H. and M. Valizadeh, *Properties of fibers and fabrics that contribute to human comfort*, in *Improving comfort in clothing*. 2011, Elsevier. p. 61-78.

91. Olausson, H., et al., *The neurophysiology of unmyelinated tactile afferents.* 2010. **34**(2): p. 185-191.
92. Vigário, R., et al., *Independent component approach to the analysis of EEG and MEG recordings.* 2000. **47**(5): p. 589-593.
93. van Ede, F., et al., *Orienting attention to an upcoming tactile event involves a spatially and temporally specific modulation of sensorimotor alpha-and beta-band oscillations.* Journal of Neuroscience, 2011. **31**(6): p. 2016-2024.
94. De Vico Fallani, F., et al., *Evaluation of the brain network organization from EEG signals: a preliminary evidence in stroke patient.* The Anatomical Record: Advances in Integrative Anatomy and Evolutionary Biology: Advances in Integrative Anatomy and Evolutionary Biology, 2009. **292**(12): p. 2023-2031.
95. Fallani, F.D.V., et al., *Cortical network analysis in patients affected by schizophrenia.* Brain topography, 2010. **23**(2): p. 214-220.
96. Shapiro, S.S. and M.B. Wilk, *An analysis of variance test for normality (complete samples).* Biometrika, 1965. **52**(3/4): p. 591-611.
97. Jones, T.A., *Motor compensation and its effects on neural reorganization after stroke.* Nature Reviews Neuroscience, 2017. **18**(5): p. 267-280.
98. Carmichael, S.T., *Cellular and molecular mechanisms of neural repair after stroke: making waves.* Annals of Neurology: Official Journal of the American Neurological Association and the Child Neurology Society, 2006. **59**(5): p. 735-742.
99. Liu, K., et al., *Neuronal intrinsic mechanisms of axon regeneration.* Annual review of neuroscience, 2011. **34**: p. 131-152.
100. Grefkes, C., et al., *Cortical connectivity after subcortical stroke assessed with functional magnetic resonance imaging.* Annals of neurology, 2008. **63**(2): p. 236-246.
101. Kastrup, A., et al., *Behavioral correlates of negative BOLD signal changes in the primary somatosensory cortex.* Neuroimage, 2008. **41**(4): p. 1364-1371.
102. Kim, S., J. Lee, and L. Kim. *ERS differences between stroke patients and healthy controls after hand movement*. in *2016 4th International Winter Conference on Brain-Computer Interface (BCI)*. 2016. IEEE.
103. Näätänen, R., A. Gaillard, and S. Mäntysalo, *Brain potential correlates of voluntary and involuntary attention*, in *Progress in brain research*. 1980, Elsevier. p. 343-348.

104. Vossel, S., J.J. Geng, and G.R. Fink, *Dorsal and ventral attention systems: distinct neural circuits but collaborative roles.* The Neuroscientist, 2014. **20**(2): p. 150-159.
105. Johansen-Berg, H., et al., *Correlation between motor improvements and altered fMRI activity after rehabilitative therapy.* Brain, 2002. **125**(12): p. 2731-2742.
106. Rinne, P., et al., *Triple dissociation of attention networks in stroke according to lesion location.* Neurology, 2013. **81**(9): p. 812-820.
107. Volz, L.J., et al., *Motor cortex excitability and connectivity in chronic stroke: a multimodal model of functional reorganization.* Brain Structure and Function, 2015. **220**(2): p. 1093-1107.
108. Liu, J., et al., *Enhanced interhemispheric functional connectivity compensates for anatomical connection damages in subcortical stroke.* Stroke, 2015. **46**(4): p. 1045-1051.
109. Bartolomeo, P. and M.T. de Schotten, *Let thy left brain know what thy right brain doeth: inter-hemispheric compensation of functional deficits after brain damage.* Neuropsychologia, 2016. **93**: p. 407-412.
110. Geffen, G.M., D.L. Jones, and L.B. Geffen, *Interhemispheric control of manual motor activity.* Behavioural brain research, 1994. **64**(1-2): p. 131-140.
111. Ebner, F.F. and R.E. Myers, *Corpus callosum and the interhemispheric transmission of tactual learning.* Journal of Neurophysiology, 1962. **25**(3): p. 380-391.
112. Rubinov, M. and O. Sporns, *Complex network measures of brain connectivity: uses and interpretations.* Neuroimage, 2010. **52**(3): p. 1059-1069.
113. Gerloff, C. and M. Hallett, *Big news from small world networks after stroke.* Brain, 2010. **133**(4): p. 952-955.
114. Levin, M.F., J.A. Kleim, and S.L. Wolf, *What do motor "recovery" and "compensation" mean in patients following stroke?* Neurorehabilitation and neural repair, 2009. **23**(4): p. 313-319.
115. Dewald, J.P., et al., *Abnormal muscle coactivation patterns during isometric torque generation at the elbow and shoulder in hemiparetic subjects.* Brain, 1995. **118**(2): p. 495-510.
116. Cirstea, M. and M.F.J.B. Levin, *Compensatory strategies for reaching in stroke.* 2000. **123**(5): p. 940-953.
117. Jones, T.A., et al., *Motor system plasticity in stroke models: intrinsically use-*

dependent, unreliably useful. 2013. **44**(6_suppl_1): p. S104-S106.

118. Dayan, E. and L.G.J.N. Cohen, *Neuroplasticity subserving motor skill learning.* 2011. **72**(3): p. 443-454.
119. Takeuchi, N. and S.-I.J.N.p. Izumi, *Maladaptive plasticity for motor recovery after stroke: mechanisms and approaches.* 2012. **2012**.
120. Marigold, D.S., et al., *Contribution of muscle strength and integration of afferent input to postural instability in persons with stroke.* Neurorehabilitation and neural repair, 2004. **18**(4): p. 222-229.
121. Sober, S.J. and P.N.J.J.o.N. Sabes, *Multisensory integration during motor planning.* 2003. **23**(18): p. 6982-6992.
122. Taube, J.S.J.A.R.N., *The head direction signal: origins and sensory-motor integration.* 2007. **30**: p. 181-207.
123. Macdonell, R.A., G.A. Donnan, and P.F.J.A.o.n. Bladin, *A comparison of somatosensory evoked and motor evoked potentials in stroke.* 1989. **25**(1): p. 68-73.
124. Williams, E.R., D.S. Soteropoulos, and S.N. Baker, *Coherence between motor cortical activity and peripheral discontinuities during slow finger movements.* Journal of neurophysiology, 2009. **102**(2): p. 1296-1309.
125. Guo, Z., et al., *Altered corticomuscular coherence (CMCoh) pattern in the upper limb during finger movements after stroke.* Frontiers in Neurology, 2020. **11**: p. 410.
126. Colebatch, J., et al., *Preliminary report: activation of the cerebellum in essential tremor.* 1990. **336**(8722): p. 1028-1030.
127. Pundik, S., et al., *Recovery of post stroke proximal arm function, driven by complex neuroplastic bilateral brain activation patterns and predicted by baseline motor dysfunction severity.* 2015. **9**: p. 394.
128. Yao, J. and J.P.A. Dewald. *Cortico-muscular Communication during the Generation of Static Shoulder Abduction Torque in Upper Limb Following Stroke*. in *2006 International Conference of the IEEE Engineering in Medicine and Biology Society*. 2006.
129. Chen, R., et al., *The clinical diagnostic utility of transcranial magnetic stimulation: report of an IFCN committee.* 2008. **119**(3): p. 504-532.
130. Talelli, P., R. Greenwood, and J.J.C.n. Rothwell, *Arm function after stroke: neurophysiological correlates and recovery mechanisms assessed by*

transcranial magnetic stimulation. 2006. **117**(8): p. 1641-1659.

131. Kristeva, R., L. Patino, and W.J.N. Omlor, *Beta-range cortical motor spectral power and corticomuscular coherence as a mechanism for effective corticospinal interaction during steady-state motor output.* 2007. **36**(3): p. 785-792.
132. Mima, T. and M.J.C.N. Hallett, *Electroencephalographic analysis of cortico-muscular coherence: reference effect, volume conduction and generator mechanism.* 1999. **110**(11): p. 1892-1899.
133. Peterson, S.M. and D.P. Ferris, *Group-level cortical and muscular connectivity during perturbations to walking and standing balance.* NeuroImage, 2019. **198**: p. 93-103.
134. Meng, F., et al., *Study on connectivity between coherent central rhythm and electromyographic activities.* 2008. **5**(3): p. 324.
135. Kong, K.-H., K.S. Chua, and J. Lee, *Recovery of upper limb dexterity in patients more than 1 year after stroke: frequency, clinical correlates and predictors.* NeuroRehabilitation, 2011. **28**(2): p. 105-111.
136. Folstein, M.F., S.E. Folstein, and P.R. McHugh, *"Mini-mental state": a practical method for grading the cognitive state of patients for the clinician.* Journal of psychiatric research, 1975. **12**(3): p. 189-198.
137. Fugl-Meyer, A.R., et al., *The post-stroke hemiplegic patient. 1. a method for evaluation of physical performance.* Scandinavian journal of rehabilitation medicine, 1975. **7**(1): p. 13-31.
138. Kamper, D., et al., *Relative contributions of neural mechanisms versus muscle mechanics in promoting finger extension deficits following stroke.* 2003. **28**(3): p. 309-318.
139. Divekar, N.V. and L.R. John, *Neurophysiological, behavioural and perceptual differences between wrist flexion and extension related to sensorimotor monitoring as shown by corticomuscular coherence.* Clinical neurophysiology, 2013. **124**(1): p. 136-147.
140. Delorme, A. and S. Makeig, *EEGLAB: an open source toolbox for analysis of single-trial EEG dynamics including independent component analysis.* Journal of neuroscience methods, 2004. **134**(1): p. 9-21.
141. Oostenveld, R., et al., *FieldTrip: open source software for advanced analysis of MEG, EEG, and invasive electrophysiological data.* 2011. **2011**.

142. Mima, T., T. Matsuoka, and M.J.C.N. Hallett, *Information flow from the sensorimotor cortex to muscle in humans.* 2001. **112**(1): p. 122-126.
143. Geweke, J.J.J.o.t.A.s.a., *Measurement of linear dependence and feedback between multiple time series.* 1982. **77**(378): p. 304-313.
144. Delorme, A., et al., *EEGLAB, SIFT, NFT, BCILAB, and ERICA: new tools for advanced EEG processing.* 2011. **2011**.
145. Ding, M., et al., *Short-window spectral analysis of cortical event-related potentials by adaptive multivariate autoregressive modeling: data preprocessing, model validation, and variability assessment.* 2000. **83**(1): p. 35-45.
146. Babiloni, F., et al., *Estimation of the cortical functional connectivity with the multimodal integration of high-resolution EEG and fMRI data by directed transfer function.* 2005. **24**(1): p. 118-131.
147. Mima, T., et al., *Electroencephalographic measurement of motor cortex control of muscle activity in humans.* Clinical Neurophysiology, 2000. **111**(2): p. 326-337.
148. Lim, M., et al., *Ascending beta oscillation from finger muscle to sensorimotor cortex contributes to enhanced steady-state isometric contraction in humans.* 2014. **125**(10): p. 2036-2045.
149. Shingala, M.C., A.J.I.J.o.N.T.i.S. Rajyaguru, and Engineering, *Comparison of post hoc tests for unequal variance.* 2015. **2**(5): p. 22-33.
150. Huang, Y., et al., *Measurement of sensory deficiency in fine touch after stroke during textile fabric stimulation by electroencephalography (EEG).* 2020. **17**(4): p. 045007-045007.
151. Lackmy-Vallée, A., et al., *Anodal transcranial direct current stimulation of the motor cortex induces opposite modulation of reciprocal inhibition in wrist extensor and flexor.* 2014. **112**(6): p. 1505-1515.
152. Glover, I.S. and S.N.J.J.o.N. Baker, *Cortical, Corticospinal, and Reticulospinal Contributions to Strength Training.* 2020. **40**(30): p. 5820-5832.
153. Pennisi, G., et al., *Transcranial magnetic stimulation after pure motor stroke.* 2002. **113**(10): p. 1536-1543.
154. Takeuchi, N., et al., *Disinhibition of the premotor cortex contributes to a maladaptive change in the affected hand after stroke.* 2007. **38**(5): p. 1551-1556.
155. Ward, N.S. and L.G.J.A.o.n. Cohen, *Mechanisms underlying recovery of motor*

function after stroke. 2004. **61**(12): p. 1844-1848.

156. Nowak, D.A., et al., *Dexterity is impaired at both hands following unilateral subcortical middle cerebral artery stroke.* 2007. **25**(10): p. 3173-3184.
157. Bowden, J.L., J.L. Taylor, and P.A.J.F.i.n. McNulty, *Voluntary activation is reduced in both the more-and less-affected upper limbs after unilateral stroke.* 2014. **5**: p. 239.
158. Baker, S.N.J.C.o.i.n., *Oscillatory interactions between sensorimotor cortex and the periphery.* 2007. **17**(6): p. 649-655.
159. Bartley, K., et al., *Corticospinal volleys and compound muscle action potentials produced by repetitive transcranial stimulation during spinal surgery.* 2002. **113**(1): p. 78-90.
160. Stinear, C.M., et al., *Functional potential in chronic stroke patients depends on corticospinal tract integrity.* 2007. **130**(1): p. 170-180.
161. O'Dwyer, N.J., L. Ada, and P.D. Neilson, *Spasticity and muscle contracture following stroke.* Brain, 1996. **119**(5): p. 1737-1749.
162. Bertolasi, L., et al., *Inhibitory action of forearm flexor muscle afferents on corticospinal outputs to antagonist muscles in humans.* The Journal of physiology, 1998. **511**(3): p. 947-956.
163. Martin, P.G., et al., *Fatigue-sensitive afferents inhibit extensor but not flexor motoneurons in humans.* Journal of Neuroscience, 2006. **26**(18): p. 4796-4802.
164. Ackerley, R., et al., *Insights and perspectives on sensory-motor integration and rehabilitation.* 2016. **29**(6-7): p. 607-633.
165. Sarmento, R.M., et al., *Automatic neuroimage processing and analysis in stroke—A systematic review.* IEEE reviews in biomedical engineering, 2019. **13**: p. 130-155.
166. Karbasforoushan, H., J. Cohen-Adad, and J. Dewald, *Brainstem and spinal cord MRI identifies altered sensorimotor pathways post-stroke.* Nature communications, 2019. **10**(1): p. 1-7.
167. Haller, S. and A.J. Bartsch, *Pitfalls in fMRI.* European radiology, 2009. **19**(11): p. 2689-2706.
168. Zhou, S., et al., *Impairments of cortico-cortical connectivity in fine tactile sensation after stroke.* Journal of NeuroEngineering and Rehabilitation, 2021. **18**(1): p. 34.
169. Kaiser, V., et al., *Relationship between electrical brain responses to motor*

imagery and motor impairment in stroke. Stroke, 2012. **43**(10): p. 2735-2740.

170. Xie, P., et al., *Effect of pulsed transcranial ultrasound stimulation at different number of tone-burst on cortico-muscular coupling.* BMC neuroscience, 2018. **19**(1): p. 1-10.
171. Zhou, S., et al., *Optimization of relative parameters in transfer entropy estimation and application to corticomuscular coupling in humans.* Journal of neuroscience methods, 2018. **308**: p. 276-285.
172. Zeman, B. and C. Yiannikas, *Functional prognosis in stroke: use of somatosensory evoked potentials.* Journal of Neurology, Neurosurgery & Psychiatry, 1989. **52**(2): p. 242-247.
173. Qiu, S., et al., *Event-related beta EEG changes during active, passive movement and functional electrical stimulation of the lower limb.* IEEE Transactions on Neural Systems and Rehabilitation Engineering, 2015. **24**(2): p. 283-290.
174. Ye, F., et al., *A Data-driven Investigation on Surface Electromyography (sEMG) based Clinical Assessment in Chronic Stroke.* Frontiers in Neurorobotics, 2021. **15**: p. 94.
175. Calautti, C., et al., *Displacement of primary sensorimotor cortex activation after subcortical stroke: a longitudinal PET study with clinical correlation.* 2003. **19**(4): p. 1650-1654.
176. Grandchamp, R. and A. Delorme, *Single-trial normalization for event-related spectral decomposition reduces sensitivity to noisy trials.* Frontiers in psychology, 2011. **2**: p. 236.
177. Cohen, M.X., *A better way to define and describe Morlet wavelets for time-frequency analysis.* NeuroImage, 2019. **199**: p. 81-86.
178. Chen, L., et al., *EEG-controlled functional electrical stimulation rehabilitation for chronic stroke: system design and clinical application.* Frontiers of medicine, 2021. **15**(5): p. 740-749.
179. Wang, Y., et al., *Low-intensity pulsed ultrasound modulates multi-frequency band phase synchronization between LFPs and EMG in mice.* Journal of neural engineering, 2019. **16**(2): p. 026036.
180. Maris, E. and R. Oostenveld, *Nonparametric statistical testing of EEG-and MEG-data.* Journal of neuroscience methods, 2007. **164**(1): p. 177-190.
181. Mangold, S., et al., *Motor training of upper extremity with functional electrical stimulation in early stroke rehabilitation.* Neurorehabilitation and neural repair,

2009. **23**(2): p. 184-190.

182. Garnsworthy, R., et al., *Transcutaneous electrical stimulation and the sensation of prickle.* Journal of neurophysiology, 1988. **59**(4): p. 1116-1127.
183. Forst, J.C., et al., *Surface electrical stimulation to evoke referred sensation.* Journal of Rehabilitation Research & Development, 2015. **52**(4).
184. Shi, Y., et al., *Self-powered electro-tactile system for virtual tactile experiences.* Science Advances, 2021. **7**(6): p. eabe2943.
185. Wolny, T., P. Linek, and P. Michalski, *Inter-rater reliability of two-point discrimination in acute stroke patients.* Neurorehabilitation, 2017. **41**(1): p. 127-134.
186. Suda, M., et al., *Validity and reliability of the Semmes-Weinstein Monofilament test and the thumb localizing test in patients with stroke.* Frontiers in neurology, 2021. **11**: p. 1957.
187. Zhao, Y., et al., *Event-Related Beta EEG Changes Induced by Various Neuromuscular Electrical Stimulation: A Pilot Study.* IEEE Transactions on Neural Systems and Rehabilitation Engineering, 2021. **29**: p. 1206-1212.
188. Chen, S., et al., *Relation between sensorimotor rhythm during motor attempt/imagery and upper-limb motor impairment in stroke.* Clinical EEG and Neuroscience, 2022. **53**(3): p. 238-247.
189. Tangwiriyasakul, C., et al., *Temporal evolution of event-related desynchronization in acute stroke: a pilot study.* Clinical neurophysiology, 2014. **125**(6): p. 1112-1120.
190. Pfurtscheller, G. and F.L. Da Silva, *Event-related EEG/MEG synchronization and desynchronization: basic principles.* Clinical neurophysiology, 1999. **110**(11): p. 1842-1857.
191. Lilin, C., et al., *Correlation of N30 somatosensory evoked potentials with spasticity and neurological function after stroke: A cross-sectional study.* Journal of Rehabilitation Medicine, 2021. **53**(9).
192. Frías, I., et al., *Interhemispheric connectivity of primary sensory cortex is associated with motor impairment after stroke.* Scientific Reports, 2018. **8**(1): p. 1-10.
193. Behrmann, M., J.J. Geng, and S. Shomstein, *Parietal cortex and attention.* Current opinion in neurobiology, 2004. **14**(2): p. 212-217.
194. Kaas, J.H., *Theories of visual cortex organization in primates: areas of the third*

level. Progress in brain research, 1996. **112**: p. 213-221.

195. Levy, B.J. and A.D. Wagner, *Cognitive control and right ventrolateral prefrontal cortex: reflexive reorienting, motor inhibition, and action updating.* Annals of the New York academy of sciences, 2011. **1224**(1): p. 40-62.
196. Kenzie, J.M., et al., *Errors in proprioceptive matching post-stroke are associated with impaired recruitment of parietal, supplementary motor, and temporal cortices.* Brain Imaging and Behavior, 2019. **13**(6): p. 1635-1649.
197. Bhakta, B.B., *Management of spasticity in stroke.* British medical bulletin, 2000. **56**(2): p. 476-485.
198. Sloan, R., et al., *Inter-rater reliability of the modified Ashworth Scale for spasticity in hemiplegic patients.* International journal of rehabilitation research, 1992. **15**(2): p. 158-161.
199. Gladstone, D.J., C.J. Danells, and S.E. Black, *The Fugl-Meyer assessment of motor recovery after stroke: a critical review of its measurement properties.* Neurorehabilitation and neural repair, 2002. **16**(3): p. 232-240.